AFFDL-TR-76-91
Volume I

A GUIDE FOR ESTIMATION OF AEROACOUSTIC LOADS ON FLIGHT VEHICLE SURFACES

BOLT BERANEK AND NEWMAN INC.
50 MOULTON STREET
CAMBRIDGE, MASSACHUSETTS 02138

FEBRUARY 1977

FINAL REPORT JANUARY 1975 - JULY 1976

Approved for public release; distribution unlimited

AIR FORCE FLIGHT DYNAMICS LABORATORY
AIR FORCE WRIGHT AERONAUTICAL LABORATORIES
AIR FORCE SYSTEMS COMMAND
WRIGHT-PATTERSON AIR FORCE BASE, OHIO 45433

NOTICE

When Government drawings, specifications, or other data are used for any purpose other than in connection with a definitely related Government procurement operation, the Unites States Government thereby incurs no responsibility nor any obligation whatsoever; and the fact that the government may have formulated, furnished, or in any way supplied the said drawings, specifications, or other data, is not to be regarded by implication or otherwise as in any manner licensing the holder or any other person or corporation, or conveying any rights or permission to manufacture, use, or sell any patented invention that may in any way be related thereto.

This technical report has been reviewed and is approved.

Robert W. Gordon

ROBERT W. GORDON
Project Engineer

R.M. Bader

ROBERT M. BADER, Chief
Structural Integrity Branch

FOR THE COMMANDER

Howard L Farmer

HOWARD L. FARMER, Col, USAF
Chief, Structural Mechanics Division

This report has been reviewed by the Information Office (IO) and is releasable to the National Technical Information Service (NTIS). At NTIS, it will be available to the general public, including foreign nations.

Copies of this report should not be returned unless return is required by security considerations, contractual obligations, or notice on a specific document.

AIR FORCE - 19 MAY 77 - 150

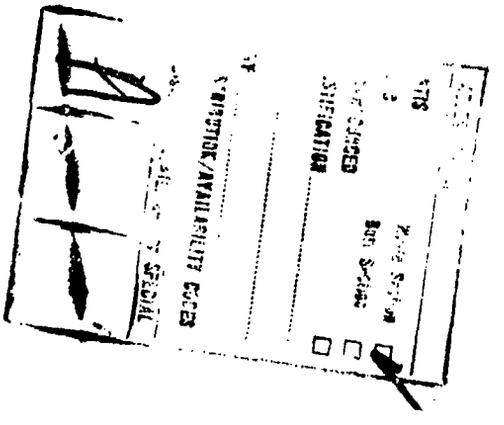

UNCLASSIFIED
SECURITY CLASSIFICATION OF THIS PAGE (When Data Entered)

REPORT DOCUMENTATION PAGE

READ INSTRUCTIONS BEFORE COMPLETING FORM

1. REPORT NUMBER: AFFDL-TR-76-91-Vol-I	2. GOVT ACCESSION NO.
3. RECIPIENT'S CATALOG NUMBER	
4. TITLE (and Subtitle): A Guide for Estimation of Aeroacoustic Loads on Flight Vehicle Surfaces	5. TYPE OF REPORT & PERIOD COVERED: Final Report, January 1975-July 1976
6. PERFORMING ORG. REPORT NUMBER: BBN-3215-Vol-I	
7. AUTHOR(s): Eric E. Ungar, John F. Wilby, Donald B. Bliss, B. Pinkel, A. Galaitsis	8. CONTRACT OR GRANT NUMBER(s): F33615-75-C-3017
9. PERFORMING ORGANIZATION NAME AND ADDRESS: Bolt Beranek and Newman Inc., 50 Moulton Street, Cambridge, Massachusetts 02138	10. PROGRAM ELEMENT, PROJECT, TASK AREA & WORK UNIT NUMBERS: Project No. 1471, 14710226
11. CONTROLLING OFFICE NAME AND ADDRESS: Air Force Flight Dynamics Laboratory (AFFDL/FBE), Air Force Systems Command, Wright-Patterson AFB, OH 45433	12. REPORT DATE: February 1977
	13. NUMBER OF PAGES: 198
14. MONITORING AGENCY NAME & ADDRESS (if different from Controlling Office): 206p.	15. SECURITY CLASS. (of this report): Unclassified
	15a. DECLASSIFICATION/DOWNGRADING SCHEDULE

16. DISTRIBUTION STATEMENT (of this Report)

Approved for public release; distribution unlimited

17. DISTRIBUTION STATEMENT (of the abstract entered in Block 20, if different from Report)

18. SUPPLEMENTARY NOTES

19. KEY WORDS (Continue on reverse side if necessary and identify by block number)

Aeroacoustic loads, surface pressures, nearfield noise, jet noise, noise from powered lift systems, propeller noise, engine noise, blasts from armament, boundary layer pressures, cavity noise

20. ABSTRACT (Continue on reverse side if necessary and identify by block number)

A compilation is presented of the best available methods for estimating the magnitudes, spectra and correlations of pressures that act on the surfaces of flight vehicles due to propulsion and powered lift systems, surface flows and armament.

DD FORM 1 JAN 73 1473 EDITION OF 1 NOV 65 IS OBSOLETE

UNCLASSIFIED
SECURITY CLASSIFICATION OF THIS PAGE (When Data Entered)

060100

FOREWORD

This report was prepared by Bolt Beranek and Newman Inc., Cambridge, Massachusetts, for the Structural Integrity Branch, Strucutral Mechanics Division, Air Force Flight Dynamics Laboratory, Wright-Patterson Air Force Base, Ohio under Contract F33615-75-C-3017. The work described herein is a part of the Air Force System Command continuing program to establish methods of predicting and controlling the aero-acoustic environment of flight vehicles. The work was directed under Project 1471, "Aero-Acoustic Problems in Flight Vehicles, Task 147102 Aero-Acoustics." Messrs. Robert Gordon and Davey L. Smith of AFFDL/FBE served as Air Force Project Engineers. Their cooperation is gratefully acknowledged.

The work presented herein was performed by several members of the staff of Bolt Beranek and Newman Inc., under the technical direction of Dr. Eric E. Ungar, who also was responsible for integration and presentation of the results. Dr. John Wilby and Mr. B. Pinkel contributed the portions dealing with jet noise, and Dr. A. Galaitsis provided the part addressing fan/compressor noise. Mr. Richard Hayden prepared the part pertaining to powered lift devices, Mr. Joseph Smullin contributed the section dealing with propeller noise, and Mr. Robert White developed the portion concerned with armament. Dr. Donald Bliss contributed the sections dealing with surface flows and cavity noise.

This report summarizes information which served as the basis for "A Guide for Estimation of Aeroacoustic Loadings on Flight Vehicle Surfaces," AFFDL-TR-76-91, Vol. I.

This report concludes the work on Contract F33651-75-C-3017, which covered a period from January 1975 to October 1976. The manuscript was released by the authors in October 1976.

TABLE OF CONTENTS

TABLE OF CONTENTS (Cont.)

LIST OF FIGURES

LIST OF FIGURES *(Cont.)*

LIST OF FIGURES *(Cont.)*

LIST OF FIGURES *(Cont.)*

LIST OF FIGURES *(Cont.)*

LIST OF TABLES

SECTION I
INTRODUCTION

1.1 Background, Objective and Scope

The fluctuating pressures that act on the surfaces of flight vehicles due to propulsion systems, surface flows and armament tend to induce oscillatory motions of these surfaces. These motions can induce structural fatigue, result in degradation of equipment performance, and produce acoustic noise inside the aircraft - and this noise, in turn, can have adverse effects on the crew and on sensitive equipment. In order to avoid these problems, the designers of aircraft must take account of the fluctuating pressures and their potential effects early in the design/development cycle, usually long before prototype test data are available.

It is the purpose of this report to provide the aircraft designer with a compilation of the best available methods for predicting the salient parameters of the fluctuating pressure fields, in a form in which this information can be applied readily by nonspecialists in aeroacoustics. However, the user of this report is assumed to have a basic understanding of the fundamental definitions and concepts of acoustics.

The prediction methods presented in this report were selected on the basis of extensive review and evaluation of alternative techniques, and in some cases represent extensions, clarifications and simplifications of earlier methods. Although all methods presented here are believed to reflect the best available information, in some cases the state of the art is such that even the best methods are of uncertain validity. Discussions of the background and limitations of the estimation

methods included in the present report appear in a companion volume, together with reviews of alternative methods. However, where such discussions are brief and/or necessary for the proper use of the recommended estimation techniques, these discussions are included here.

SECTION II
CHARACTERIZATION OF AEROACOUSTIC LOADS

Complete characterization of the pressure field on an aircraft surface requires description of both its temporal and its spatial variations. Such complete characterization is rarely possible in practice, because most pressure fields exhibit complex - usually, random - variations with space and time. Thus, one usually has to settle for some rather limited descriptions of the average properties of the pressure fields of interest.

For most practical purposes, one may simplify the analysis and representation of pressure fields acting on aircraft surfaces by considering these fields to be statistically stationary - i.e., to have statistical properties that essentially do not vary with time for the particular time-interval of interest. (Or, conversely, one can usually select meaningful time intervals - typically, several seconds or longer - for which the pressure fields of interest can be considered statistically stationary.)

Additional simplifications may be obtained by assuming that the temporal statistics of the pressure field vary slowly (or not at all) with the spatial coordinates. This assumption and that of stationarity in essence permit one to consider the spatial and temporal variations separately.

2.1 Time and Frequency Characterization of Pressure At a Point

The most obvious way of representing the variation of the pressure p at a point is in terms of the corresponding time-function p(t). Clearly, this representation tends to be at the very least extremely complicated in most practical cases. The extent to which the function p(t) repeats itself in a time

interval τ is revealed by the autocorrelation function $R(\tau)$, defined by

$$R(\tau) = \lim_{T\to\infty} \left[\frac{1}{T} \int_{-T/2}^{T/2} p(t)\, p(t+\tau)\, dt \right] , \tag{1}$$

and this function provides a simple and meaningful representation of the pressure variation.

For $\tau = 0$ one finds that $R = R(0)$ here represents the time-average value of the square of the pressure. Thus, the values of $R(\tau)$ show how closely the mean-square value of the pressure is approached for delay intervals τ.

Instead of representing $p(t)$ in terms of the distribution of periods (repetition time intervals), one may represent it in terms of its frequency components. This may be done by use of the Fourier integral $P(\omega)$, which is defined by*

$$P(\omega) = \frac{1}{2\pi} \int_{-\infty}^{\infty} p(t) e^{i\omega t}\, dt , \tag{2}$$

where $\omega = 2\pi f$ represents the radian frequency. For most For most practical applications, however, it is preferable to deal with the real quantity

$$S(\omega) = |P(\omega)|^2, \tag{3}$$

which is called the spectral density, and which is a real function and thus discards tne phase information inherent in the complex function $P(\omega)$.

---

* Note that other definitions of the Fourier integral, differing from the present one by a factor of π or 2π, are also often used in the literature.

For a pressure p(t) that is sampled only for a (long) time interval T_0 and that is assumed to vanish outside that time interval, Parseval's theorem indicates that

$$\frac{\pi}{2}\int_{-\infty}^{\infty} S(\omega)\, d\omega = \pi \int_{0}^{\infty} S(\omega)\, d\omega = T_0\, \overline{p^2} \qquad (4)$$

where

$$\overline{p^2} = \frac{1}{T_0}\int_{0}^{T_0} p^2(t)\, dt \qquad (5)$$

represents the mean-square pressure.* One may thus interpret $\pi\, S(\omega)/T_0$ as representing the contribution to the mean-square pressure at the radian frequency ω. Similarly, one may interpret

$$\frac{\pi}{T_0}\int_{\omega_1}^{\omega_2} S(\omega)\, d\omega = \frac{2\pi^2}{T_0}\int_{f_1}^{f_2} S(f)\, df = \int_{f_1}^{f_2} s(f)\, df = p^2_{\Delta f}\ , \qquad (6)$$

as representing the contribution to $\overline{p^2}$ made in the frequency interval between ω_1 and ω_2 (or between $f_1 = \omega_1/2\pi$ and $f_2 = \omega_2/2\pi$).

The function $s(f) = 2\pi^2\, S(f)/T_0$ has the dimensions of (pressure)^2/Hz and represents the contribution of $\overline{p^2}$ per Hz made at the frequency f. This function is often called the "power spectral

---

*It is of interest to note that here the spectral density and the autocorrelation function are a Fourier transform pair:

$$R(\tau) = \frac{2\pi}{T_0}\int_{-\infty}^{\infty} S(\omega)\, e^{-i\omega\tau}\, d\omega$$

$$\frac{2\pi}{T_0}\, S(\omega) = \frac{1}{2\pi}\int_{-\infty}^{\infty} R(\tau)\, e^{-i\omega\tau}\, d\tau$$

density" (PSD) of the pressure. The spectrum level L_s is defined as

$$L_s = 10 \log [L_3 \cdot (1.0 \text{ Hz})/p_{ref}^2] \quad , \text{ dB} \tag{7}$$

where p_{ref} represents a reference pressure.*

The sound pressure level L_p in the band between frequencies f_1 and f_2 is defined as

$$L_p = 10 \log [\overline{p_{\Delta f}^2}/p_{ref}^2] \quad , \text{ dB} \tag{8}$$

It is common practice to present data in terms of the sound pressure levels in contiguous standard octave or one-third octave bands; a corresponding plot of L_p versus the band center frequency is called a sound pressure level spectrum.

2.2 Spatial Characterization of Pressure Distributions

At any given instant, the pressure on a surface may be represented as a function of p(x,y) of two spatial coordinates measured along the surface. Again, complete specification of p(x,y) is generally difficult. Therefore one usually employs a spatial autocorrelation function to display the content of spatial periodicities, in complete analogy to the time autocorrelation function of Eq. (1):

$$R(\eta,\xi) = \lim_{X,Y\to\infty} \left[\frac{1}{XY} \int_{-Y/2}^{Y/2} \int_{-X/2}^{X/2} p(x,y)\, p(x+\eta,\, y+\xi)\, dx\, dy \right] . \tag{9}$$

Although R here in general may depend on the location (x,y), as well as on the intervals η and ξ, it has been assumed here that the pressure field is statistically homogeneous, so that R is independent of x,y.

* The standard value of p_{ref} is $2\times10^{-5} N/m^2 \approx 2.90\times10^{-9}$ psi. Note that here and everywhere in this report all logarithms are to the base 10.

For $\eta = \xi = 0$, one finds that R (0,0) represents the spatial average of $p^2(x,y)$. Thus, the values of $R(\eta, \xi)$ indicate how close R remains to the spatial mean-square pressure values for various separation distances η, ξ; that is, $R(\eta, \xi)$ displays the spatial coherence of the pressure field.

In complete analogy to what is done in the time and frequency domains, one can also form spatial Fourier transforms and define spatial spectral densities and spectra. (The spatial analog of the frequency f is $1/\lambda$, where λ denotes the wavelength; the spatial analog of the radian frequency ω is the wavenumber $\kappa = 2\pi/\lambda$.) Because these functions are only rarely known in practical applications, and because they are relatively difficult to use for structural response estimation, they are not discussed further here.

2.3 Combined Frequency and Spatial Characterization

One can readily generalize the foregoing discussions so as to arrive at representations that apply to the time (or frequency) and space domains simultaneously. For example, one may combine Equations (1) and (9) into a single space-time autocorrelation function that involves a triple integral, and one may develop corresponding space-time spectra. Again, these representations are only of limited use for practical estimation purposes and will therefore not be belabored here.

For most practical purposes it is convenient to present pressure estimates in the form of frequency-band spectra (applicable to selected locations) and corresponding spatial correlations – the latter separately for each frequency band, if necessary. Most practical spatial correlations (in a given frequency band) may be approximated by exponential functions of the form

$$R(\eta, \xi) = C \exp[-a(\eta/\ell_x)^b] \cdot \exp[-h(\xi/\ell_y)^k] \qquad (10)$$

where C, a, b, h, k, ℓ_x and ℓ_y are positive constants. Typically a, h = ½ and b, k = 2. Note that for $\eta << \ell_x$ the value of the first exponential is near unity, whereas for $\eta >> \ell_x$ that value is very small; thus ℓ_x, which is called the correlation length in the x-direction, indicates over what spatial extent in that direction the pressure remains coherent. An analogous statement applies for ℓ_y.

The form of Equation (10) implies that the correlation is separable in the x and y directions. This is often the case, but not always. However, in most practical circumstances, an equation of the form of that of Equation (10) applies in relation to a suitably chosen (e.g., polar) coordinate system.

The spatial correlation function is often given in terms of the corresponding correlation coefficient $\rho(\eta,\xi)$, which is defined as

$$\rho(\eta,\xi) = \frac{R(\eta,\xi)}{R(0,0)} = \frac{R(\eta,\xi)}{p^2} \qquad (11)$$

2.4 List of Symbols for Sec. II

Symbol	Definition	Units*	
C	constant	---	---
L_p	sound pressure level	---	---
L_s	spectrum level	---	---
P(ω)	Fourier integral	lb in^{-2}sec	($Nm^{-2}s$)
R	autocorrelation function	lb^2in^{-4}	(N^2m^{-4})
S(ω)	spectral density	$lb^2in^{-4}sec^2$	($N^2m^{-4}s^2$)
T	period	sec	s
a,b	constants	---	---
f	frequency	sec^{-1}	(s^{-1})
h,k	constants	in^{-1}	(m^{-1})
l_x,l_y	correlation lengths	in	(m)
p	pressure	lb in^{-2}	(N m^{-2})
p_{ref}	reference pressure	lb in^{-2}	(N m^{-2})
$\overline{p^2}$	mean square pressure	lb^2in^{-4}	(N^2m^{-4})
s(f)	power spectral density	$lb^2in^{-4}sec$	($N^2m^{-4}s$)
t	time	sec	s
x,y	coordinates	in	(m)
η,ξ	spatial separations	in	(m)
κ	wavenumber	in^{-1}	(m^{-1})
λ	wavelength	in	(m)
ρ	correlation coefficient	---	---
τ	time interval	sec	s
ω	radian frequency	sec^{-1}	(s^{-1})

*SI units are given in parentheses where appropriate.

SECTION III
USE OF PREDICTION GUIDE

3.1 Predominant Sources and Combinations of Sources

Which source makes the greatest contribution to the fluctuating pressure field at a given point on an aircraft surface at a given instant generally depends on the aircraft configuration and on its instantaneous operating characteristics (including its propulsion parameters and flight regime).

In many practical instances, it is intuitively obvious which sources make significant and which make insignificant contributions. For example, propeller noise obviously is significant at points on a fuselage near the edge of the propeller disk, thrust reverser noise is likely to dominate at locations near a thrust reverser, and gun blast may be expected to make significant contributions at positions near the nozzle; on the other hand, boundary layer turbulence is likely to have an insignificant effect where the flow is smooth, and the mechanical (casing) noise of an engine usually will be overwhelmed by contributions from other sources, except perhaps very near the engine.

However, quite often one may not be able to select intuitively the sources that do or do not make major contributions. Although a strong source near the observation point clearly may be expected to predominate, the effects of a strong source that is far from the point of interest may be comparable to those of a weaker source that is nearer. Where the situation is not clear, one needs to develop estimates for all potentially significant contributions from all sources.

In applying this prediction guide to a given aircraft, one needs to consider one set of operating conditions at a time. For this set of conditions and for each aircraft surface location of interest, one needs to evaluate the noise/fluctuating-pressure contributions made by each source. These contributions may be determined for one source at a time, using the procedures given in the later sections of this report, and using the considerations of Paragraph 3.2 to account for the effects of reflections from the ground and from aircraft surfaces. The contributions from all sources may then be combined as indicated in Paragraph 3.3.

3.2 Effects of Reflections

3.2.1 Reflection at the receiving surface

Sound waves that impinge on a surface give rise to reflected waves. The pressures associated with these reflected waves combine with those associated with the incoming wave, so that the pressures that act at a given point on a structural surface generally are higher than those experienced at the same point in the freefield, i.e., if no structural surface were present.

For plane waves impinging on a rigid flat surface, the pressure on the surface increases by 6 dB over the free-field value. The increase is between 0 and 6 dB for non-rigid surfaces, depending on the surface's impedance and on the angle of incidence of the wave. However, increases of up to 9 dB can occur at intersections of two planes (due to multiple reflection), such as at the junction of an aircraft's horizontal stabilizer and fuselage.

Source Far From Nearly Flat Receiving Surface

If the separation distance s between the source and the receiving surface exceeds 10 λ, where λ denotes the acoustic wavelength at the frequency of interest, and if also the radius of curvature of the receiving surface exceeds 10 λ, then take the pressure at the receiving surface as 6 dB higher than the freefield value.

Source Near Flat or Curved Receiving Surface

For a source that is within 10 λ of the receiving surface* that is, for s< 10 λ - find the increase ΔL_{pr} in the sound pressure level due to reflection at the receiving surface from

$$\Delta L_{pr} = 20 \log \left[\frac{3 + \cos 2\alpha}{2} \right] \qquad (12)$$

where, as shown in Figure 3.1, α denotes the angle between the direction of sound propagation and the normal to the receiving surface at the point of interest.

Source Far From Cylindrical Receiving Surface

For a source that is more than 10 λ from a cylindrical receiving surface - or for jets whose centerlines are more than 10 jet diameters from the receiving surface, find the increase ΔL_{pr} in the sound pressure level at the receiving point due to reflection from

$$\Delta L_{pr} = 10 \log \left(r^2 + A^2 \right) \qquad (13)$$

---

* or, in the case of a jet, for jets whose centerlines are within 10 jet diameters from the surface

where

$$\Gamma = D_o(EG - FH)$$

$$\Lambda = D_o(FG + EH)$$

$$D_o = \frac{4}{\pi \kappa r \cos\beta}$$

$$E = \sum_{m=o}^{\infty} \frac{\cos m}{C_m} \sin\left(-\gamma_m + \frac{\pi m}{2}\right)$$

$$F = \sum_{m=o}^{\infty} \frac{\cos m\psi}{C_m} \cos\left(-\gamma_m + \frac{\pi m}{2}\right)$$

$$G = \cos(\kappa x \sin\beta)$$

$$H = \sin(\kappa x \sin\beta) \qquad (14)$$

$$C_o = 2\left[J_1^2(\kappa r_c \cos\beta) + N_1^2(\kappa r_c \cos\beta)\right]^{\frac{1}{2}}$$

$$C_m = \frac{1}{2}\left[\left\{J_{m+1}(\kappa r_c \cos\beta) - J_{m-1}(\kappa r_c \cos\beta)\right\}^2 + \left\{N_{m-1}(\kappa r_c \cos\beta) - N_{m+1}(\kappa r_c \cos\beta)\right\}^2\right]^{\frac{1}{2}}$$

$$\gamma_o = \tan^{-1}\left[\frac{-J_1(\kappa r_c \cos\beta)}{N_1(\kappa r_c \cos\beta)}\right]$$

$$\gamma_m = \tan^{-1}\left[\frac{J_{m+1}(\kappa r_c \cos\beta) - J_{m-1}(\kappa r_c \cos\beta)}{N_{m-1}(\kappa r_c \cos\beta) - N_{m+1}(\kappa r_c \cos\beta)}\right]$$

and where J and N are Bessel functions of the first and second kind, respectively, with r_c denoting the radius of the cylinder and $\kappa = 2\pi/\lambda$ the wavenumber of the sound at the frequency of interest, the angles ψ and β are defined in Fig. 6.

3.2.2 Reflections from ground and other surfaces

A reflecting surface located in the vicinity of a source and receiver directs toward the receiver some of the sound that would propagate elsewhere if no reflecting surface were present. Thus, a reflecting surface generally serves to increase the pressure that reaches the receiver due to a given source.*

The pressure increase resulting from a reflecting surface depends on the geometry of the source, receiver and reflector, and also on the acoustical impedance of the reflector. For most ground and structural surfaces it is adequate to assume this impedance to be infinite.

To estimate the pressure increase resulting from a reflecting surface, proceed as follows:

(a) Approximate that surface by a plane in the vicinity of the source and receiver.

(b) Refer to Figure 3 and determine the distances H_1 and H_2 of the source and receiver points from the reflecting plane. Also determine the length $L = \overline{P'S'}$.

(c) Find the increase ΔL_{ps} in the sound pressure level at the receiving point due to reflection from the surface under consideration from

$$\Delta L_{ps} = 10 \log \left[\frac{2}{1 + A} \right] \tag{15}$$

where

$$A_H = \frac{2H_1H_2}{L^2 + H_1^2 + H_2^2} \tag{16}$$

* For pure tones, the reflected component may be out of phase with the direct component, resulting in a decrease in the net amplitude. For uncorrelated and/or broad-band noise, such "destructive interference" is less important and the relations presented in this section may be used for upper-bound estimates.

(d) If more than one reflecting surface is present, follow steps (a) and (b) for each. Calculate A for each from Equation (16) and find the total increase in the sound pressure level due to all reflecting surfaces from

$$\Delta L_{ps} = 10 \log \left[1 + \sum \frac{1 - A}{1 + A} \right] \qquad (17)$$

where the summation extends over all reflecting surfaces considered.

3.3 Combination of Pressures

3.3.1 Mean-square pressures

The mean-square pressure $\overline{p}^2$ due to the simultaneous presence of components with individual mean-square pressures $\overline{p}_1^2$, $\overline{p}_2^2$, $\overline{p}_3^2$, ... is found from*

$$\overline{p}^2 = \overline{p}_1^2 + \overline{p}_2^2 + \overline{p}_3^2 + \ldots \qquad (18)$$

*Strictly, this expression holds only if the various components are uncorrelated - that is, if the (long-duration) time-averages of all products of pairs of the pressure signals vanish, i.e., if

$$\frac{1}{T}\int_0^T p_1(t)p_2(t)\,dt = \frac{1}{T}\int_0^T p_2(t)p_3(t)\,dt =$$

$$= \frac{1}{T}\int_0^T p_1(t)p_3(t) = \ldots = 0$$

For practical purposes, pressure components associated with different sources and mechanisms may be taken to be uncorrelated.

3.3.2 Sound pressure levels

Since the sound pressure level L_1 associated with a fluctuating pressure component to which corresponds the mean-square pressure $\overline{p_1^2}$ is defined as

$$L_1 = 10 \log [\overline{p_1^2} / p_{ref}^2] , \qquad (19)$$

where p_{ref} represents a constant reference pressure, the sound pressure level L_p associated with the total mean-square pressure $\overline{p^2}$ of equation [18] may be found from

$$L_p = 10 \log [\overline{p^2}/p_{ref}^2]$$

$$= 10 \log [10^{L_1/10} + 10^{L_2/10} + 10^{L_3/10} + \ldots]. \qquad (20)$$

3.4 List of Symbols for Sec. III

Symbol	Definition	Units*
A_H	function defined by Eq. (16)	---
B	Bessel function of second kind	---
C_0, C_m, C	function defined in Eq. (14)	---
E,F,G,H	functions defined in Eq. (14)	---
H_1, H_2	distances from reflecting plane (see Fig. 3)	in (m)
J	Bessel function of first kind	---
L	length	in (m)
r_c	radius of cylinder	in (m)
Γ, Λ	functions defined by Eq. (14)	---
ΔL_p	increase in sound pressure level due to reflection	dB
α	angle (see Fig. 1)	rad
β	angle (see Fig. 2)	rad
γ_0, γ_m	function defined in Eqs.(14)	---
ψ	angle (see Fig. 2)	rad

*SI units are given in parentheses where appropriate.

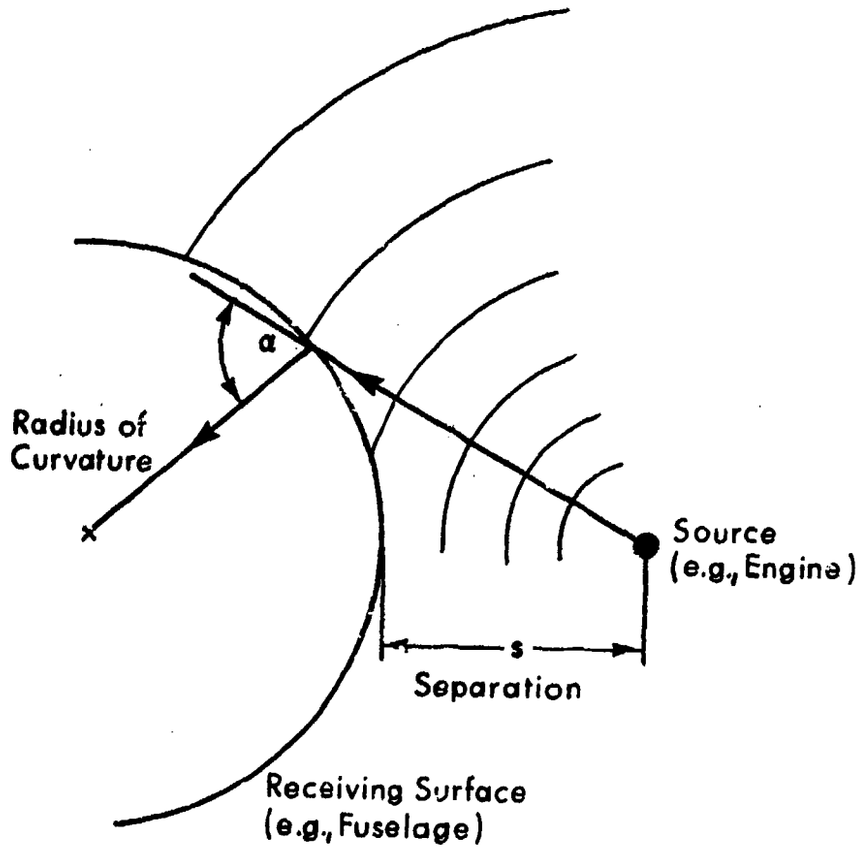

FIG. 1. GEOMETRY OF SOURCE NEAR RECEIVING SURFACE.

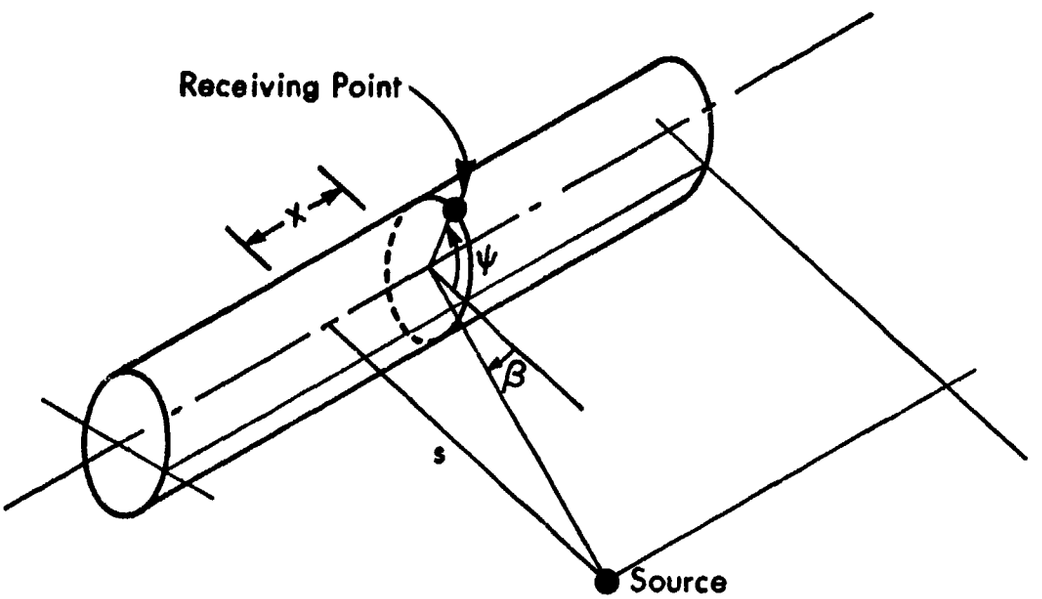

Note: β is in Plane Containing Cylinder Axis and Source Point

FIG. 2. GEOMETRY OF SOURCE FAR FROM CYLINDRICAL RECEIVING SURFACE.

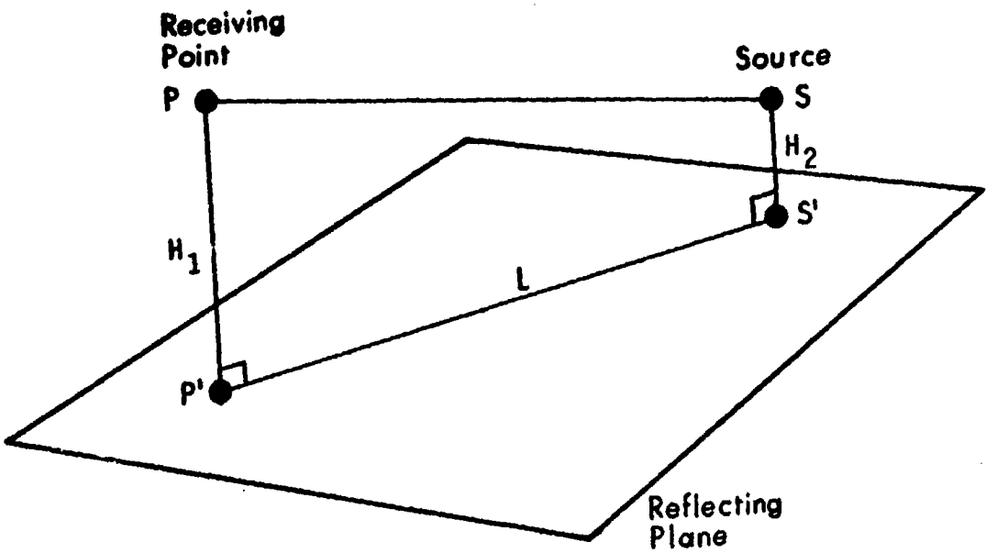

FIG. 3. GEOMETRY OF SOURCE AND RECEIVER LOCATION WITH RESPECT TO REFLECTING PLANE

SECTION IV
JET ENGINE NOISE

4.1 General

The noise associated with a jet engine consists primarily of components due to the jet stream and due to the fan and compressor.

Paragraph 4.2 deals with noise due to undeflected jets of various configurations. Deflected jets, such as are encountered in powered lift devices, are treated in Sec. V. The noise due to thrust reversers is treated in Paragraph 4.4.

Paragraph 4.3 addresses the nearfield noise of fans and compressors.

4.2 Jet Noise

4.2.1 Free-field noise on stationary aircraft

The sound pressure levels applicable to the free-field pertain to observation points that are remote from any reflecting surfaces. For observation points on or near surfaces, correct the results calculated for the free-field by using the procedures given in Paragraph 3.2.

Engines with Circular Nozzles

Shock-Free Flow Noise

The estimation procedures described here apply for subsonic jet flows and for supersonic jet exhausts that are free of shocks. The *same procedures apply with and without afterburning*, as long as the appropriate values of the jet parameters are used.

Overall Levels and Levels in Three Basic Octave-Bands

(1a) Refer to Figure 4 for definitions of coordinates of field point and source point and of related distances and angles.

(1b) Use Table 1 to identify the frequency bands to be considered.

(1c) For each band, determine the reduced source coordinates on the jet boundary from

$$X_o = x_o/D = a_{i,13}\, M^{\,a_{i,14}\,(T_T/1000)^{[a_{i,15} + a_{i,16}\, M]}}$$

$$Y_o = y_o/D = 0.5 + 0.131\, X_o \qquad (21)$$

using the appropriate values of $a_{i,j}$ listed in Table 2. T_T denotes the total temperature of the jet, in ^oR. Then calculate the (reduced) source/observer distance and angle from

$$R_s = [(X - X_o)^2 + (Y - Y_o)^2]^{1/2}$$

$$\theta_s = \tan^{-1}[(Y - Y_o)/(X - X_o)]. \qquad (22)$$

(1d) For each band, calculate the mean-square acoustic pressure $\bar{p}^2$ (in psi) at the observation point from

$$p^2 = \frac{C_8 C_9}{C_{10}}\, T_T^{\,1.54}\, M^4\, (1 + \cos^4\theta_s)\left[\frac{C_1}{R_s^{\,2}} + \frac{C_2}{R_s^{\,4}} + \frac{C_3}{R_s^{\,6}}\right] \qquad (23)$$

where

$$C_9 = \left[\frac{1 + \alpha^2 M^2}{\alpha^2 M^2 + \left(1 - \dfrac{M\cos\theta_s}{1 + C_6 e^{-C_7 R_s}}\right)^2}\right]^{5/2} \qquad (24)$$

TABLE 1

IDENTIFICATION OF FREQUENCY BANDS FOR JET NOISE ESTIMATION

Index i	Band	Strouhal Number $S = fD/c_o$	
		Band Center	Range
1	Overall	1.25	0.078 to 20
2	Octave	0.221	0.156 to 0.312
3	Octave	0.442	0.312 to 0.625
4	Octave	0.884	0.625 to 1.25

TABLE 2

COEFFICIENTS $a_{i,j}$ FOR JET NOISE PARAMETERS

		Index i			
		1	2	3	4
Coefficient Number j	1	0.8239	0.4176	0.32555	0.74038
	2	-1.24	-1.7269	0.2482	-3.4538
	3	-2.3019	-1.3226	-4.0206	-4.7181
	4	1.4745	1.3507	2.6807	3.2662
	5	45.759	18.932	202.88	331.55
	6	-2.1086	-3.2199	3.8424	0.53294
	7	3.3692	1.3276	10.520	9.5983
	8	-2.3864	-0.1765	-8.0248	-6.829
	9	12.808	8.4045	10.491	10.429
	10	-1.8167	-1.5494	-0.019983	0.36732
	11	-1.7894	-.16571	0.73551	0.89132
	12	1.1641	0.22007	-0.76495	-0.87600
	13	4.512	5.2846	4.5428	2.6963
	14	-0.028729	1.3015	0.20763	1.8687
	15	0.789	0.85116	0.27691	3.0174
	16	-0.51772	-0.60053	0.036298	-2.1329
	17	5.50×10^9	4.78×10^8	1.45×10^9	1.15×10^9

$$C_{10} = 1 + \frac{C_4 \, e^{-C_5\theta_s}}{1 + C_6 \, e^{-C_7 R_s/4}} \qquad (25)$$

and where C_1, C_2, C_3, C_6, and C_7 do not depend on frequency (or the index i) and are given by

$$C_1 = M^{2.34}$$

$$C_2 = 10.65\left(\frac{T_T}{T_o}\right)^{0.93}$$

$$C_3 = -15.18\left(\frac{T_T}{T_o}\right)^{1.11} M^{0.89}$$

$$C_6 = 17.5\left(\frac{T_T}{3000}\right)^{0.890(M^2-1)}$$

$$C_7 = 0.41\left(\frac{T_T}{3600}\right)^{0.566(M^2-1)} \qquad (26)$$

and T_o denotes the ambient air temperature (^oR). The parameters α^2, C_4, C_5, and C_8 do depend on the index i and are given by

$$\alpha^2 = a_{i,1} \, M^{a_{i,2}} \, (T_T/1000)^{(a_{i,3}+a_{i,4}M)}$$

$$C_4 = a_{i,5} \, M^{a_{i,6}} \, (T_T/1000)^{(a_{i,7}+a_{i,8}M)}$$

$$C_5 = a_{i,9} \, M^{a_{i,10}} (T_T/1000)^{(a_{i,11}+a_{i,12}M)}$$

$$C_8 = a_{i,17} \qquad (27)$$

where the values of the coefficients $a_{i,j}$ are given in Table 2.

(1e) For each observation point and frequency band, calculate the sound pressure level L_p (in dB, re $2 \times 10^{-5} N/m^2$)

from

$$L_p = 171 + 10 \log_{10} \overline{p^2} \tag{28}$$

Note: A computer program for evaluation of Eq. (23) is given in AFFDL-TR-67-43.*

Levels in Additional Octave Bands

For *higher frequencies* than those calculated previously;

(2a) calculate the jet-velocity-based Strouhal number S_4 for the center frequency f_4 of the band with index i=4 from

$$S_4 = \frac{f_4 D}{V_j} = 0.884 \frac{c_o}{V_j} . \tag{29}$$

(2b) Calculate the jet-velocity-based Strouhal number for any octave band with center frequency f_+ that is greater than f_4 from

$$S_+ = \frac{f_+ D}{V_j} = \frac{f_+}{f_4} S_4 \tag{30}$$

(2c) Use Figure 5 to determine the reduced sound pressure levels L_4 and L_+ that correspond to S_4 and S_+, for the measurement location of interest.

(2d) Calculate the sound pressure level in the octave band with center frequency f_+ from

$$L_p\ (f_+) = L_p\ (f_4) + L_+ - L_4 \tag{31}$$

where $L_p\ (f_4)$ is calculated from Eq. [28] for the i=4 band.

For *lower frequencies* than those calculated for the three basic octave bands,

---

* Plumblee, H.E., Ballentine, J.R., Passinos, B., "Nearfield noise analysis of aircraft propulsion system with emphasis on prediction techniques for jets," August 1967.

(2e) calculate the jet-velocity-based Strouhal number S_2 corresponding to the center frequency f_2 of the octave band with index i=2 from

$$S_2 = \frac{f_2 D}{V_j} = 0.221 \frac{c_o}{V_j} \tag{32}$$

(2f) Find the jet-velocity-based Strouhal numbers for any octave band with center frequency f_- that is less than f_2 from

$$S_- = \frac{f_- D}{V_j} = \frac{f_-}{f_2} S_2 . \tag{33}$$

(2g) Use Figure 5 to determine the reduced sound pressure levels L_2 and L_- that correspond to S_2 and S_- for the observation position of interest.

(2h) Calculate the sound pressure level in the octave band with center frequency f_- from

$$L_p\ (f_-) = L_p\ (f_2) + L_- - L_2 \tag{34}$$

where $L_p\ (f_2)$ is calculated from Eq. (28) for the i=2 band.

Shock Noise

Shocks occur in supersonic flows in convergent nozzles or in convergent-divergent nozzles operating at supersonic conditions that do not correspond to the design pressure ratio. Broadband shock noise occurs whenever shocks are present; discrete-frequency shock noise occurs infrequently and its onset generally can not be predicted reliably.

Discrete-Frequency Shock Noise

(3a) Calculate the fundamental shock noise frequency f_{S1} from

$$f_{S1} = c_o / 2D\sqrt{R_p - 1.893} \tag{35}$$

where R_p denotes the nozzle pressure ratio. (1.893 is the value of the critical pressure ratio.) Also find the frequency of the first harmonic (i.e. the second pure tone) from

$$f_{S2} = 2\, f_{S1} \tag{36}$$

(3b) Find the reference sound pressure levels Φ associated with the fundamental and first harmonic shock noise components from Figure 6.

(3c) Find the reduced axial location X_{SD} of the noise source from

$$X_{SD} = x_{SD}/D = 3.5\sqrt{PR - 1.893} \tag{37}$$

and evaluate the reduced axial distance of the observation point from the source,

$$X - X_{SD} = \frac{x - x_{SD}}{D} \tag{38}$$

Use Figure 7 to determine the adjustment values $\Delta\Phi$ applicable to the observation point of interest.

(3d) Calculate the upper-bound sound pressure levels at the observation point for the fundamental and for the first harmonic from

$$L_{p_{SD}} = \Phi + \Delta\Phi + 10 \log\left(\frac{A_n}{0.028\ ft^2}\right) + 10 \log\left(\frac{\rho_o c_o}{\rho_{SL}\, c_{SL}}\right) - 40 \log\left(\frac{y}{4D}\right) \tag{39}$$

where ρ_o and c_o denote the density and soundspeed for the ambient air and ρ_{SL} and c_{SL} denote those same parameters at standard sealevel conditions.

Broad-Band Shock Noise

For a *convergent nozzle*,

(4a) Calculate f_{S1} from Eq. (35). The presence of

shocks provides no significant increase Δ_{SB} in the sound level (over the shock-free case) for frequency bands below f_{S1}.

(4b) Determine the angle θ between the jet axis and the observation point. For $\theta \leq 45°$, take the sound-level increase Δ_{SB} as zero. For $\theta > 45°$, find Δ_{SB} from Figure 8. Find the total broadband noise by adding Δ_{SB} to each of the band values calculated for shock-free noise.

For *a convergent-divergent nozzle*, use the same procedure as for a convergent nozzle; however, take $\Delta_{SB} = 0$ if the pressure ratio is between 0.9 and 1.1 times the nozzle's design pressure ratio.

Engines with Plug Nozzles

Shock-Free Flow Noise

The estimation procedures described here apply for subsonic jet flows and for supersonic jet exhausts that are free of shocks. The *same procedures apply with and without afterburning*, as long as the appropriate values of the jet parameters are used.

Overall Levels and Levels in Three Basic Octave Bands

(a) Refer to Figure 9 for definition of the nozzle geometry.

(b) Calculate the equivalent diameter D_e and the ratio R_d of the Hydraulic diameter to the equivalent diameter from

$$D_e = 2\sqrt{h(D-h)} \qquad (40)$$

$$R_d = 2h/D_e$$

(c) Use Table 1 to identify the basic frequency bands to be considered. Here, use the equivalent Strouhal number

$$S_o = \frac{fD_e}{c_o} R_d^{0.4} \tag{41}$$

instead of that shown in the table.

(d) Proceed as in Step (1c) of 4.2.1. Note that here all actual dimensions are nondimensionalized with respect to D_e instead of D; for example, $X_o = x_o/D_e$. (This has no effect on the calculations indicated by Eqs. (21) and (22).)

(e) Calculate the mean square pressure $\overline{p}^2$ at the location of interest for each basic frequency band by following Step (1d) of 4.2.1.

(f) Find the sound pressure level at the point of interest, in each basic frequency band, from

$$L_p = 10 \log \overline{p}^2 + 3 \log [0.10 + 2h/D] + 171 \tag{42}$$

Levels in Additional Octave Bands

Proceed as the corresponding part of Section 4.2.1 for circular jets, but use $D_e R_d^{0.4}$ in place of D in Equations (29), (30), (32), and (33).

Shock Noise

Proceed as in Section 4.2.1 for circular nozzles, using Eqs. (35) - (39), but use the equivalent diameter D_e (as given by Equation (40)) in place of the nozzle diameter D.

Engines with Slot Nozzles

Shock-free flow noise

The estimation procedures described here apply for subsonic jet flows and for supersonic jet exhausts that are free of shocks. The *same procedures apply with and without afterburning*, as long as the appropriate values of the jet parameters are used.

Overall Levels and Levels in Three Basic Octave Bands

(1a) Calculate the effective diameter D_e and the diameter ratio R_d from

$$D_e = 2\sqrt{A_N/\pi}$$
$$R_d = 2\sqrt{\pi A_N}/P_N \qquad (43)$$

where A_N denotes the nozzle area and P_N its perimeter.

(1b) Using the values calculated above, evaluate the mean square pressure in the overall band and in three basic octave bands by following steps (c), (d),(e) of the section, *Engines with Plug Nozzles*. Calculate the corresponding sound pressure levels by use of Equation (28).

Levels in Additional Octave Bands

Follow the procedure described in the section, *Engines with Circular Nozzles* for circular jets, but use $D_e R_d^{0.4}$ in place of D in Equations (29), (30), (32), and (33).

Shock noise

Proceed as in Section 4.2.1 for circular nozzles, but use the equivalent diameter D_e from Equation (43) in place of the nozzle diameter D.

Engines with Coaxial Jets

See Figure 10 for the general geometry. The sound field due to two coaxial jets is calculated by estimating the contribution of each jet and combining the results.

Noise of primary jet

(1a) Calculate the (uncorrected) shock-free flow noise of the primary (central circular) jet by using the parameters for the primary jet in the procedure of Section 4.2.1 for circular jets.

(1b) Evaluate the correction term

$$\Delta L_p = 10 m_c \log \left[1 - \frac{V_{j2}}{V_{j1}} \right] \qquad (44)$$

where V_{j1} and V_{j2} are the velocities of the primary and secondary jets, respectively, and m_c is found from Figure 11. Add this correction term to the sound pressure levels obtained in step (1a), above, to obtain the sound pressure level due to shock-free flow in the primary jet.

(1c) Calculate the shock noise contribution of the primary jet by using the parameters applicable to that jet in the procedure of Section 4.2.1. Add this term to the sound pressure level from (1b), above, to obtain the total sound pressure level of the primary jet.

Noise of secondary jet

(2a) Calculate the effective parameters for the secondary jet from

$$r_w = W_2/W_1$$

$$T_{Te} = \frac{T_{T1} + r_w T_{T2}}{1 + r_w}$$

$$V_{je} = \frac{\rho_1 A_1 V_{j1}^2 + \rho_2 A_2 V_{j2}^2}{\rho_1 A_1 V_{j1} + \rho_2 A_2 V_{j2}}$$

$$D_e = D_2$$

$$M_e = \frac{V_{je}}{\left[\gamma R_g \left(T_{Te} - \frac{V_{je}^2}{2c_p}\right)\right]^{\frac{1}{2}}} \qquad (45)$$

where W_1 and W_2 denote the mass flows of the primary and secondary jets, γ represents the ratio of specific heats and R_g the gas constant appropriate to the jet exhaust.

(2b) Determine the flow noise of the secondary jet by using the above-determined parameters in the procedure of Section 4.2.1.

Combined noise of both jets

Determine the sound pressure level L_p (in a given frequency band) resulting at a given observation point by combining the sound pressure levels L_{p1} and L_{p2} resulting from the two individual jets (in the same frequency band) from

$$L_p = 10 \log \left[10^{L_{p1}/10} + 10^{L_{p2}/10} \right] \qquad (46)$$

4.2.2 Free-field noise on moving aircraft

The sound pressure levels applicable to the free-field pertain to observation points that are remote from any reflecting surfaces. For observation points near reflecting surfaces, correct the results calculated for the free-field by using the procedures given in Section 3.2

Engines with Circular Nozzles

Shock-free flow noise

The estimation procedures described here apply for subsonic jet flows and for supersonic jet exhaust flows that are free of shocks. The same procedures apply *with and without afterburner operation*, as long as the appropriate values of the jet parameters are used.

Aircraft motion changes the acoustic power radiated by the jet, introduces a shift in frequency, and changes the effective relative locations of noise sources and receivers.

Overall Levels and Levels in Three Basic Octave Bands

(1a) Refer to Figure 12 for definitions of coordinates of observation point (receiver) and source in jet. Identify the (uncorrected) frequencies to be considered by referring to Table

(1b) Calculate the effective jet Mach number from

$$M^* = M_a(1 - V_a/V_j)^{0.75} \qquad (47)$$

(1c) Use Equation (21), with M^* replacing M and with the values of $a_{i,j}$ given in Table 2, to calculate the reduced source coordinates X_o and Y_o.

(1d) Find R_s and θ_s by use of Equation (22).

(1e) Calculate the effective angle θ_s^* between the source/receiver line and the jet axis from

$$\cot \theta_s^* = \frac{1}{1-M_a^2} \left[\cot \theta_s - M_a \sqrt{1-M_a^2 + \cot^2 \theta_s} \right] \qquad (48)$$

and find the effective source/receiver distance from

$$R_s^* = (Y - Y_o) \Big/ \sin \theta_s^* \qquad (49)$$

(1f) As in steps (1d) and (1e) of Section 4.2.1, find $\overline{p}^2$ and SPL from Equations (23) - (27) and the parameter values listed in Table 2, but here using the above-calculated values of M^*, θ_s^* and R_s^* in place of the corresponding parameters without the asterisk.

(1g) Determine the corrected frequencies associated with the various bands by using Table 1, but with f replaced by

$$f^* = f (1 + M_a \cos \theta_s^*) \qquad (50)$$

Levels in Additional Octave Bands

(2a) Proceed as in corresponding part of Section 4.2.1.

(2b) Correct the frequencies associated with the bands considered by multiplying each by $(1 + M_a \cos \theta_s^*)$.

Shock noise

Shocks occur in supersonic flows in convergent nozzles or in convergent-divergent nozzles operating at supersonic conditions that do not correspond to the design pressure ratio. Broadband shock noise occurs whenever shocks are present; discrete-frequency shock noise occurs infrequently and its onset generally can not be predicted reliably.

Discrete-Frequency Shock Noise

(3a) Calculate the fundamental shock noise frequency f^*_{SL} from

$$f^*_{S1} = \frac{c_o \left[M_a + 0.625 \left(M_{jo} - M_a\right)\right] \left(1 - M_a\right)\left(1 + 0.625\, M_{jo}\right)}{1.25 \left(PR - 1.893\right)^{\frac{1}{2}} \left[1 + 0.625 \left(M_{jo} - M_a\right)\right] M_{jo}\, D} \qquad (51)$$

and calculate the frequency f^*_{S2} of the first harmonic (i.e., of the second natural frequency) of this noise from

$$f^*_{S2} = 2f^*_{S1} \qquad (52)$$

where

M_{jo} = jet Mach number relative to ambient speed of sound

M_a = airplane Mach number

(3b) Find X_{SD} from Equation (37)

(3c) Find θ_s from

$$\theta_s = \tan^{-1} \left[Y/(X - X_{SD})\right] \qquad (53)$$

(3d) Find R^*_s from

$$R^*_s = \sqrt{Y^2 + X^2_{SD}} \qquad (54)$$

(3e) Find θ^*_s from Equation (48) or Figure 13.

(3f) Calculate $[X - X_{SD}]^*$ from

$$[X - X_{SD}]^* = R_s^* \cos \theta_s^* \qquad (55)$$

and use this value in place of $X - X_D$ to find $\Delta\Phi$ from Figure 7.

(3g) Follow step (3d) of 4.2.1 to determine the sound pressure levels at the observation point due to the fundamental and first harmonic frequency components.

Broadband Shock Noise

(4a) Follow steps (3a) - (3e) as for discrete-frequency shock noise, above, but omit step (3d).

(4b) Find the amount Δ_{SB} by which the shock-free sound-pressure level is increased (in any band under consideration) due to shock noise, as follows:

For a *convergent nozzle*,

If $\theta_s^* \leq 45°$ and/or the frequency f of interest is lower than f_{S1}^*, then $\Delta_{SB} = 0$.

If both $\theta_s^* > 45°$ and $f > f_{S1}^*$, find Δ_{SB} from Figure 8.

For a *convergent-divergent nozzle*, proceed as above, but take $\Delta_{SB} = 0$ if the pressure ratio at which the nozzle is operating is between 0.9 and 1.1 times its design pressure ratio.

(4c) Find the total broadband noise due to shock noise and shock-free noise by adding Δ_{SB} to each of the band values calculated for shock-free noise (in Section 4.2.2.).

Engines with Plug Nozzles

Shock-free flow noise

The estimation procedures described here apply for subsonic jet flows and for supersonic jet exhaust flows that are free of shocks. The same procedures apply *with and without afterburner operation*, as long as the appropriate values of the jet parameters are used.

Overall Levels and Levels in Three Basic Octave Bands

(1a) Refer to Figure 9 for definition of nozzle geometry and calculate D_e and R_d from Equations (40).

(1b) Use Equations (21), with D replaced by D_e, to determine the reduced source coordinates X_o and Y_o. Find the reduced receiver (observation point) coordinates X and Y from

$$X = x/D_e, \qquad Y = y/D_e \tag{56}$$

(1c) Follow steps (1b) - (1f) of Section 4.2.2 to determine the sound pressure levels in the various bands.

(1d) Determine the frequency associated with each of the bands considered by using Table 1, but with the Strouhal number given in that Table replaced by

$$S^* = \frac{fD_e}{c_o} R_d^{0.4} \quad (1 + M_a \cos \theta_s^*). \tag{57}$$

Levels in Additional Octave Bands

Follow the procedure of the corresponding part of Section 4.2.1, but use Equation (57) as the relation between the frequencies and Strouhal numbers instead of the simpler relations appearing in Equations (29), (30), (32), and (33).

Shock noise

Shocks occur in supersonic flows in covergent nozzles or in convergent-divergent nozzles operating at supersonic conditions that do not correspond to the design pressure ratio. Broadband shock noise occurs whenever shocks are present; discrete-frequency shock noise occurs infrequently and its onset generally can not be predicted reliably.

(2a) Calculate the equivalent diameter D_e from Equation (40).

(2b) Proceed as in Section 4.2.2 for circular nozzles, but use D_e in place of the nozzle diameter D.

Engines with Slot Nozzles

Shock-free flow noise

The estimation procedures described here apply for subsonic jet flows and for supersonic jet exhaust flows that are free of shocks. The same procedures apply *with and without afterburner operation*, as long as the appropriate values of the jet parameters are used.

Overall Levels and Levels in Three Basic Octave Bands

(a) Calculate the effective diameter D_e and the diameter ratio R_d from Equations (42).

(b) Proceed as for plug-nozzles with steps (1b) - (1d) of Section 4.2.2.

Levels in Additional Octave Bands

Follow the procedure of Section 4.2.1.1.1.2, but use Equation (57) as the relation between the frequencies and Strouhal numbers, in place of the simpler relations appearing in Equations (29), (30), (32), and (33).

Shock noise

Proceed as in Section 4.2.2 for circular nozzles, but use the effective diameter D_e, as calculated from Equation (43), in place of the nozzle diameter D.

Engines with Coaxial Jets

See Figure 9 for the general geometry. The sound field due to two coaxial jets is determined by estimating the contribution of each jet and combining the results.

Noise of primary jet

Shock-Free Flow Noise

(a) Calculate the (uncorrected) shock-free flow noise of the primary (central circular) jet by using the parameters for

the primary jet in the procedure of Section 4.2.2 for circular jets, but use $M^* = M_a$ in place of Equation (47).

(b) Evaluate the correction term ΔL_p from Equation (44) as in Step (1b) of Section 4.2.1, and add this term to the uncorrected sound pressure levels calculated in step (a), above, to obtain the sound pressure levels due to shock-free flow in the primary jet.

Shock Noise

Proceed as in Section 4.2.2 for circular jets, using the parameters for the primary jet.

Noise of secondary jet

(a) Calculate the effective parameters of this jet from Equations (45) and evaluate the corrected effective Mach number M_e^* from

$$M_e^* = M_e \left(1 - V_a/V_{je}\right)^{0.75} \qquad (58)$$

(b) Follow the procedure of Section 4.2.2, but here use T_{Te}, M_e^* and D_2 in place of T_T, M and D.

Combined noise of both jets

Proceed as in Section 4.2.1.

4.2.3 Pressure correlations

(a) Refer to Figure 14. Approximate the aircraft surface at the location of interest by a plane parallel to the jet axis.

(b) Determine the coordinates (x,y,z) of the observation point (P) of interest, noting that the z-coordinate is equal to the (perpendicular) distance from the jet axis to the aircraft surface plane and that the x and y axes are parallel to this plane.

(c) For a selected frequency of interest, determine the coordinate x_o of the effective noise source locations (S) by use of Figure 15.

For an engine with a plug nozzle, use D_e from Equation (40) in place of D in calculations pertaining to this figure. For an engine with a slot nozzle, use D_e from Equation (43) in place place of D.

For coaxial jets, treat the effects of the jets separately, using D_e and V_{je} from Equations (45) in place of D and V_j for the secondary jet and considering the primary jet as a simple circular jet.

(d) Evaluate

$$\overline{PS} = [(x-x_o)^2 + y^2 + z^2]^{\frac{1}{2}} \tag{59}$$

and

$$\alpha_1 = \frac{\omega}{c_o} \frac{x-x_o}{\overline{PS}}$$

$$\alpha_2 = \frac{\omega}{c_o} \frac{y}{\overline{PS}} \tag{60}$$

(e) Find the spatial correlation coefficient corresponding to separation distances ξ_1 and ξ_2 (in the x and y directions, respectively, in inches) and to radian frequency ω from

$$\rho(\xi_1,\xi_2,0) = \exp(-0.23\alpha_1\xi_1)\cos(\alpha_1\xi_1) \cdot \exp(-1.21\alpha_2\xi_2)\cos(4.17\alpha_2\xi_2) \tag{61}$$

(f) Repeat steps (c) through (e) for all frequencies of interest.

4.2.4 List of symbols for Sec. 4.2

Symbol	Definition	Units*
A_N	nozzle area	in.^{2} (m^2)
A_1, A_2	areas of primary and secondary jets	in.^{2} (m^2)
C_n	functions defined by Eqs. 24 – 27	
D	jet nozzle exit diameter	in. (m)
D_e	equivalent diameter	in. (m)
M	Mach number	
M_e	equivalent jet Mach number	
M_j	jet exit Mach number	
P_N	nozzle perimeter	in. (m)
R	reduced radial coordinate	
R_d	ratio of hydraulic diameter to equivalent diameter	
R_g	gas constant for jet exhaust	
R_p	nozzle pressure ratio	
R_s	reduced source/observer distance (see Figs. 4, 12)	
S	Strouhal number	
T_T	jet total temperature	°R (°K)
T_{T_e}	equivalent total temperature	°R (°K)
T_{T1}, T_{T2}	total temperatures of primary and secondary jets	°F (°K)
T_θ		
V_j	jet exit velocity	in./sec (m/s)
V_{je}	equivalent jet velocity	in./sec (m/s)

*SI units are given in parentheses where appropriate. Consistent units must be used for any given set of calculations.

Symbols	Definition	Units
V_{j1}, V_{j2}	velocities of primary and secondary jets	in./sec (m/s)
W_1, W_2	mass flows of primary and secondary jets	lb/sec (kg/s)
X,Y	reduced coordinates	
X_0, Y_0	reduced jet noise source coordinates	in. (m)
$a_{i,j}$	jet noise parameter coefficients (see Table 2)	
c_p	specific heat at constant pressure, for jet exhaust	$in.^2/sec^2$ °R (m/s^2°K)
c_{SL}	speed of sound in air at standard sea level condition	in./sec (m/s)
c_0	speed of sound in ambient air	in./sec (m/s)
f_{s1}	fundamental shock noise frequency	Hz
f_{s2}	second shock noise frequency	Hz
m_c	sound pressure level correction parameter (Eq. 44)	
r	radial coordinate	in. (m)
r_w	mass flow ratio	
x_0, y_0	jet noise source coordinates	in. (m)
ΔL_p	sound pressure level correction	dB
Δ_{SB}	increase in broadband sound pressure level	dB
$\Delta\Phi$	sound pressure level adjustment (Fig. 7)	dB
Φ	reference sound pressure level for discrete frequency shock noise	lb $in.^{-2}$ (Nm^{-2})

Symbol	Definition	Units
γ	ratio of specific heats of exhaust gas	
θ	angle between jet axis and observation point	rad
θ_s	source/observer angle (see Figs. 4, 12)	rad
ρ_{SL}	density of air at standard sea level conditions	in./sec (m/s)
ρ_0	density of ambient air	lb in.$^{-3}$ (kg m^{-3})
ρ_1, ρ_2	densities of exhaust of primary and secondary jets	lb/m^{-3} (kg m^{-3})

4.3 Fan/Compressor Noise

4.3.1 Introduction

Available Prediction Techniques

Essentially only two of the techniques available in the literature appear to be useful for estimation of fan/compressor nearfield noise [4.3.1, 4.3.2].* Both of these involve semi-empirical procedures that have been computer-programmed. Both programs require detailed geometric and aerodynamic engine descriptions as input and print out the 1/3-octave band sound pressure levels at various angular positions, at a distance of 150 or 250 ft. From these levels one may extrapolate to the nearfield by assuming a hemispherical spreading.

In the event the user plans to perform many calculations, he obviously should use the aforementioned computer programs. However, if he needs to carry out only a few computations, he would do well to make use of the procedure described here.

The approach of Burdsall *et al* [4.3.1] is preferred here, because it accounts for the fan and compressor contributions simultaneously, and thus requires much less numerical computations than the approach of Benzakein *et al* [4.3.2]. Furthermore, the computer-free version of Burdsall's approach is considerably less complicated.

Fan/Compressor Noise Mechanisms

The noise signature of a high-speed fan/compressor engine contains three main components:

---

* See Section 4.3.4 for references.

(1) broad-band noise,

(2) pure tones at the blade passage frequency and its harmonics

(3) multiple pure tones or combination tones resulting from the interaction of the blade passage frequency with the engine shaft frequency.

The broad-band noise extends over a wide range of the spectrum, contains no sharp predominant peaks, and is random in character. It is radiated from both inlet and fan discharge, and it is generated by (a) unsteady forces on the blades due to random fluctuations in the boundary layer and the flow, (b) random inflow turbulence interacting with the blade row, and (c) air scrubbing action over the blade, vane and duct wall surfaces.

The blade passage frequency corresponds to the product of the fan blade number and the fan rotational speed (in Hz). Noise at this frequency (and its harmonics) is generated by (a) the interaction of a wake produced by a rotor (or stator) stage with the next stator (rotor) stage, and (b) the pressure fields generated by the blades themselves.

The third type of noise is known by several names, such as combination tone noise, buzz-saw noise, supersonic tip-speed noise, or multiple pure-tone noise. Indeed, these names are quite descriptive of the spectral composition and the generating mechanisms. This type of noise is due to inaccuracies (manufacturing tolerances) in the blade shapes, which result in shock waves of dissimilar shapes and strengths. This noise consists of components at the shaft rotational frequency, its harmonics and its combination tones with the blade-pass-frequency, and it is radiated only from the inlet.

Limitation of Recommended Prediction Procedure

The recommended prediction procedure is based on a semi-empirical scheme that uses relations obtained by curve-fitting to experimental data in absence of suitable theoretical expressions. The actual noise-generation processes are highly complex and are under continuing study. Thus, the entire procedure is approximate; although results have been favorable in several test cases, this scheme does not provide highly accurate answers, and its output must be considered only as a guide or a rough estimate, even for farfield noise.

The computed farfield noise levels (the method of Reference [4.3.1] gives the sound pressure levels at 150 ft) need to be interpreted to yield the nearfield levels. This is done here by extrapolation, assuming hemispherical spreading. Although this rather aggressive assumption undoubtedly will result in some discrepancies, the farfield prediction scheme incorporates other approximations of similar weight; therefore, the hemispherical spreading assumption is likely not to be a damaging one. Furthermore, in many cases the locations (e.g., on the fuselage) at which the sound pressures are to be determined will be in the acoustic farfield of the engine (that is, several wavelengths away), although being geometrically near, so that this assumption may not be as restricting as may appear at first glance.

4.3.2 Overview of prediction procedure

The steps involved in the procedure may be visualized with the aid of the flow diagram of Figure 16, which shows the nine computational actions as nine blocks.

The notation used here is identical to that of Ref. [4.3.1.] in order to facilitate cross-referencing with it.

and the computer program included in it.

Block b1 refers to input of all the geometrical (fan diameter, bypass ratio, etc.) and performance parameters (engine speed, etc.) needed in the noise prediction. In block b2; these input parameters are used to calculate additional parameters.

In block b3 the broadband noise power (BBN) is calculated and distributed over 24 one-third octave bands (from 50 Hz to 10 kHz), with an appropriate directivity pattern. In block b4 are calculated similarly the contributions at the blade passage frequency (BPF) and at its second harmonic (BPF2) that occur in each 1/3-octave band, at each angular position.

In block b5, it is determined whether there is any contribution from the multiple pure tones (MPT). There is no such contribution if the relative tip Mach number MTIP is less than or equal to unity. Otherwise, the MPT contribution is calculated in block b6. Block b7 ensures that the acoustic energy accounted for by the BPF and BPF2 component is not included again through the MPT calculation.

The effects of the three noise sources are added (and checked) in blocks b8 and b9 to produce the total fan/compressor noise.

4.3.3 Calculation procedure

Input and Preliminary Parameters

(a) Determine the values of the input parameters [block b1] that must be available for the prediction scheme. These parameters (and the units used in the present procedure) are listed in

Table 3.

The first column of this table shows the symbols used in the subsequent calculations. The last three columns indicate which input quantities are needed for each of the three types of noise.

(b) Evaluate the additional parameters [block b2], as follows:

$$
\begin{aligned}
\text{THETA} &= (\text{TT2} + 459.688)/518.688 \\
\text{DELTA} &= \text{PT2}/29.92, \\
\text{SPAFC} &= \text{SPAF}\,\frac{\sqrt{\text{THETA}}}{\text{DELTA}}\,, \\
\text{XMXAVE} &= 1 - \sqrt{0.9708126 - 0.0196508.5 \cdot \text{SPAFC}}\,, \\
\text{RPMC} &= \text{RPM}/\sqrt{\text{THETA}}\,, \\
\text{AREA} &= \pi \cdot \text{DIAT}^2/4\,, \\
\text{TAU} &= \pi \cdot \text{DIAT}/\text{B}\,, \\
\text{E1} &= \text{RPM}/60.0\,, \\
\text{BPF} &= \text{B} \cdot \text{E1}\,, \\
\text{XMTIP} &= \frac{\pi \cdot \text{DIAT} \cdot \text{RPMC}}{60 \cdot 12 \cdot 1117}\,, \\
\text{XMREL} &= \sqrt{\text{XMXTIP}^2 + \text{XMTIP}^2}
\end{aligned}
\qquad (62)
$$

The meaning of these parameters, together with the associated units used here, are given in Section 4.3.5.

TABLE 3. INPUT PARAMETERS FOR FAN/COMPRESSOR NOISE PREDICTION.

Name	Description	Units	Broadband	Discrete Tone	Combination Tone
DIAT	fan tip diameter	inches	X	X	X
DIAH	fan hub diameter	inches			X
B	number of blades	--	X	X	X
NV	number of vanes	--		X	
BPR	by-pass ratio	--	X		
GAP	rotor/stator spacing	inches		X	
CHORD	blade tip chord	inches	X	X	
DDDXT	fan tip diameter gradient	--			X
DDDXH	fan hub diameter gradient	--			X
RS	blade suction surface radius of curvature	inches			X
SIGPHI = σ_ϕ	standard deviation of blade tip metal angle	radians			X
DL	inlet duct length	feet		X	
PPR	radius to observer	feet	X	X	X
RPM	fan speed	rpm	X	X	X
SPAP	specific airflo rate	lb/sec/ft^2	X	X	X
XMXTIP	tip axial Mach number	--			X
PR	fan pressure ratio	--		X	
DF	diffusion factor	--	X		
TT2	ambient inlet temperature	°F	X	X	X
PT2	ambient inlet pressure	in Hg		X	X
C	speed of sound	in/sec			

Broadband Noise [Block b3]

Calculate broadband noise contribution BBN (I,J) at each angular location (indicated by I) and in each one-third octave band (indicated by the value of J)*, by taking the steps indicated below.

*The angular locations θ_I are measured from the engine centerline. Ten degree intervals are taken for θ_I between 10° and 150°, and $I = \theta_I$ (degrees)/10. The one-third octave bands are coded as shown in Table 4.

TABLE 4. CODING OF ANGULAR POSITION AND FREQUENCY-BAND INDICES I AND J FOR FAN/COMPRESSOR NOISE PREDICTION.

Index I	Angle Θ_I (deg)
1	10
2	20
3	30
4	40
5	50
6	60
7	70
8	80
9	90
10	100
11	110
12	120
13	130
14	140
15	150

Index J	1/3-OB Center Frequency (Hz)
1	50
2	63
3	80
4	100
5	125
6	160
7	200
8	250
9	315
10	400
11	500
12	630
13	800
14	1000
15	1250
16	1600
17	2000
18	2500
19	3150
20	4000
21	5000
22	6300
23	8000
24	10,000

(a) Calculate FSTAR, the index number of the band that contains a critical frequency that influences the directivity indices, by using

$$F1 = \frac{1}{2}\left[1 - \tanh\left(\frac{XMREL - 0.95}{2}\right)\right],$$

$$F2 = \frac{1}{2}\left\{1 - \tanh[15(XMREL - 0.95)]\right\},$$

$$FSTAR = 10 \cdot F2 \cdot \log_{10}\left[\frac{50 \cdot CHORD}{c \cdot XMREL}\ MAX\left(\sqrt{|1 - XMREL^2|},\ 0.5\right)\right] + 10(1 - F2)\left[\log_{10}\left(\frac{DIAT}{24}\right) - 21\right], \qquad (63)$$

(b) Find the overall sound pressure level $OLSPL_{60}$ at the 60° angular position from

$$OLSPL_{60} = TABLE\ (DF, XMREL) + 20 \log_{10}\left(\frac{DIAT}{52}\right) - 20 \log_{10}\left(\frac{FFR}{150}\right) + \left[10 \log_{10}\left(\frac{BPR}{BPR + 1}\Big/.833\right)\right] \sigma_0(90°) \qquad (64)$$

where

$$\sigma_0(90°) = \begin{cases} 0 \text{ for } \theta \leq 90° \\ 1 \text{ for } \theta > 90° \end{cases} \qquad (65)$$

applies a bypass ratio correction to the aft-end angles where the values of the function TABLE (DF, XMREL) are given by Table 5.

(c) Calculate the overall sound pressure level $OLSPL_I$ at angular positions other than 60° from

$$OLSPL_I = OLSPL_{60} + F1 \cdot D_{sub} + (1-F1) \cdot D_{sup} \qquad (66)$$

where F1 is given by Eq. (63). The subsonic and supersonic directivity corrections D_{sub}, D_{sup} are given by Fig. 17. (The subscript I here corresponds to Table 4, as before.)

TABLE 5. VALUES OF THE FUNCTION: TABLE (DF, XMREL).

DF \ XMREL	0.70	0.75	0.80	0.85	0.90	0.95	1.00	1.05	1.10	1.15	1.20	1.25	1.30	1.35	1.40
.28	87.2	88.4	89.5	90.6	91.6	92.6	93.7	94.8	96.0	96.9	97.9	98.7	99.5	100.1	100.7
.29	87.3	88.4	89.5	90.6	91.6	92.7	93.8	94.9	96.1	97.0	98.0	98.7	99.5	100.1	100.7
.30	87.4	88.4	89.6	90.6	91.7	92.8	93.9	95.1	96.2	97.0	98.1	98.7	99.5	100.1	100.7
.31	87.5	88.6	89.6	90.7	91.7	92.9	94.0	95.2	96.3	97.2	98.2	98.8	99.6	100.1	100.7
.32	87.6	88.7	89.8	90.8	91.8	93.0	94.1	95.3	96.4	97.3	98.3	99.0	99.6	100.2	100.8
.33	87.9	88.9	89.9	91.0	92.0	93.2	94.2	95.5	96.6	97.5	98.4	99.1	99.6	100.2	100.8
.34	88.1	89.2	90.2	91.3	92.2	93.5	94.5	95.6	96.8	97.7	98.6	99.2	99.7	100.3	100.9
.35	88.5	89.5	90.5	91.6	92.5	93.6	94.7	95.8	97.0	97.9	98.7	99.4	99.9	100.4	101.1
.36	88.9	89.9	90.9	92.0	92.8	93.9	95.0	96.1	97.2	98.1	98.9	99.6	100.0	100.6	101.3
.37	89.3	90.3	91.4	92.4	93.2	94.3	95.3	96.4	97.5	98.4	99.2	99.8	100.3	100.9	101.5
.38	89.7	90.8	92.0	92.9	93.8	94.8	95.7	96.8	97.8	98.7	99.5	100.0	100.5	101.2	101.8
.39	90.3	91.4	92.7	93.5	94.4	95.3	96.2	97.3	98.2	99.1	99.8	100.4	101.0	101.5	102.1
.40	90.9	92.0	93.2	94.1	95.0	95.9	96.8	97.8	98.7	99.5	100.2	100.8	101.4	102.0	102.5
.41	91.5	92.6	93.8	94.8	95.7	96.5	97.4	98.4	99.3	100.0	100.7	101.3	102.0	102.5	102.9
.42	92.0	93.1	94.3	95.3	96.4	97.2	98.0	98.9	99.8	100.5	101.3	101.9	102.5	103.0	103.3
.43	92.4	93.6	94.8	95.8	97.1	97.8	98.6	99.5	100.3	101.1	101.9	102.4	103.9	103.4	103.8
.44	92.8	94.0	95.3	96.4	97.7	98.4	99.2	100.1	101.0	101.7	102.4	103.0	103.5	103.8	104.2
.45	93.1	94.4	95.8	96.9	98.3	98.9	99.8	100.6	101.5	102.2	102.9	103.4	104.0	104.3	104.6
.46	93.4	94.6	96.2	97.2	98.7	99.4	100.2	101.0	101.9	102.7	103.4	103.9	104.4	104.7	105.0
.47	93.5	94.9	96.5	97.8	99.1	99.8	100.6	101.5	102.3	103.1	103.7	104.2	104.7	105.0	105.2
.48	93.6	95.1	96.8	98.2	99.4	100.2	101.0	101.8	102.7	103.4	104.1	104.5	105.0	105.3	105.2
.49	93.6	95.3	97.0	98.3	99.6	100.5	101.4	102.1	103.0	103.7	104.4	104.8	105.3	105.5	105.7
.50	93.7	95.4	97.2	98.4	99.9	100.8	101.7	102.4	103.3	104.0	104.7	105.1	105.5	105.7	105.9
.51	93.9	95.6	97.3	98.6	100.0	101.0	101.9	102.6	103.6	104.3	105.0	105.3	105.7	105.9	106.1
.52	94.1	95.8	97.4	98.7	100.1	101.1	102.1	102.8	103.8	104.5	105.2	105.6	105.9	106.1	106.3
.53	94.2	95.9	97.4	98.8	100.2	101.2	102.3	103.0	104.1	104.7	105.4	105.8	106.0	106.2	106.4
.54	94.4	96.0	97.5	98.9	100.3	101.4	102.4	103.3	104.4	105.0	105.6	105.9	106.2	106.4	106.5
.55	94.6	96.1	97.5	98.9	100.3	101.4	102.5	103.6	104.5	105.2	105.8	106.0	106.3	106.5	106.6
.56	94.7	96.2	97.6	98.9	100.4	101.5	102.6	103.7	104.7	105.3	106.0	106.2	106.4	106.6	106.7

(d) Determine from each overall level $OLSPL_I$ the one-third octave band levels by using

$$BBN(I,J) \begin{cases} OASPL_I - 10.7 + J & \text{, for } J \leq FSTAR \\ OASPL_I - 10.7 + J - 1.6(FSTAR + J - 1) & \text{, for } J > FSTAR \end{cases} \quad (67)$$

where FSTAR is given by Eq. (63).

Discrete Tone Noise [Block 64]

(a) Calculate ξ_{RF}, the cutoff ratio of the rotor field, from

$$XMSTAR = 1.0 + 0.84 \cdot B^{-2/3},$$

$$RF = \frac{XMTIP}{XMSTAR} \frac{1}{\sqrt{1 - XMXAVE^2}} \quad (68)$$

(b) Find the forward and aft radiated power levels PWL1F and PWL1R corresponding to the fundamental blade-passage frequency from the curves of Fig. 18.

(c) Calculate NCOR as the integer value nearest that given by

$$NCOR_o = 1 + (\xi_{RF}/0.91) \quad (69)$$

and find CORF from

$$CORF = \begin{cases} 3.3, \text{ for} & NCOR = 1 \\ 7.5, \text{ for} & NCOR = 2 \\ 6.8, \text{ for} & NCOR = 3 \end{cases} \quad (70)$$

Then evaluate the forward-radiated power level PWL2F at the second harmonic from

$$PWL2F = PWL1F - CORF \tag{71}$$

(d) Calculate CORR from

$$CORR = \begin{cases} 3.2, & \text{for NCOR} = 1 \\ 3.5, & \text{for NCOR} = 2 \\ 2.5, & \text{for NCOR} = 3 \end{cases} \tag{72}$$

and find the aft-radiated power PWL2R at the second harmonic from

$$PWL2R = PWL1R - CORR \tag{73}$$

(e) Find the mean sound pressure levels SPLMF and SPLMR in the forward and aft quadrants, at the observer distance, at the blade-passage frequency, from

$$\begin{aligned} SPLMF &= PWL1F - 20 \log_{10}(FFR) + 5.55 \\ SPLMR &= PWL1R - 20 \log_{10}(FFR) + 5.55 \end{aligned} \tag{74}$$

(f) Find the sound pressure level SPL1 at the blade-passage frequency, at specific angular locations, from

$$SPL1 = \begin{cases} SPLMF + \Delta 1, & \text{for } 0<\theta<90^\circ,\ \xi_{RF} \geq 1.05 \\ SPLMF + \Delta 2, & \text{for } 0<\theta<90^\circ,\ \xi_{RF} \leq 1.05 \\ SPLMF + \Delta 3, & \text{for } 90<\theta<180^\circ \end{cases} \tag{75}$$

where $\Delta 1$, $\Delta 2$ and $\Delta 3$ are given in Fig. 19.

(g) Find the sound pressure levels SPL2 associated with the second harmonic from

$$SPL2\ (\theta) = SPL1(\theta) - CORF \qquad (76)$$

where CORF is given by Eq. (70).

(h) For $\theta = 90°$, select the larger of the two values of SPL1 calculated from Eq. (75), and also choose the larger of the two values of SPL2.

(i) Record all SPL1 and SPL2 values at the various angles and locations in a table (matrix) of values relabeled BPN (I,J), corresponding to the indexes given in Table 4.

COMBINATION TONE NOISE [Blocks 66, 67]

No combination tones arise if XMREL < 1; in that case, no further computation is needed. For XMREL > 1, proceed as described here.

(a) Evaluate the auxiliary parameters, given below.

$$\mu = \tan^{-1}\left(\frac{1}{XMREL}\right),$$

$$\beta^* = \tan^{-1}\left(\frac{XMXTIP}{XMTIP}\right),$$

$$RF = \left(\frac{1}{2\cos\beta^*}\right)\left(\frac{(1 - XMXTIP^2)\cdot XMREL^2}{\left(1 + \frac{XMXTIP^2}{5}\right) XMXTIP \cdot XMTIP}\right)\left(\frac{DIAT^2 - DIAH^2}{DIAT \cdot DDDXT + DIAH\ DDDXH}\right)$$

$$RS' = \frac{RS \cdot RF}{RF - RS}, \text{ for } RF \neq RS,$$

$$\alpha = \frac{RS'}{\tau}\left[\frac{\sin\mu}{\sin(\mu - \beta^*)}\right],$$

$$\theta_a = 13.5\,\alpha^{-0.8575} \text{ (degrees)} \qquad (77)$$

$$\alpha' = \frac{RS'}{\tau}\left[\frac{\sin(\mu + \theta_a)}{\sin(\mu - \beta^*)}\right],$$

$$\theta_e = 2\tan^{-1}\left[\frac{-\sin\mu + \sqrt{(\sin\mu)^2 + \frac{\tau}{RS'}\sin(\mu-\beta^*)\left[2\cos\mu - \frac{\tau}{RS'}\sin(\mu-\beta^*)\right]}}{2\cos\mu - \frac{\tau}{RS'}\sin(\mu-\beta^*)}\right]$$

$$\psi_1 = \frac{\theta_a}{\sqrt{2}\,\sigma_\phi}$$

$$\psi_2 = \frac{\theta_e - \theta_a}{\sqrt{2}\,\sigma_\phi}$$

$$\eta = \frac{1 + \mathrm{erf}(\psi_2)}{2}$$

$$\sigma_\varepsilon^2 = 2n\alpha'^2 \left\{ \sigma_\phi^2 + 2\sqrt{\frac{2}{\pi}}\,\sigma_\phi^3 \left[(\psi_1^2 + 2^{1.5}\sigma_\phi\,\psi_1 + (2\sigma_\phi)^2 e^{-\psi_1^2}) - (\psi_2^2 + 2^{1.5}\sigma_\phi\,\psi_2 + (2\sigma_\phi)^2 e^{-\psi_2^2}) \right] \right\}$$

$$\xi_c = 1 - 0.1\, e^{23.0259\,(1-\mathrm{XMREL})}$$

The meanings of these parameters are indicated in Sec. 4.3.5.

(b) Calculate the overall power level OLPWL of the combination tones from

$$\mathrm{OLPWL} = 189.16 + 727.24\ \mathrm{XMREL} - 488.93\ \mathrm{XMREL}^2 + 107.69\ \mathrm{XMREL}^3 + 10\log_{10}(\mathrm{AREA}/144) - 20\log_{10}(n\cdot B)\ , \tag{78}$$

(c) Determine the 1/3 octave band power levels PWL(K) from*

$$\mathrm{PWL}(K) = 170.8 + 10\log_{10}\mathrm{PRMS} \tag{79}$$

*Here K is the index designating the band; it is the same as the index J of Table 4.

where

$$PRMS = \frac{1+\sigma_a^2 + (B\delta-1)\exp[-(2Q\sigma_\varepsilon)^2]}{8Q^3K\,[1-\cos(2Q)+Q]\,[1-(\sin 2Q)/Q]} \tag{80}$$

$$\delta = \begin{cases} 0, & \text{for } K \neq B \\ 1, & \text{for } K = B \end{cases} \tag{81}$$

(d) Calculate the cutoff ratio ξ_K for each band from

$$\xi_K = \frac{XMTIP}{XMSTAR} \cdot \frac{1}{\sqrt{1 - XMXAVE^2}} \tag{82}$$

where

$$XMSTAR = 1 + 0.84\ K^{-2/3}, \tag{83}$$

and find ξ_K/ξ_c, where ξ_c is given by Eq. (77).

For those tones for which $\xi_K/\xi_c < 1$, set the sound pressure equal to zero.

(e) Calculate the average sound pressure level $\overline{SPL}_K$ at the appropriate distance, for each 1/3 octave band, from

$$\overline{SPL}_K = PWL_K - 20\log_{10}(FFR) - 3.85 \tag{84}$$

(f) Find the sound pressure level $SPL_{K,\theta}$, in each 1/3 octave band at each angular location θ, from

$$SPL_{K,\theta} = \overline{SPL}_K + \sum_{i=0}^{5} D_{\theta i}\,(\xi_K)^i, \tag{85}$$

where the directivity coefficients $D_{\theta i}$ are obtained from Table 6 and ξ_K is given by Eq. (82).

(g) Record the $\overline{SPL}_{K,\theta}$ values calculated above in a corresponding list (matrix) of values, relabeled CTN (I,J), where the indexes I and J correspond to Table 4.

Total Noise [Blocks b8, b9]

(a) For each set of indices I and J (that is, for each angular location and frequency band), compare BPN (I,J) and CTN (I,J), and omit the lower of the two values from the calculation in the next step.

(b) Calculate the total noise TON (I,J) by summing the contribution of each mechanism in each 1/3 octave band and at each angular position, from

$$TON\ (I,J) = 10 \log_{10} \left[10^{BPN(I,J)/10} + 10^{CTN(I,J)/10} + 10^{BBN(I,J)/10} \right] \qquad (86)$$

TABLE 6. DIRECTIVITY COEFFICIENTS $D_{\theta 1}$

θ \ 1	0	.1	2	3	4	5
10°	- 475.92	1088.41	832.01	207.78	0	0
20°	- 488.88	1164.19	929.26	244.73	0	0
30°	- 491.57	1202.70	987.87	269.86	0	0
40°	14.22	7.71	2.85	0	0	0
50°	419.53	- 1046.58	867.72	238.17	0	0
60°	12.96	- 43.78	53.02	20.72	0	0
70°	- 286.74	635.16	432.44	105.71	-48.71	-26.11
80°	181.25	- 411.47	295.32	67.81	0	0
90°	1618.24	- 3933.70	3133.88	821.89	0	0
100°	4033.55	- 9869.94	7937.61	-2104.66	0	0
110°	6613.32	-16167.2	12994.70	-3443.76	0	0

4.3.4 References for Sec. 4.3

4.3.1. E.A. Burdsall *et al*, "Fan/Compressor Noise: Prediction, Research and Reduction Studies," Pratt and Whitney Aircraft, East Hartford, Connecticut, Feb. 1971.

4.3.2. M.J. Benzakein *et al*, "Fan/Compressor Noise Research," General Electric Co., Cincinnati, Ohio, Oct. 1971.

4.3.5 List of symbols for Sec. 4.3

Symbol	Definition	Units*
AREA	total inlet area	$in.^2$
B	number of blades	
BBN	broadband noise power	
BPF	blade passage frequency	Hz
BPF2	harmonic of blade passage frequency	Hz
BPR	by-pass ratio	
C	speed of sound	in./sec
CHORD	blade tip chord	in.
DDDXH	fan hub diameter gradient	
DDDXT	fan tip diameter gradient	
DELTA	ambient inlet pressure	
DF	diffusion factor	
DIAH	fan hub diameter	in.
DIAT	fan tip diameter	in.
DL	inlet duct length	ft
$D_{\theta i}$	directivity coefficients (Table 6)	
D_{sub}, D_{sup}	subsonic and supersonic directivity corrections	dB
E1	shaft rotation frequency	Hz
FFR	distance to observer	ft
FSTAR	index number of critical frequency band	
GAP	rotor/stator spacing	in.
M*	effective jet Mach number, with aircraft forward motion	

*The calculations in this section are based on use of the specific units cited here.

Symbol	Definition	Units
M_a	Mach number of aircraft	
M_e^*	corrected effective Mach number	
M_{jo}	jet Mach number relative to speed of sound in ambient air	
NV	number of vanes	
OLPWL	overall sound power level of combination tones	dB
$OLSPL_I$	overall sound pressure level at angular position with index I	dB
$OLSPL_{60}$	overall sound pressure level at 60° position	dB
PR	fan pressure ratio	
PRMS	reduces mean square sound pressure	
PT2	ambient inlet pressure	in. Hg
PWL(K)	sound power level in one-third octave band with index K	dB
PWL1F,PWL1R	forward and rearward radiated power levels of fundamental blade passage tone	dB
PWL2F,PWL2R	forward and rearward radiated power levels of harmonic of blade passage tone	dB
RF	radius of curvature of streamline	in.
RPM	fan rotational speed	rpm
RPMC	corrected fan speed	rpm
RS	blade suction surface radius of curvature	in.

Symbol	Definition	Units
RS'	effective radius of curvature of suction surface	in.
R_S^*	effective reduced source/ observer distance, with aircraft forward motion	
S*	effective Strouhal number	
SIGPHI	standard deviation of blade tip metal angle	rad
SPAF	specific air flow rate	lb/sec ft^2
SPAFC	corrected specific air flow rate	lb/sec ft^2
SPL1,SPL2	sound pressure level at blade passage frequency and harmonic	dB
$\overline{SPL}_K$	average sound pressure level in band with index K	dB
$SPL_{K,\theta}$	sound pressure level in band with index K. at angle θ	dB
SPLMF,SPLMR	mean sound pressure levels in forward and rearward gradients	dB
TABLE	sound pressure correction (Table 5)	dB
TAU	gap between blade tips	in.
THETA	see Eq. 62	
TON	total tonal noise	dB
TT2	ambient inlet temperature	°F
V_a	aircraft velocity	in./sec (m/s)
XMXAVE	mean axial Mach number	
XMREL	relative tip Mach number	
XMTIP	circumferential tip Mach number	
XMXTIP	tip axial Mach number	

Symbol	Definition	Units
f^*	frequency corrected for aircraft forward motion	Hz
f^*_{s1}	fundamental shock noise frequency, corrected for aircraft forward motion	Hz
f^*_{s2}	sound shock noise frequency, corrected for aircraft forward motion	Hz
α, α'	see Eq. 77	
α_1, α_2	pressure correlation parameters (Eq. 60)	$in.^{-1}$ (m^{-1})
β^*	air inflow angle	rad
θ_a	relative camber angle at leading edge	deg
θ_e	relative camber angle at throat	deg
η	see Eq. 77	
θ_I, θ	angular locations	deg
θ^*_s	effective source/observer angle, with aircraft forward motion	rad
μ	Mach angle	rad
ξ_K	cutoff ratio for frequency band with index K	
ξ_{RF}	cutoff ratio of rotor field	
ξ_c	critical cutoff ratio	
ξ_1, ξ_2	separation distances in x and y directions (see Fig. 14)	in. (m)
σ_0	by-pass correction	
σ_ε	standard deviation of shock spacing	in.
σ_ϕ	same as SIGPHI	deg
τ	blade tip gap	in.

4.4 Thrust Reversers

Unlike the jet exhaust noise treated in Section 4.2, thrust reverser noise is produced by interaction of a jet with a solid body. This noise thus depends on the configuration of the solid body. The two common types of thrust reversers are (1) target reversers (see Figure 20), where the entire jet impinges on a single flow-turning surface, and (2) cascade reversers, (see Figure 21), where the jet impinges on a series of vane-like surfaces.

The procedures given below deal only with the thrust reverser noise component. Note that exhaust noise is also present during thrust reverser operation. Jet exhaust noise may be estimated by the methods given in Section 4.2.

4.4.1 Target reversers

(a) Refer to Figure 20 and identify whether the reverser under consideration is of the V-gutter or of the semi-cylindrical configuration.

(b) Calculate the hydraulic diameter D_h and the equivalent diameter D_e from the exit flow area A_F and flow perimeter P_F

$$D_h = 4A_F/P_F$$

$$D_e = \sqrt{4A_F/\pi} \tag{87}$$

(c) Evaluate the reference frequency f_o from

$$f_o = \frac{V_j}{D_e(D_h/D_e)^{0.4}(T_T/T_o)^{0.4}(1+\cos\theta_i'')} \tag{88}$$

where

$$\theta_i'' = \theta_i(V_j/c_o)^{0.1} \tag{89}$$

and θ_i represents the angle between the inlet axis and a line from the inlet center to the observation point. T_T denotes the total absolute temperature of the exhaust flow and T_o the absolute temperature of the ambient air.

(d) Evaluate the terms indicated below

$$\Delta_{\rho c} = 10 \log_{10} \left(\frac{\rho_j \rho_o c_o^4}{\rho_{SL}^2 c_{SL}^4} \right)$$

$$\Delta_r = 10 \log_{10} \left\{ \frac{A_e}{r^2} \left[1 + \left(\frac{c_o}{2\pi r f_o} \right)^2 \right] \right\}$$

$$\Delta_a = 10 \log_{10} (1 + M_a \cos\theta) \qquad (90)$$

where r denotes the source-to-observer distance and ρ_{SL} and c_{SL} represent the standard sea level values of air density and soundspeed.

(e) Compute the overall sound pressure level $L_p OA_{90}$ at 90° from the primary jet axis from

$$L_p OA_{90} = K_{tr} + 10 \log_{10} \left[\frac{(V_j/c_o)^{5.5}}{1 + 0.01 (V_j/c_o)^{2.5}} \right]$$

$$- 10 \cos^2\psi \log_{10} \left(\frac{D_h}{D_e} \right) + \Delta_{\rho c} + \Delta_r + \Delta_a \qquad (91)$$

where ψ is the angle between the source to observer line and the y axis (fig 4) and

$$K_{tr} = \begin{cases} 149 \text{ for semi-cylindrical reversers} \\ 154 \text{ for V-gutter reversers} \end{cases}$$

(f) Determine the overall sound pressure level OASPL at the observation point of interest by using

$$L_p OA = L_p OA_{90} + 20 \log_{10} \left[\frac{\cos(\theta_1/3)}{\cos 30^\circ} \right] \text{dB} \qquad 92$$

where θ_1 is the angle between the jet axis and the line from the reverser inlet to the observation point.

(g) Determine the corresponding one-third octave band spectrum by use of Fig. 22.

4.4.2 Cascade reversers

(a) Refer to Figure 21. Determine the number of ports NP and the magnitudes of the dimensions defined in that figure. Ascertain whether the reverser of interest has an internal flow deflector to guide the flow into the vanes. Ascertain whether the vanes are airfoil-shaped or of constant thickness. Determine the exit area A_e of the cascade system.

(b) Calculate the hydraulic and the equivalent diameter from

$$D_e = \sqrt{4(NP)(AL)(CL)/\pi}$$

$$D_h = \frac{2(AL)(CS)}{AL + CS} \tag{93}$$

(c) Evaluate the reference frequency f_o by use of Equation (88). Calculate the modified reference frequency f_r from

$$f_r = 1.4\ f_o \tag{94}$$

(d) Evaluate the terms given by Equations (90).

(e) Compute the overall sound pressure level L_pOA_{90} at 90° from the jet axis from

$$L_pOA_{90} = K_{cr} + 10 \log_{10} \left[\frac{(V_j/c_o)^5}{1 + 0.01(V_j/c_o)^2} \right] + \Delta_r + \Delta_{pc} + \Delta_a \tag{95}$$

where

$$K_{cr} = 136 + K_1 + K_2 + 7.2\ A_e/A_t \tag{96}$$

and

$$K_1 = \begin{cases} 0 \text{ if there is an internal flow deflector} \\ 5 \text{ otherwise} \end{cases}$$

$$K_2 = \begin{cases} 0 \text{ if the vanes are airfoil-shaped} \\ 6 \text{ if the vanes are of constant thickness} \end{cases}$$

A_e = cascade exit area

A_t = tailpipe area

(f) Determine the overall sound pressure level L_pOA at the observation point of interest from

$$L_pOA = L_pOA_{90} + 20 \log \left[1 + \frac{1}{2} \sin 2\theta_i\right] \quad (97)$$

where θ_i denotes the angle between the inlet axis and a line drawn from the inlet center to the observation point.

(g) Determine the corresponding one-third octave band spectrum by use of Figure 23.

4.4.3 List of Symbols for Sec. 4.4

Symbol	Definition	Units*	
A_F	area of thrust reverser exit flows	in^2	(m^2)
AL	arc length of cascade (Fig.21)	in	(m)
A_e	exit area of cascade system	in^2	(m^2)
A_t	tailpipe area	in^2	(m^2)
CL	cascade length (Fig.21)	in	(m)
CS	cascade spacing (Fig.21)	in	(m)
D_e	equivalent diameter	in	(m)
D_h	hydraulic diameter	in	(m)
L_p	sound pressure level	dB	
M_a	aircraft Mach number		---
NP	number of ports of cascade	---	
P_F	perimeter of thrust reverser exit flows	in^2	(m^2)
V_j	jet velocity	in/sec	(m/s)
c_{SL}	soundspeed in air at standard sealevel	lb/in^3	(kg/m^3)
c_0	sound speed	in/sec	(m/s)
f	frequency	Hz	
f_r	modified reference frequency (Eq. 94)	Hz	
f_0	reference frequency (Eq. 88)	Hz	
θ_i	angle between thrust reverser inlet axis and line from inlet center to observation point	rad	
θ_i''	effective flow angle (Eq. 89)	rad	
δ_j	density of exhaust flow	lb/in^3	(kg/m^3)
δ_{SL}	density of air at standard sealevel	lb/in^3	(kg/m^3)

*SI units are given in parentheses, where appropriate consistent units must be used throughout a given set of calculations.

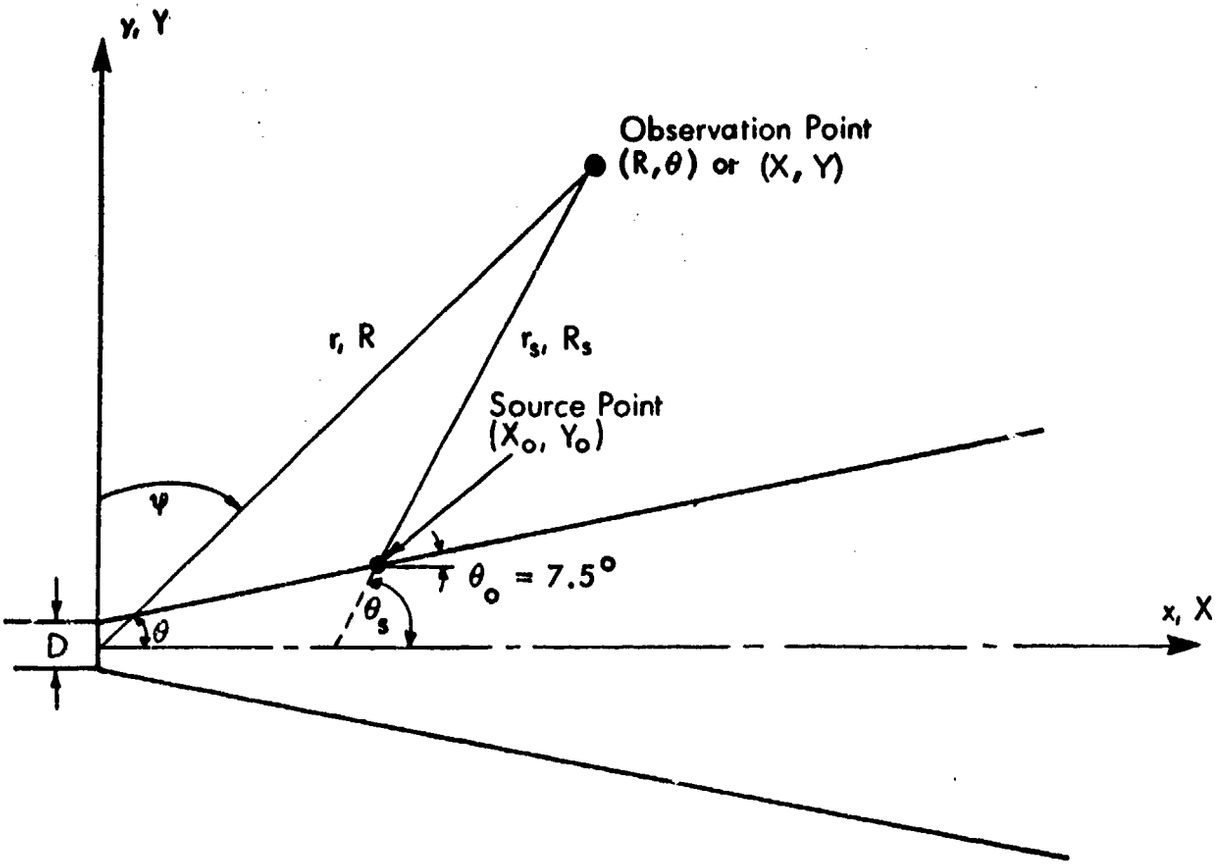

R = r/D ;
X = x/D
Y = y/D

FIG. 4. GEOMETRY FOR JET NOISE PREDICTION

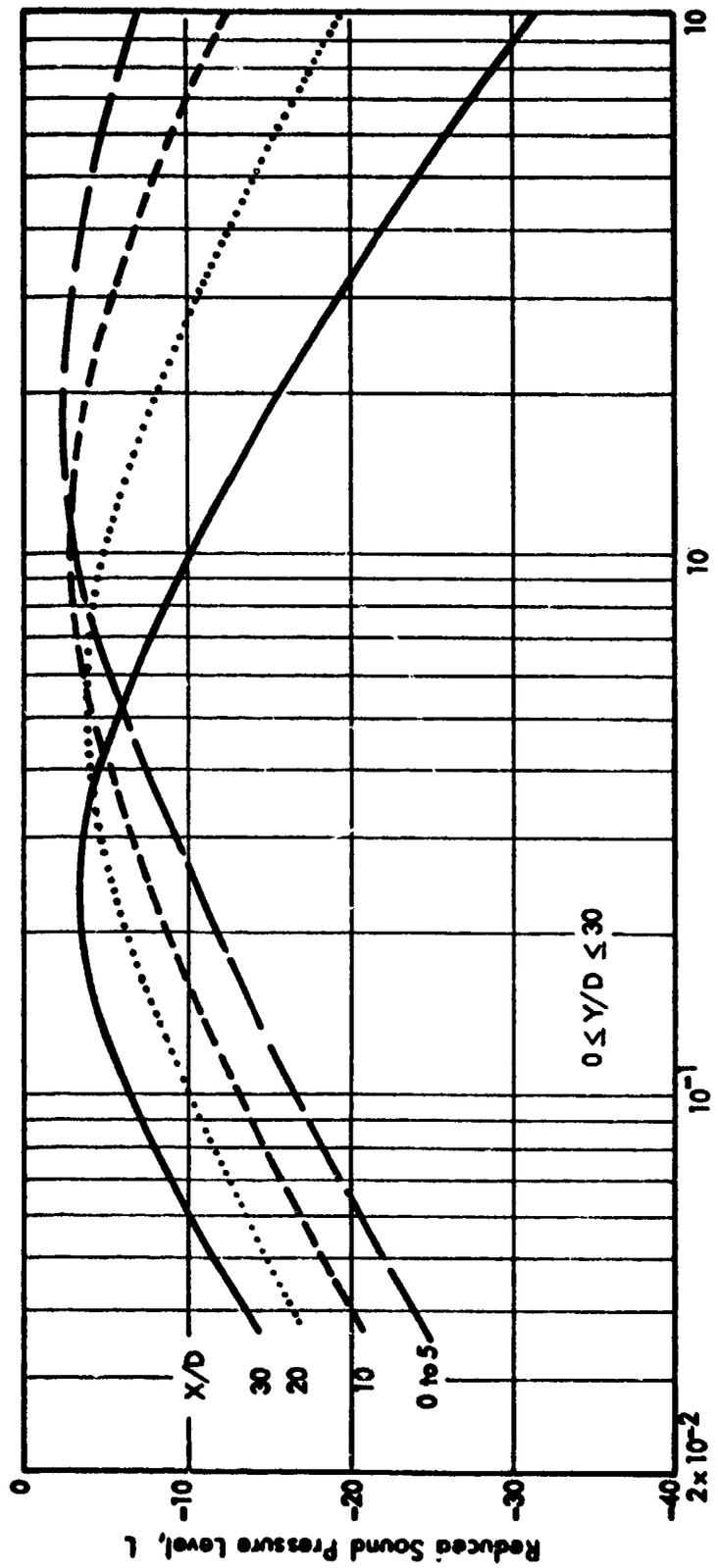

FIG. 5. REDUCED SPECTRA FOR NEARFIELD JET NOISE.

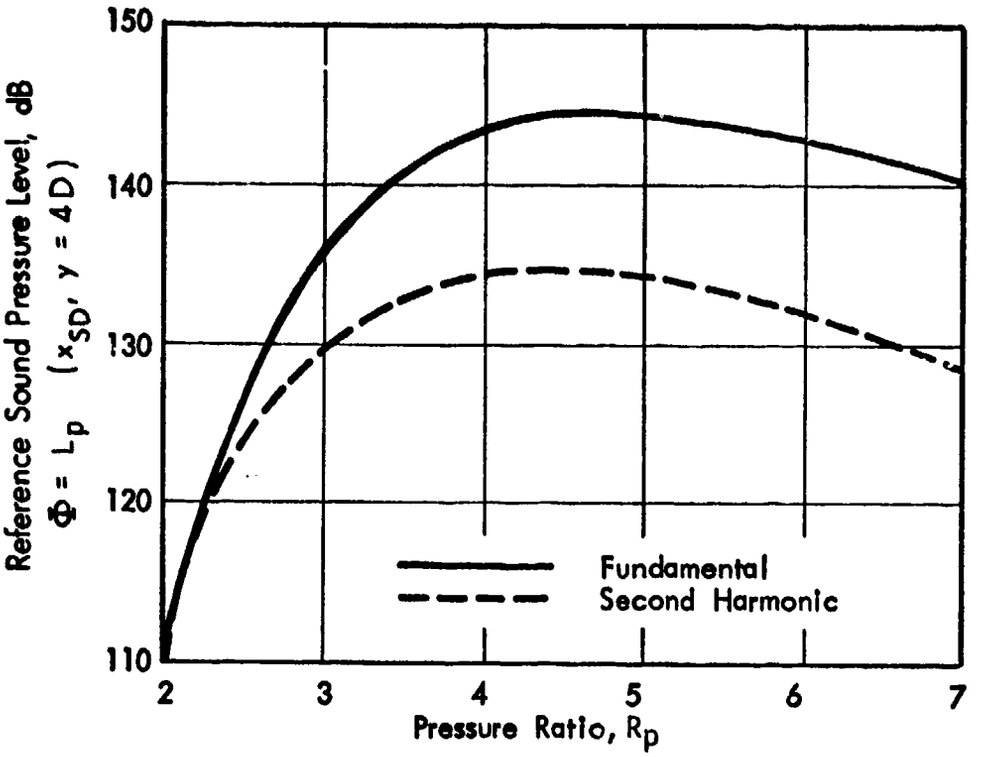

FIG. 6. REFERENCE SOUND PRESSURE LEVEL FOR DISCRETE FREQUENCY SHOCK NOISE.

(a) FUNDAMENTAL FREQUENCY

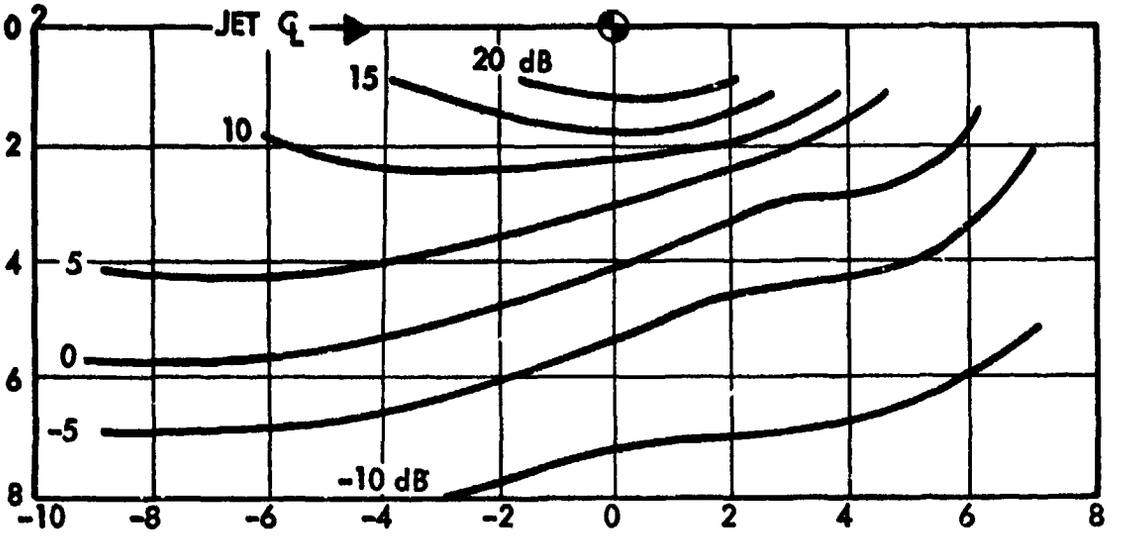

Note: numbers on curves show sound pressure level adjustment $\Delta\Phi$ to be used in Eq. [39].

(b) SECOND HARMONIC

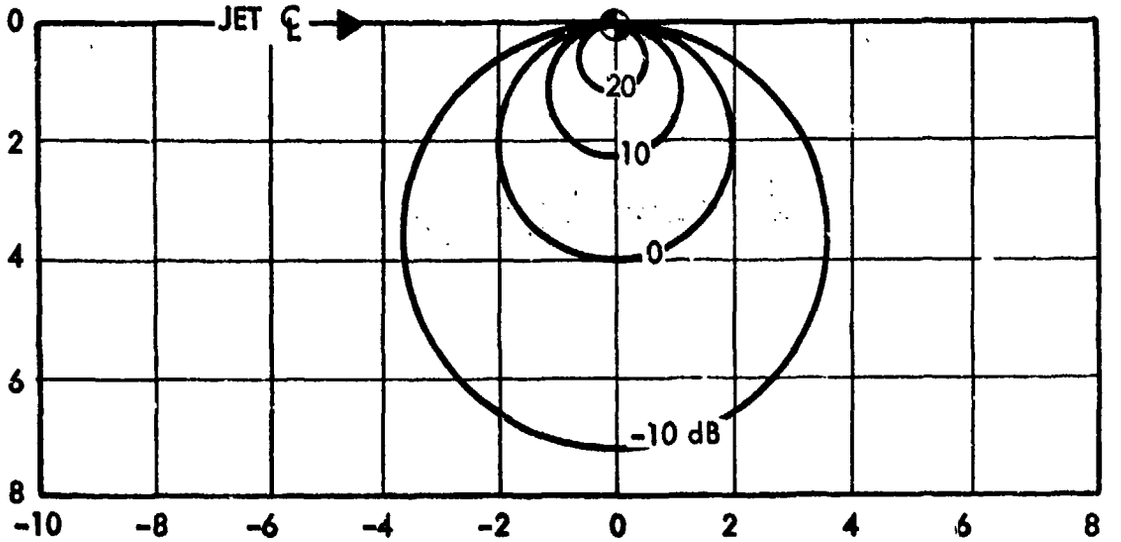

Reduced Radial Distance of Observation Point from Jet Centerline, $Y = y/D$

Reduced Axial Distance of Observation Point from Effective Source Location

$$X - X_{SD} = \frac{x - x_{SD}}{D}$$

FIG. 7. DIRECTIVITY PATTERNS FOR DISCRETE-FREQUENCY SHOCK NOISE.

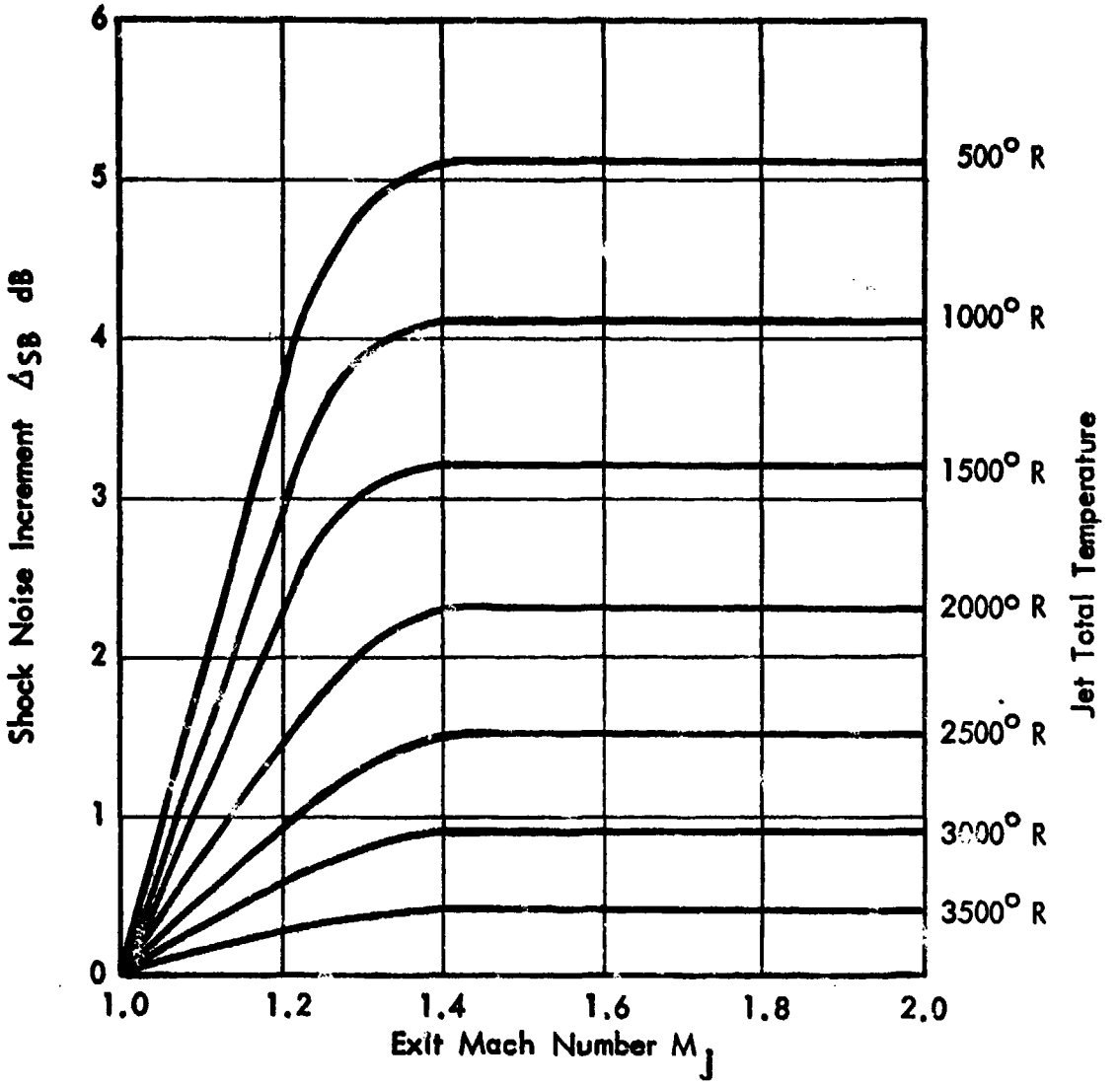

FIG. 8. INCREASE IN JET NOISE DUE TO BROADBAND SHOCK NOISE.

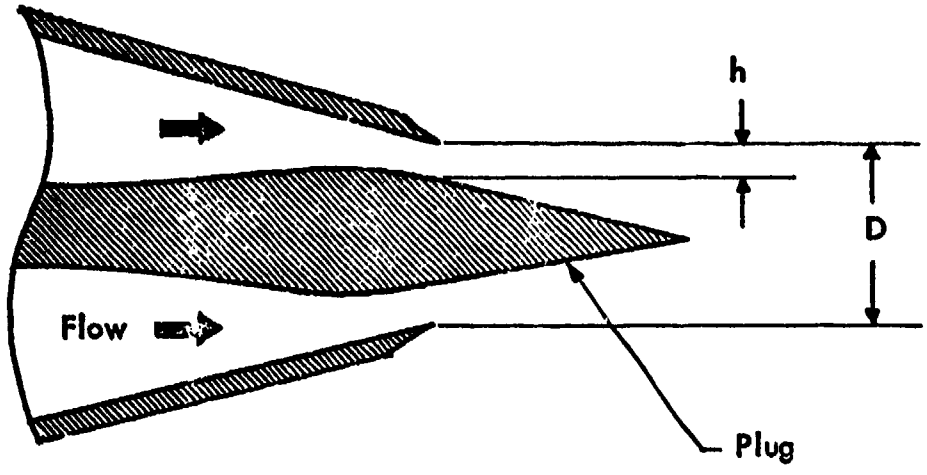

FIG. 9. PLUG NOZZLE GEOMETRY

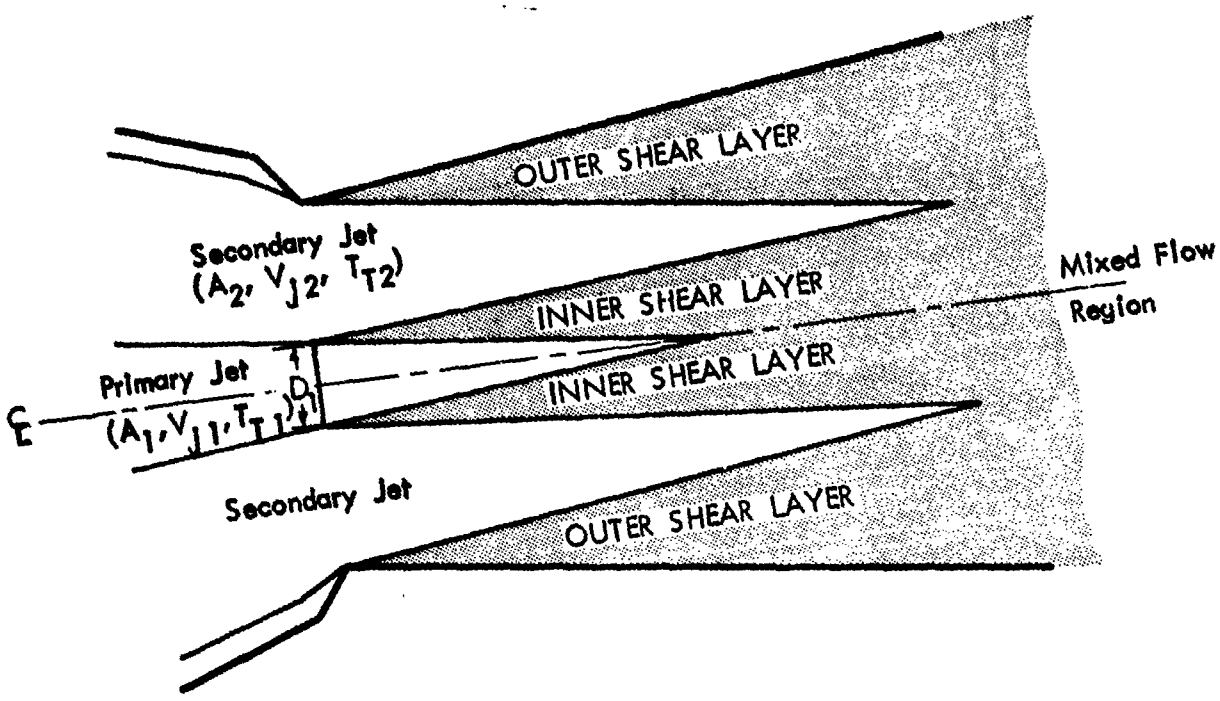

FIG. 10. SCHEMATIC SKETCH OF NOISE SOURCE REGIONS FOR CO-ANNULAR JETS.

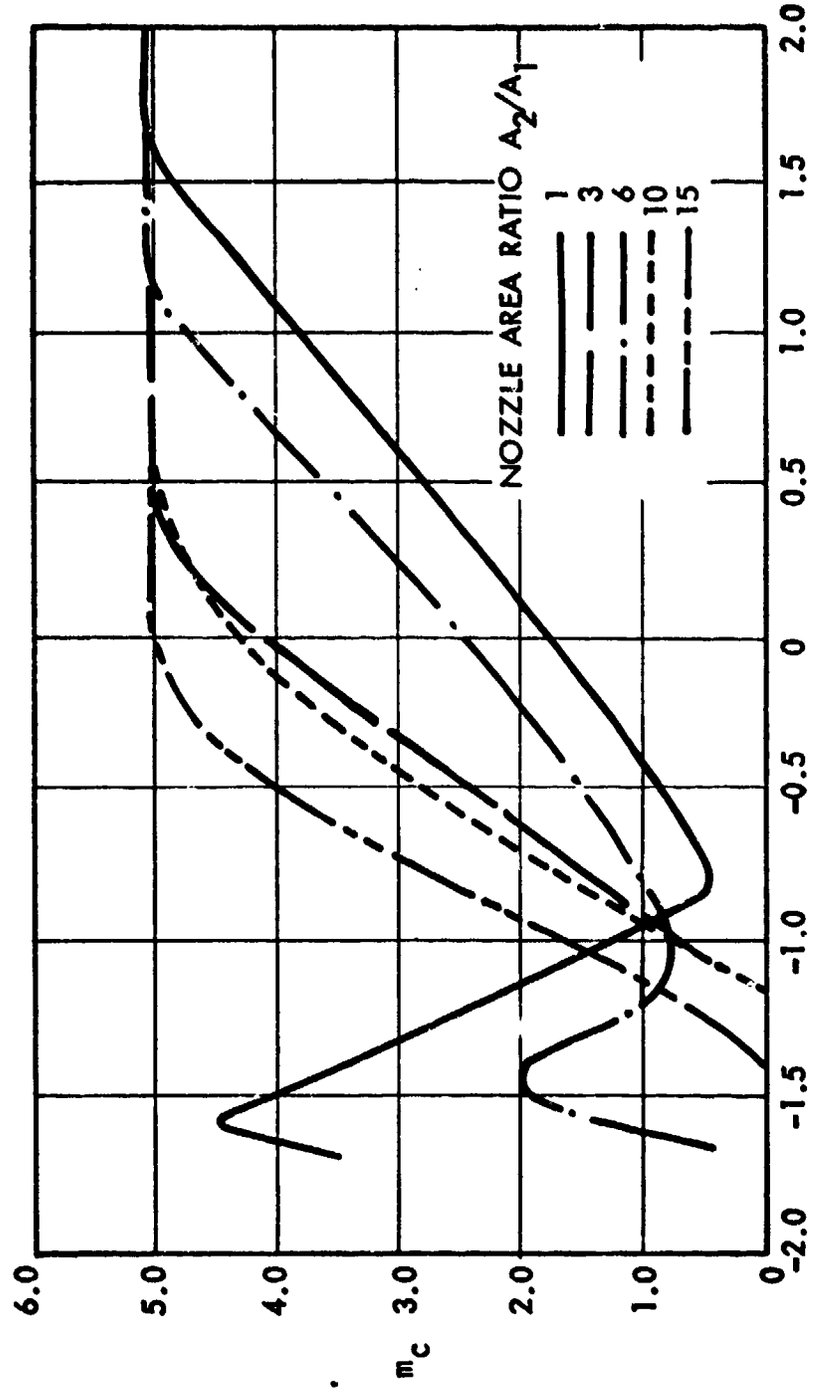

FIG. 11. PARAMETER m_c FOR CORRECTION TERM FOR NOISE OF PRIMARY JET OF TWO COAXIAL JETS

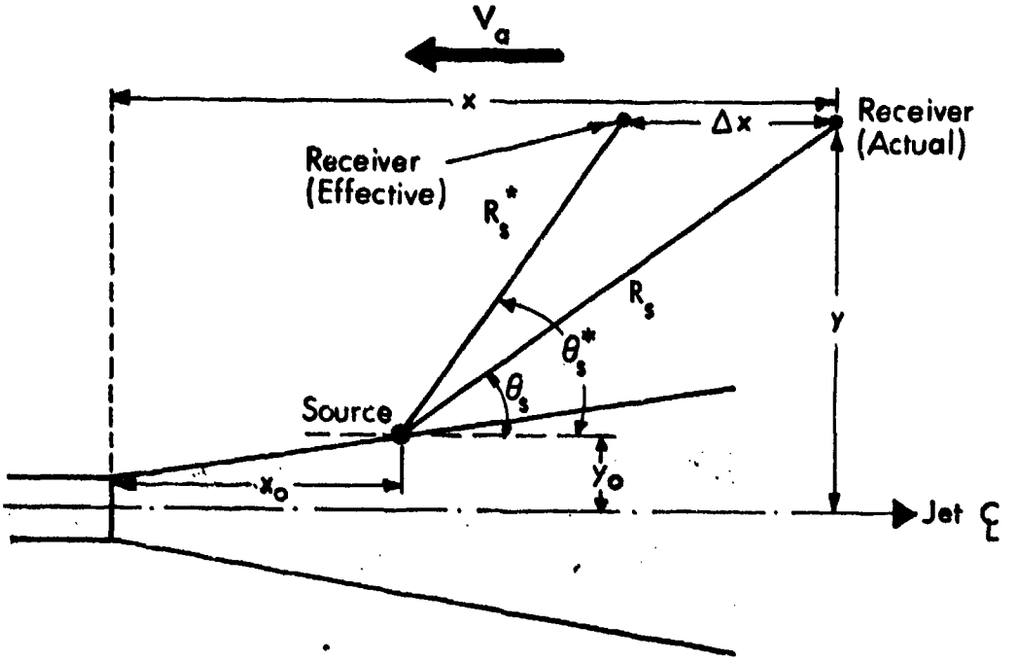

FIG. 12. GEOMETRIC RELATION BETWEEN RECEIVER AND SOURCE, WITH FORWARD MOTION OF AIRCRAFT.

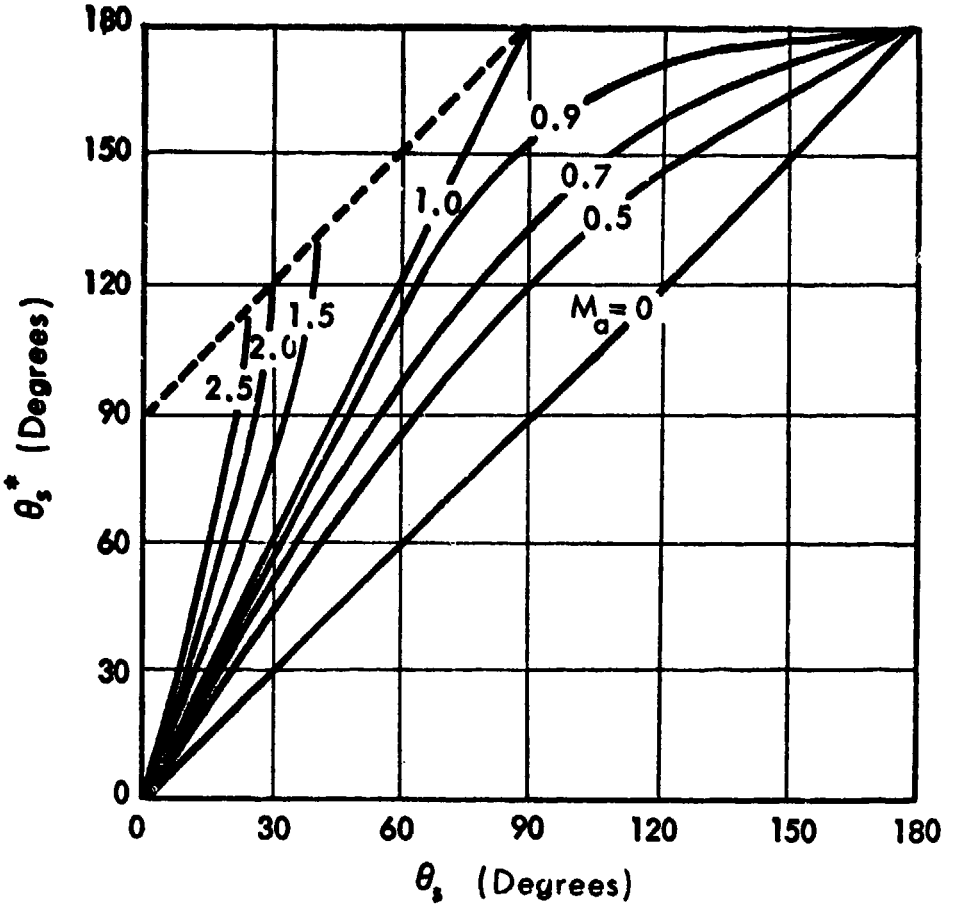

FIG. 13. EFFECT OF FORWARD MOTION ON ANGLE BETWEEN JET AXIS AND LINE FROM SOURCE TO EFFECTIVE RECEIVER LOCATION.

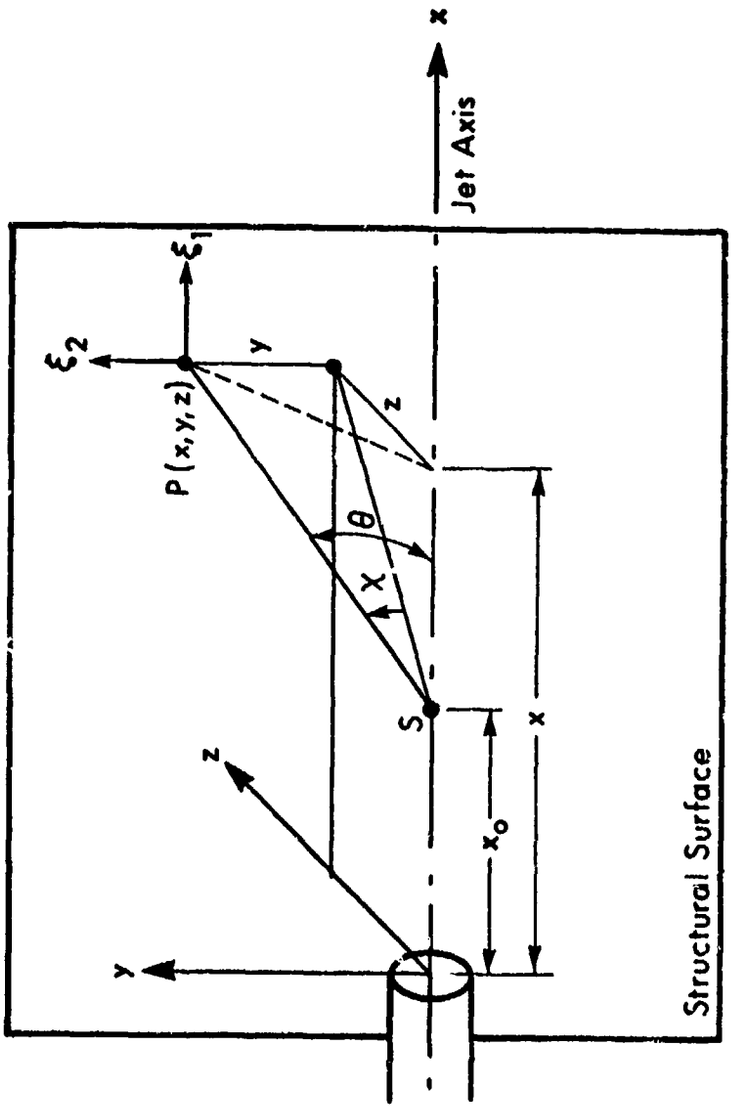

FIG. 14. GEOMETRY FOR CALCULATION OF JET NOISE PRESSURE CORRELATION COEFFICIENT

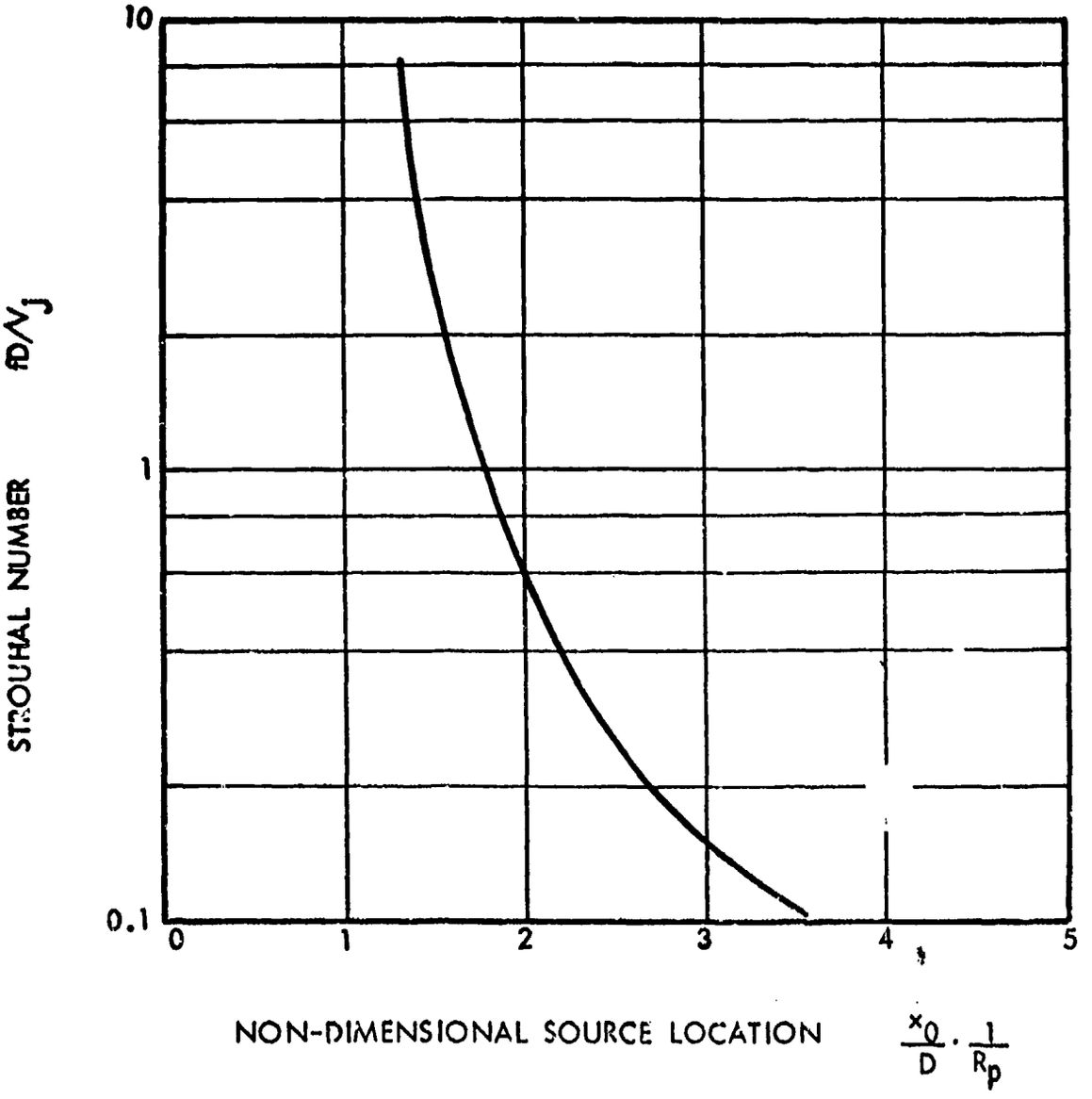

FIG. 15. EFFECTIVE NOISE SOURCE LOCATION IN ' 'ET EXHAUST.

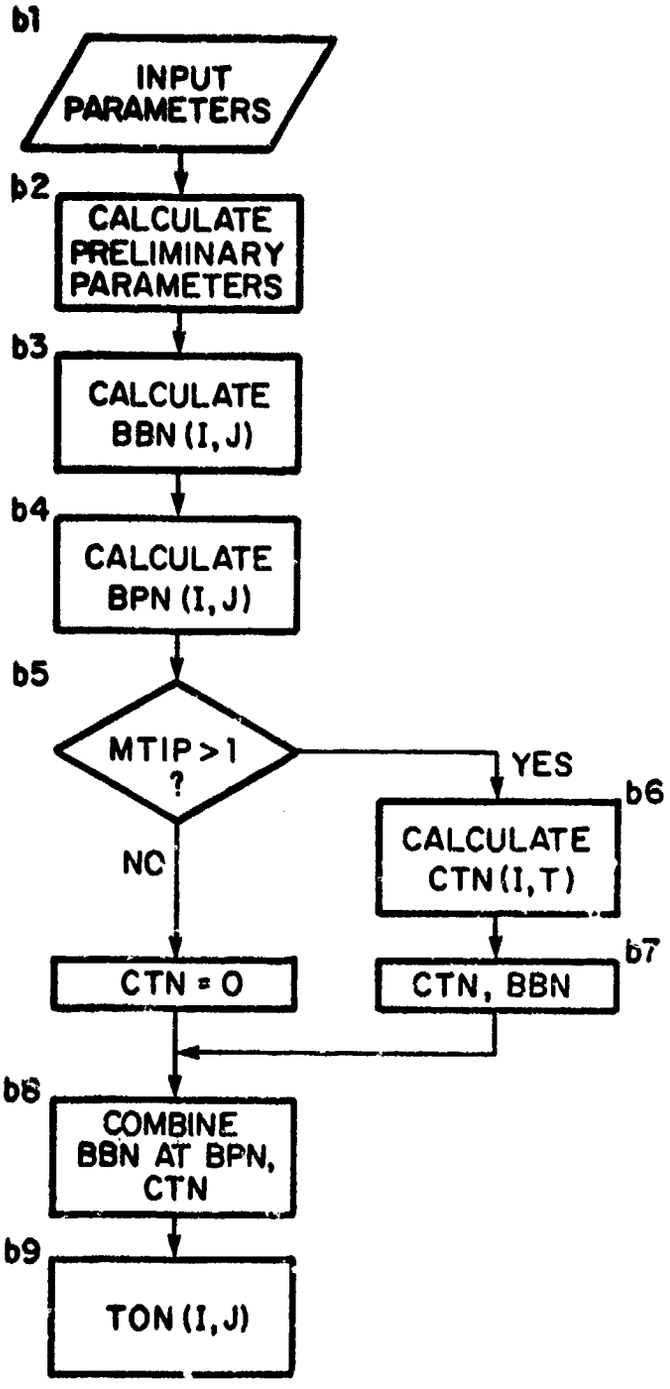

FIG. 16. FLOW DIAGRAM FOR FAN/COMPRESSOR NOISE PREDICTION.

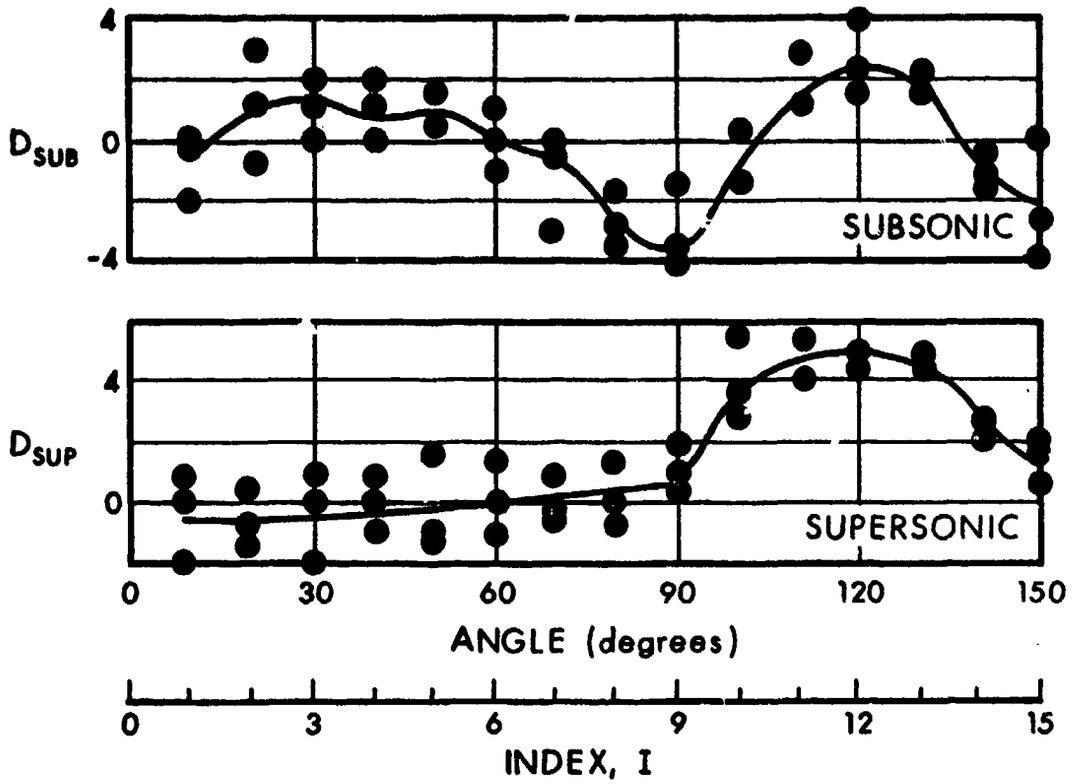

FIG. 17. SUBSONIC AND SUPERSONIC DIRECTIVITY CORRECTIONS.

(Use solid curves for prediction estimates; circles indicate range of data.)

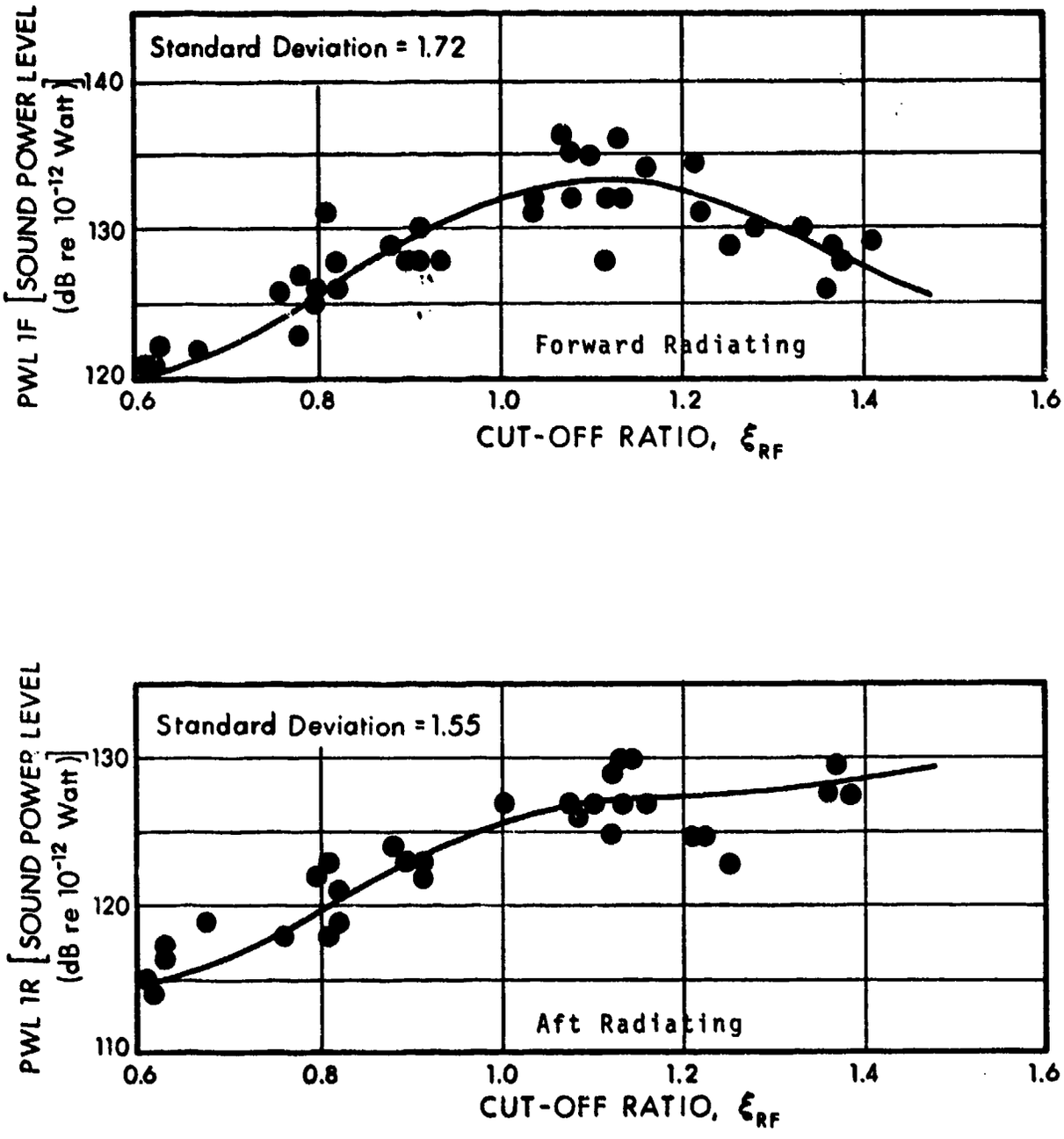

FIG. 18. NORMALIZED POWER LEVEL AT BLADE-PASSAGE FREQUENCY

(Use solid curves for prediction estimates; circles indicate range of data.)

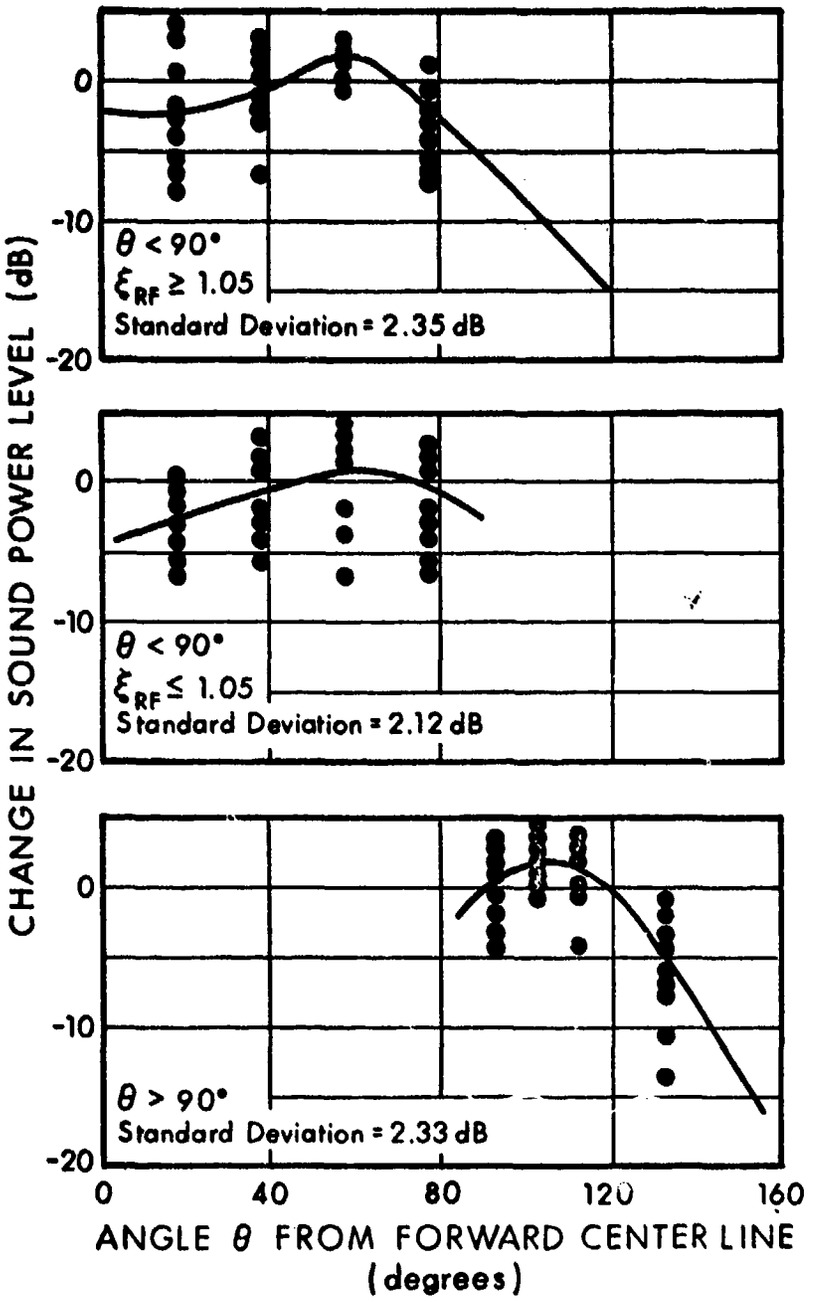

FIG. 19. DIRECTIVITY CORRECTIONS FOR BLADE-PASSAGE TONE

(Use solid curves for prediction estimates. Circles indicate spread of data.)

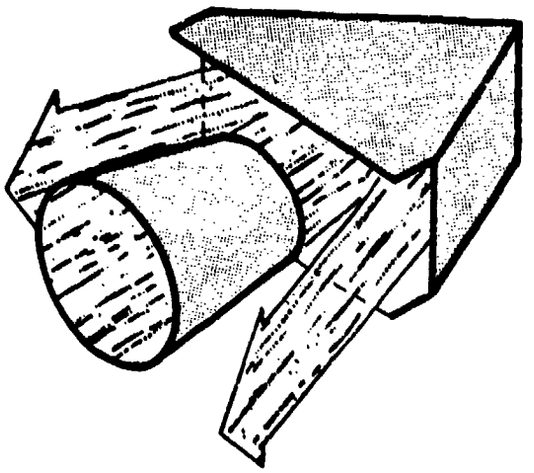

(a) V-GUTTER

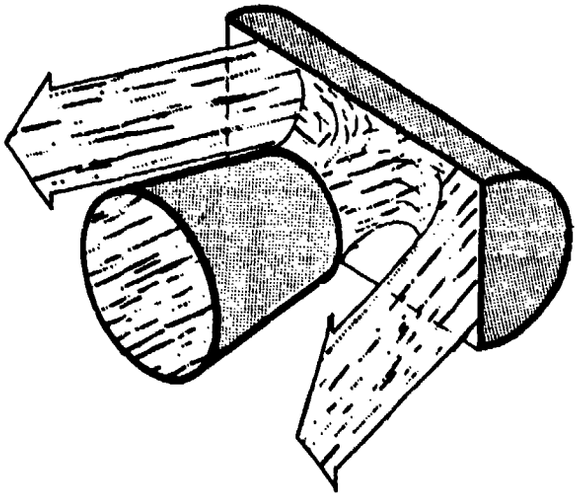

(b) SEMI-CYLINDRICAL

FIG. 20. THRUST REVERSERS OF THE TARGET TYPE.

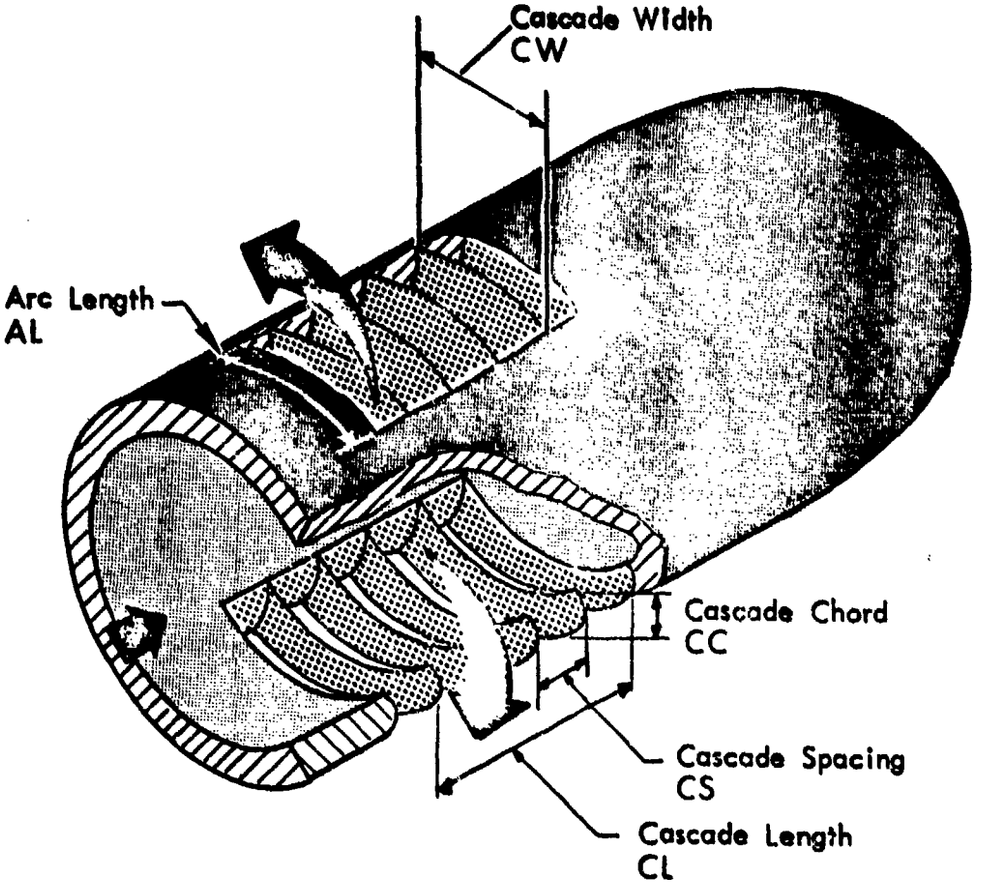

FIG. 21. TAIL PIPE CASCADE THRUST REVERSER.

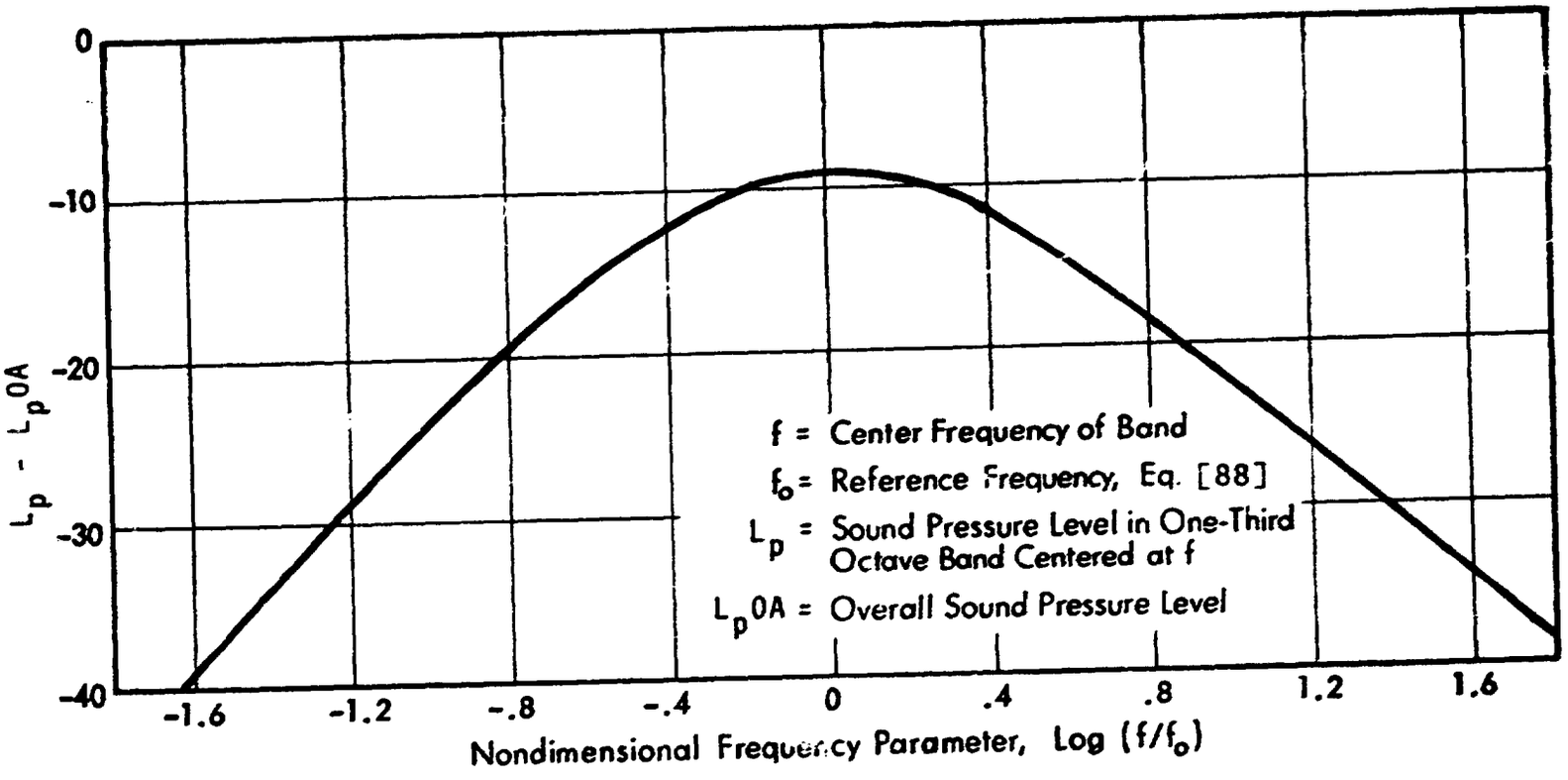

FIG. 22. NON-DIMENSIONAL ONE-THIRD OCTAVE BAND SPECTRUM FOR TARGET-TYPE THRUST REVERSERS.

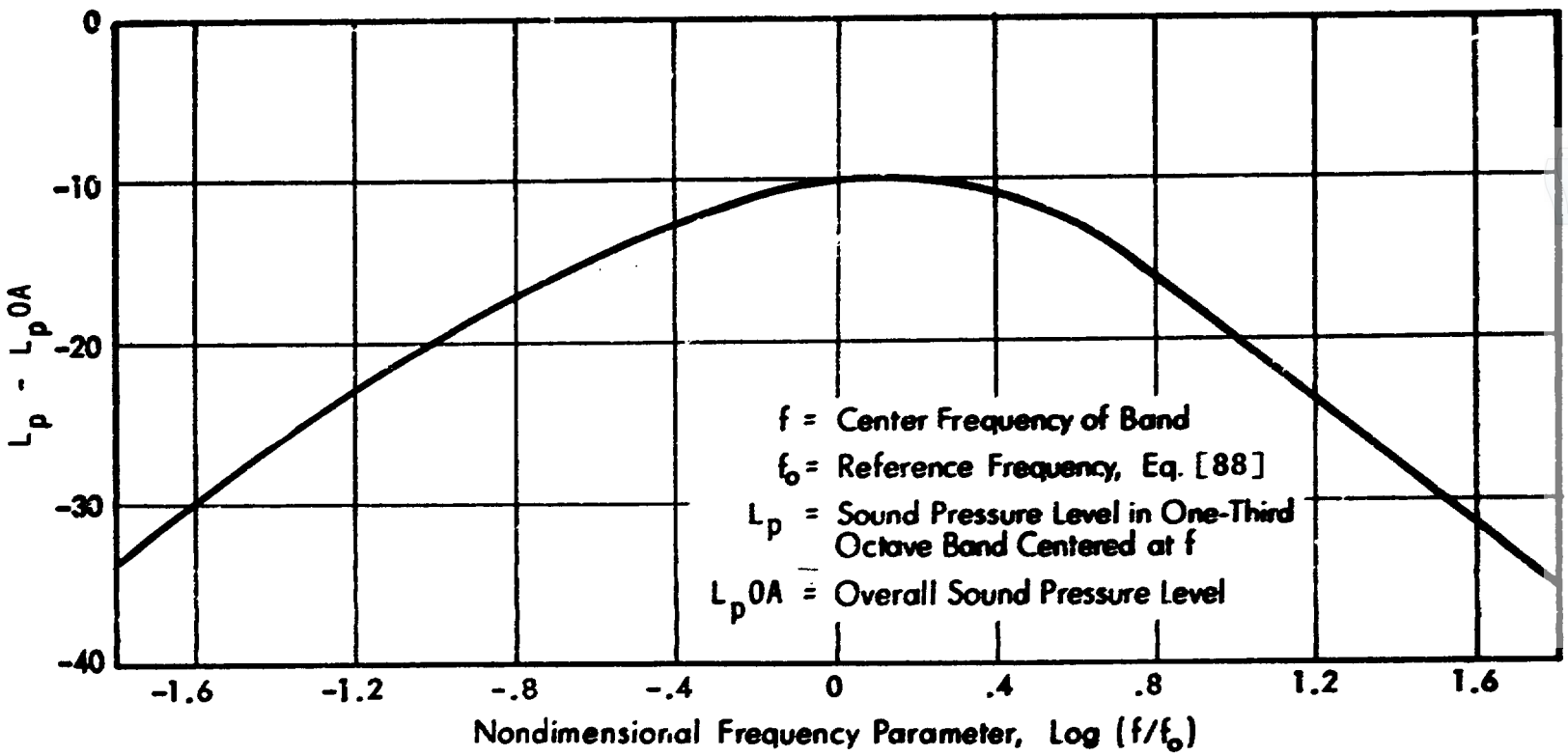

FIG. 23. NON-DIMENSIONAL ONE-THIRD OCTAVE BAND SPECTRUM FOR CASCADE-TYPE THRUST REVERSERS.

SECTION V

POWERED LIFT SYSTEMS

5.1 General

In externally blown propulsive lift systems, the jet engine exhaust is directed either at a series of flaps (externally blown flap – EBF – systems) or along the upper surface of the wing (upper surface blown – USB – systems). In both types of externally blown concepts, increased lift is obtained as the result of downward direction of the jet exhaust flow by a set of flaps, and the primary source of nearfield noise is the interaction of the jet flow with the flaps.

In internally blown systems, high pressure air is ducted either to a slot nozzle that blows along the upper surface of a flap (internally blown flap or jet flap – IBF – systems), or one that blows into an augmenter channel which also entrains ambient air (augmenter wing – AW – systems). In both types of internally blown systems, noise results due to the jet emanating from the slot nozzle, as well as due to interaction of the jet flow with the flaps.

5.2 Externally Blown Flaps

5.2.1 Engines without external mixers or decayer nozzles

Jet/Flap Interaction Noise Level and Spectrum

(a) Refer to Fig. 24 for definition of geometry and coordinates.

(b) Evaluate the effective jet diameter D_e from

$$D_e = \sqrt{\frac{4}{\pi}\left(A_{core} + A_{fan}\right)} \qquad (98)$$

where A_{core} is the area of core exit nozzle and A_{fan} is the area of bypass nozzle annulus.

(c) Find the effective jet velocity U_e from that one of the following relations that corresponds to the nozzle being used.

For a simple round nozzle,

$$U_e = U_0 = \text{mean exit velocity} \tag{99}$$

For a coannular arrangement without internal mixing,

$$U_e = \left[\frac{A_{core}\, V_{core}^6 + A_{fan}\, V_{fan}^6}{A_{core} + A_{fan}}\right]^{1/6} \tag{100}$$

where V_{core} is the core exit velocity, and V_{fan} is the bypass annulus exit velocity. For engines with internally mixed flows,

$$U_e = \frac{V_{core} + BPR \cdot V_{fan}}{1 + BPR} \quad , \tag{101}$$

where BPR is the bypass ratio.

(d) Calculate the overall sound pressure level at the observation point from

$$L_pOA = 10 \log (\rho_e^2 U_e^6 D_0^2) + 29 - 20 \log r + 0.14\delta_F + 10 \log \left[\frac{1 + \sin\psi}{2} \cos^2\left(\frac{\theta+\delta_F}{2}\right)\right] + C_A \quad , \tag{102}$$

where L_pOA is the overall sound pressure level (dB, re 2 x $10^{-5}N/m^2$) ρ_e is the mean density of jet, r is the distance from flow impingement point to observer, (see Fig. 24) δ_F is the detection angle (degrees) of the flap on which the flow centerline impinges, ψ and θ are coordinate angles, (see Fig. 24) C_A is the correction for forward speed of aircraft obtained from Sec. 5.6.1.

(e) Find the sound pressure level in every one-third octave band of interest from

$$L_p = L_pOA - 12.5 + 40 \log (fD_0/U_e) - 20 \log [0.3 + (fD_0/U_e)^{3/2}] - \Delta L_p \quad , \tag{103}$$

where L_p is the sound pressure level (dB, re 2 × 10^{-5} N/m^2) in the one-third octave band, and f is the center frequency of one-third octave band (Hz), and

$$\Delta L_p = \begin{cases} 10 \log \left[\dfrac{1 + x/D_0}{3} \right] & \text{for } fD_0/U_0 < 0.3 \\ 0 & \text{otherwise} \end{cases} \tag{104}$$

x = distance from nozzle exit plane to leading edge of first flap.

Correlation Length of Jet/Flap Interaction Noise

(a) Find the "plane wave" correlation length ℓ_p along the given surface at a given frequency f from

$$\ell_p = c/f \cos\beta \quad , \tag{105}$$

where c is the speed of sound in ambient air, and β is the angle between line from source center to observation point and the normal to the surface under consideration.

(b) Find the "spherical wave" correlation length ℓ_s from

$$\ell_s = \left[\frac{c}{2\pi f} \left(2r_0 + \frac{c}{2\pi f} \right) \right]^{\frac{1}{2}} , \qquad (106)$$

where r_0 is the distance from source center to a plane drawn tangent to the surface of interest at the observation point (measured in direction perpendicular to this plane).

(c) Take as the correlation length the lesser one of ℓ_p and ℓ_s.

Surface Pressures

For any surface on which the jet impinges, estimate the fluctuating pressure level in any one-third octave band by use of Fig. 25.

(a) Calculate the value of fD_0/U_e for the center frequency f of the one-third octave band. D_0 is the effective diameter of jet, see Eq. (98) , U_e is the effective jet velocity, see Eqs. (99) - (101).

(b) From Fig. 25, read the corresponding value of normalized fluctuating pressure level, 20 log (p/q).

(c) Calculate the dynamic pressure of the jet

$$q = \frac{1}{2} \rho_e U_e^2 \qquad (107)$$

(d) Find the fluctuating pressure level from

$$\text{FPL} = 20 \log (p/q) + 20 \log (q) + 127.5 , \qquad (108)$$

where FPL is the fluctuating pressure level in the one-third octave band (dB, re 2×10^{-5} N/m^2).

To estimate the corresponding spanwise correlation length, use Fig. 26.

(a) Calculate the reduced frequency by multiplying fD_0/U_e (found above) by $3D_0/x$, where x is the axial distance from jet exit plane to observation point.

(b) Find ℓ/D_j from Fig. 26 and calculate the spanwise correlation length ℓ. Estimate the streamwise correlation length as being approximately equal to the spanwise correlation length.

5.2.2 Engines with external mixer or decayer nozzles

Jet/Flap Interaction Noise Level and Spectrum

(a) Refer to Fig. 24 for definition of geometry and coordinates.

(b) Evaluate the effective jet diameter D_0 from Eq. (98).

(c) Find the effective jet velocity U_e that corresponds to the engine without a mixer/decayer from the appropriate one of Eqs. (99) - (101).

(d) Use Fig. 27 to find the ratio $R_U = U_{ed}/U_e$ of jet velocity U_{ed} with a mixer/decayer to the corresponding velocity U_e without a decayer, at the axial distance x from the jet exit to the impingement point. Calculate U_{ed}.

(e) Find the uncorrected overall sound pressure level OASPL from Eq. (102), using U_{ed} in place of U_e.

(f) Find the (corrected) overall sound pressure level $OASPL_c$ from

$$OASPL_c = L_pOA - 10 + \Delta OASPL_c \tag{109}$$

$$\Delta OASPL_c = \begin{cases} 60 \log R_U & \text{for } x/D_0 < 3 \\ 0 & \text{otherwise} \end{cases} . \tag{110}$$

(g) Find the frequencies f_L and f_H between which the one-third octave spectrum is nearly constant from

$$f_L = 0.1\ U_e/D_0$$

$$f_H = 40\ f_L \quad . \tag{111}$$

(h) Find the sound pressure level L_p in every one-third octave band between f_L and f_H from

$$L_p = OASPL_c - 10 \quad . \tag{112}$$

Correlation Length of Jet/Flap Interaction Noise

Follow the procedure of Sec. 5.2.1.

Surface Pressures

(a) Find the effective jet velocity U_e that corresponds to the engine without a mixer/decayer from the appropriate one of Eqs. (99) - (101).

(b) Use Fig. 27 to find $R_U = U_{ed}/U_e$; then calculate U_{ed}.

(c) Proceed as in Sec. 5.2.1 , but use U_{ed} everywhere in place of U_e.

5.3 Upper Surface Blown Flaps

5.3.1 Jet/flap interaction noise

Overall Level

(a) Evaluate the effective jet diameter D_0 by use of Eq. (98).

(b) Find the effective jet velocity U_e by use of the appropriate one of Eqs. (99) - (101).

(c) Refer to Fig. 28 for definition of the coordinates θ, ψ, and r, which are measured from the point on the flap trailing edge that is located in the middle of the jet flow.

(d) Find the overall sound pressure level at the observation point from

$$L_{pOA} = 10 \log (\rho_e^2 U_e^6 D_0^2) + 30 - 20 \log r + 0.01 \delta_F + 10 \log \left[\frac{1 + \sin\psi}{2} \cos^2\left(\frac{\theta+\delta_F}{2}\right) \right] + C_A \quad , \qquad (113)$$

where L_{pOA} is the overall sound pressure level (dB, re 2×10^{-5} N/m^2), ρ_e is the mean density of jet flow , r is the distance from jet center on trailing edge to observation point (ft), see Fig. 28 , δ_F is the flap deflection angle (degrees), θ,ψ are the coordinate angles, see Fig. 28 , and C_A is the correction for aircraft forward speed (from Sec. 5.6.1).

One-Third Octave Band Spectrum

For every one-third octave band of interest:

(a) Find the corresponding value of fD_0/U_e, where f denotes the center frequency of the band.

(b) From Fig. 29, determine the difference Δ (between the overall sound pressure level and the baseline one-third octave band level) that corresponds to this value of fD_0/U_e.

(c) Find the baseline sound pressure level L_b in the one-third octave band from

$$L_b = L_{pOA} + \Delta \quad . \tag{114}$$

(d) This baseline level pertains to a configuration with an impingement angle of 20° and a nozzle aspect ratio of 4.0, and without a deflector. Obtain the corrected one-third octave band level SPL from the baseline level, from

$$L_p = L_b + C_{AR} + C_I + C_{De} \quad , \tag{115}$$

where C_{AR}, C_I, C_{De} are corrections for aspect ratio, impingement angle, and for the presence of a deflector, obtained from Figs. 30, 31, and 32, respectively.

Note that Figs. 31 and 32 make use of the reduced frequency fD_0/U_e, but that Fig. 30 employs the reduced frequency fL_f/U_e, where L_f represents the distance along the upper wing surface from the nozzle exit to the trailing edge; see Fig. 28.

Correlation Length

Follow the procedure of Sec. 5.2.1, considering as the source center the point on the trailing edge in the jet mid-plane.

5.3.2 Surface pressures

Determine the one-third octave band spectrum for the observation point of interest by applying Fig. 33 . For lateral observation point locations other than those shown explicitly, interpolate between the given curves.

Find the corresponding axial correlation length ℓ_x and the lateral correlation length ℓ_y from Fig. 34.

5.4 Augmenter Wing

5.4.1 Noise level and spectrum

(a) Refer to Fig. 35 for definition of the coordinates.

(b) Divide the entire span into a series of contiguous elements whose spans ℓ_s are sufficiently small so that $\ell_s < r$ for each. Note ℓ_s, θ, and ψ for each element.

(c) Calculate a reference sound pressure level from

$$RSPL = 60 \log V_j + 10 \log A - 5 \log (L/h) - 30.5 , \qquad (116)$$

where V_j is the velocity of jet in the wing (ft/sec), A is the area of wing nozzle (ft^2), L is the length of flap (ft), and h is the height of nozzle (ft).

(d) Find the contribution to the one-third octave band spectrum at the observation point made by each element, as follows:

i. Find the azimuthal directivity correction D_θ from Fig. 36.

ii. Find the elevation directivity correction D_ψ from Fig. 37.

iii. Calculate the overall sound pressure level at the observation point from

$$L_{pOA} = RSPL + D_\theta + D_\psi - 10 \log (L_s/\ell_s) + C_A - 20 \log r \quad , \tag{117}$$

where L_s is the total augmenter span, r is the distance from midpoint of augmenter channel element to observation point (ft), and C_A is the correction for aircraft forward speed (dB); see Sec. 5.6.2.

iv. Use Fig. 38 to determine the one-third octave band sound pressure level L_p at each frequency of interest.

(e) Calculate the sound pressure level in each frequency band of interest by combining the contribution from all elements, using the relation

$$L_p = 10 \log \sum_i 10^{(L_{p\,i}/10)} \quad , \tag{118}$$

where $L_{p\,i}$ is the sound pressure level at observation point due to only the *ith* element, and L_p is the sound pressure level at observation point due to all elements. The summation is carried out over all elements.

(f) Find the correlation length by applying the procedure of Sec. 5.2.1, using the geometric center of the augmenter as the source center.

5.4.2 Surface pressures

Use Fig. 39 to estimate the root-mean-square fluctuating pressure in every one-third octave band of interest, for any point inside the augmenter channel.

If the fluctuating pressure level is desired, calculate it from Eq. (108), using Eq. (107) for q.

Definitive information on correlation lengths is lacking. The best one can do is to estimate ℓ_x (in the streamwise direction) and ℓ_y (in the cross-stream direction) as between 1 and 4 times the nozzle height h, with lower values occurring near the augmenter leading edge and higher values near the trailing edge. On the flap, one may expect $\ell_x > \ell_y$; on the shroud, $\ell_y > \ell_x$.

5.5 Jet Flap

5.5.1 Noise

Two mechanisms contribute to jet flap noise: the jet itself, and flow interaction with the flap.

Jet Noise

(a) Divide the slot nozzle into a series of contiguous elements, each having a spanwise length that is less than the distance from the center of the slot nozzle element to the observation point.

(b) Consider each element as a separate slot nozzle and predict its noise contribution at the observation point by using the procedure of Sec. 4.2.1.

(c) Combine the contributions from all elements by application of Eq. (118).

Flap Noise

(a) Estimate the shear layer thickness δ_{TE} (ft) at the trailing edge from

$$\delta_{TE} = \begin{cases} 0.5\ (U_0 L_f/\nu)^{-0.2} & \text{for } L_f/h < 10 \\ 0.5\ (10 U_0 h/\nu)^{-0.2} + 0.1\left(\dfrac{L_f}{h} - 10\right) & \text{for } L_f/h > 10 \end{cases} \qquad (119)$$

where L_f is the distance along flap surface from nozzle exit to trailing edge (ft), U_0 is the jet exit velocity (ft/sec), h is the slot nozzle thickness (ft), and ν is the kinematic viscosity of air (ft^2/sec).

(b) Estimate the flow velocity U_{TE} (ft/sec) at the flap trailing edge from

$$U_{TE} = \begin{cases} U_0 & \text{for } L_f/h < 10 \\ U_0\left(\dfrac{L_f}{h} - 10\right)^{0.23} & \text{for } L_f/h > 10 \end{cases} . \qquad (120)$$

(c) Divide the flap into a series of contiguous spanwise elements, each having a spanwise length ℓ_s that is less than the distance from the center of the flap element trailing edge to the observation point.

(d) Estimate the noise contribution made by each element as follows:

i. Refer to Fig. 35 for definition of the coordinates; take the nozzle shown there to correspond to the slot nozzle element under consideration.

ii. Determine the overall sound pressure level L_{pOA} due to the element under consideration from

$$L_{pOA} = 10 \log \left[\sin^2\psi \cos^2\left(\frac{\theta+\delta_F}{2}\right) \right] - 20 \log r$$

$$+10 \log [\delta_{TE} \ell_S \overline{U}^6_{TE}] - 16.5 + C_A \quad , \qquad (121)$$

where ψ, θ are the coordinate angles, see Fig. 35 r is the distance from center of trailing edge of the flap element to observation point (ft), ℓ_s is the span of the flap element (ft.), and C_A is the correction for forward speed of the aircraft (dB) from Sec. 5.6.3.

iii. Find the one-third octave band sound pressure level SPL corresponding to any band center frequency of interest by application of Fig. 40.

(e) Combine the contributions from all elements by use of Eq. (118).

(f) Estimate the correlation lengths by means of the procedure of Sec. 5.2.1 considering as the source center the midpoint of the trailing edge of the entire flap.

5.5.2 Surface pressures

(a) Estimate the local boundary layer thickness δ_x(ft) at the observation point from

$$\delta_x = \begin{cases} 0.5\ (U_0 L_x/\nu)^{-0.2} & \text{for } L_x/h < 10 \\ 0.5\ (10\ U_0 h/\nu)^{-0.2} + 0.1\left(\dfrac{L_x}{h} - 10\right) & \text{for } L_x/h > 10 \end{cases} \qquad (122)$$

and the local flow velocity U_x (ft/sec) from

$$U_x = \begin{cases} U_0 & \text{for } L_x/h \leq 10 \\ U_0\left(\dfrac{L_x}{h} - 10\right)^{-0.23} & \text{for } L_x/h > 10 \end{cases} \qquad (123)$$

where L_x is the streamwise distance along the flap surface from nozzle exit to observation point (ft), U_0 is the jet exit velocity (ft/sec), ν is the kinematic viscosity of air (ft^2/sec), and h is the thickness of slot nozzle (ft).

(b) Find 20 log (p_1/q) from Fig. 41 corresponding to the center frequency f of each band of interest.

(c) Evaluate

$$20 \log (p/q) = 20 \log (p_1/q) + 10 \log f - 6.5 \ , \qquad (124)$$

where p is the rms pressure in the one-third octave band (lb/ft^2) p_1 is the rms pressure in the one-Hertz band (lb/ft^2), q is the dynamic pressure of the jet (lb/ft^2), and f is the center frequency of one-third octave band (Hz). If desired, calculate the corresponding one-third octave band fluctuating pressure level from Eq. (108).

(d) Use the procedure of Sec. 5.3.2 and Fig. 110 to estimate the corresponding correlation lengths.

5.6 Correction for Foward Speed of Aircraft

5.6.1 Externally blown configurations

For externally blown flaps or upper surface blown flaps, evaluate the forward speed correction factor of Eq. (102) or (113) from

$$C_A = 10\ K_1 \log \left[1 - \frac{V_a}{U_e}\right] \tag{125}$$

using the appropriate value of K_1 taken from Fig. 42 . Here, V_a is the aircraft forward velocity (ft/sec), and U_e is the effective jet velocity (ft/sec); see Eqs. 99 - 101 . (In the presence of external mixer/decayers, use U_{ed} in place of U_e.)

5.6.2 Augmenter wings

Evaluate the forward speed correction term that appears in Eq. (117) from

$$C_A = 10\ K_2 \log \left[1 - \frac{V_a}{V_j}\right] \tag{126}$$

where V_a is the aircraft forward speed (ft/sec), V_j is the velocity of jet in the wing (ft/sec), and K_2 is found from Fig. 43.

5.6.3 Jet flaps

Evaluate the forward speed correction C_A that appears in Eq. (121) from

$$C_A = 50 \log \left[1 - \frac{V_a \cos \delta_F}{U_{TE}} \right] , \qquad (127)$$

where V_a is the aircraft forward speed (ft/sec), δ_F is the flap deflection angle, and U_{TE} is the flow velocity at the flap trailing edge (ft/sec); see Eq. (120) .

5.7 List of Symbols for Sec. V

Symbol	Definition	Units*
A	area of wing nozzle	ft^2 (m^2)
A_{core}	area of core exit nozzle	ft^2 (m^2)
A_{fan}	area of by-pass nozzle annulus	ft^2 (m^2)
BPR	by-pass ratio	
C_A	correction for forward speed	dB
D_e	effective jet diameter	ft (m)
FPL	fluctuating pressure level	dB
L	length of flap	ft (m)
L_F	distance along upper wing surface from nozzle exit to trailing edge (Fig. 28)	ft (m)
L_p	sound pressure level in one-third octave band	dB
L_pOA	overall sound pressure level	dB
L_s	augmentor span	ft (m)
L_x	axial distance along upper wing surface from nozzle exit to observation point	ft (m)
P	perimeter of wing nozzle section area	ft (m)
R_U	velocity ratio	
U_{TE}	flow velocity at flap trailing edge	ft/sec (m/s)

*SI units are shown in parentheses where appropriate. The units given here are typical. In some cases, use of specific units is required; this is indicated in the text, where necessary.

Symbol	Definition	Units
U_e	effective jet velocity	ft/sec (m/s)
U_{ed}	mean jet velocity with mixer/decayer	ft/sec (m/s)
U_x	flow velocity at observation point	ft (m)
U_0	mean jet velocity	ft/sec (m/s)
V_a	aircraft forward velocity	ft/sec (m/s)
V_{core}	core exit velocity	ft/sec (m/s)
V_{fan}	by-pass annulus exit velocity	ft/sec (m/s)
V_j	velocity of jet in wing	ft/sec (m/s)
c_0	speed of sound in ambient air	ft/sec (m/s)
f	center frequency of one-third octave band	Hz
f_L, f_H	lower and upper limiting frequencies of flat spectrum	Hz
h	height or thickness of nozzle	ft (m)
ℓ	spanwise correlation length	ft (m)
ℓ_p	plane wave correlation length	ft (m)
ℓ_s	spherical source correlation length	ft (m)
ℓ_x	correlation length in streamwise direction	ft (m)
ℓ_y	correlation length in	
p	sound pressure or fluctuating pressure	lb/ft^2 (N/m^2)
p_1	rms pressure in 1 Hz band	lb/ft^2 (N/m^2)

Symbol	Definition	Units
q	dynamic pressure	lb/ft^2 (N/m^2)
r	distance from jet action point to observation point (see Figs. 24, 28)	ft (m)
r	source-to-observer distance	ft (m)
r_0	distance from source center to a plane tangent to the surface at the observation point	ft (m)
x	axial distance from nozzle exit to leading edge of flap (see Fig. 24)	ft (m)
Δ	sound pressure level difference (see Fig. 29)	ft (m)
β	angle between line from source center to observation point and the normal to the surface under consideration	
δ_F	flap angle (see Figs. 24, 35)	deg
δ_{TE}	shear layer thickness at flap trailing edge	ft (m)
δ_x	boundary layer thickness at observation point	ft (m)
θ	angle to observation point or fuselage (see Figs. 24, 28, 35)	rad
ν	kinematic viscosity of air	ft^2/sec (m^2/s)
ρ_e	mean jet exhaust density	$slug/ft^3$ (kg/m^3)
ψ	angle to observation point, as measured from jet section pont (see Figs. 24, 28, 35)	rad

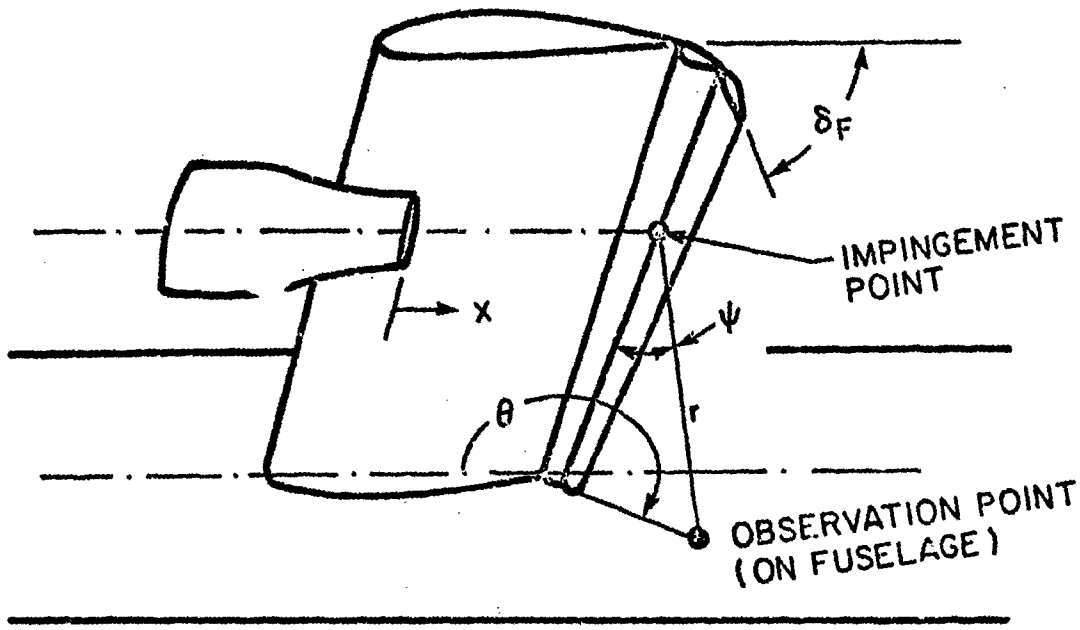

FIG. 24. DEFINITION OF COORDINATES FOR EXTERNALLY BLOWN NEAR-FIELD RADIATED NOISE CALCULATION

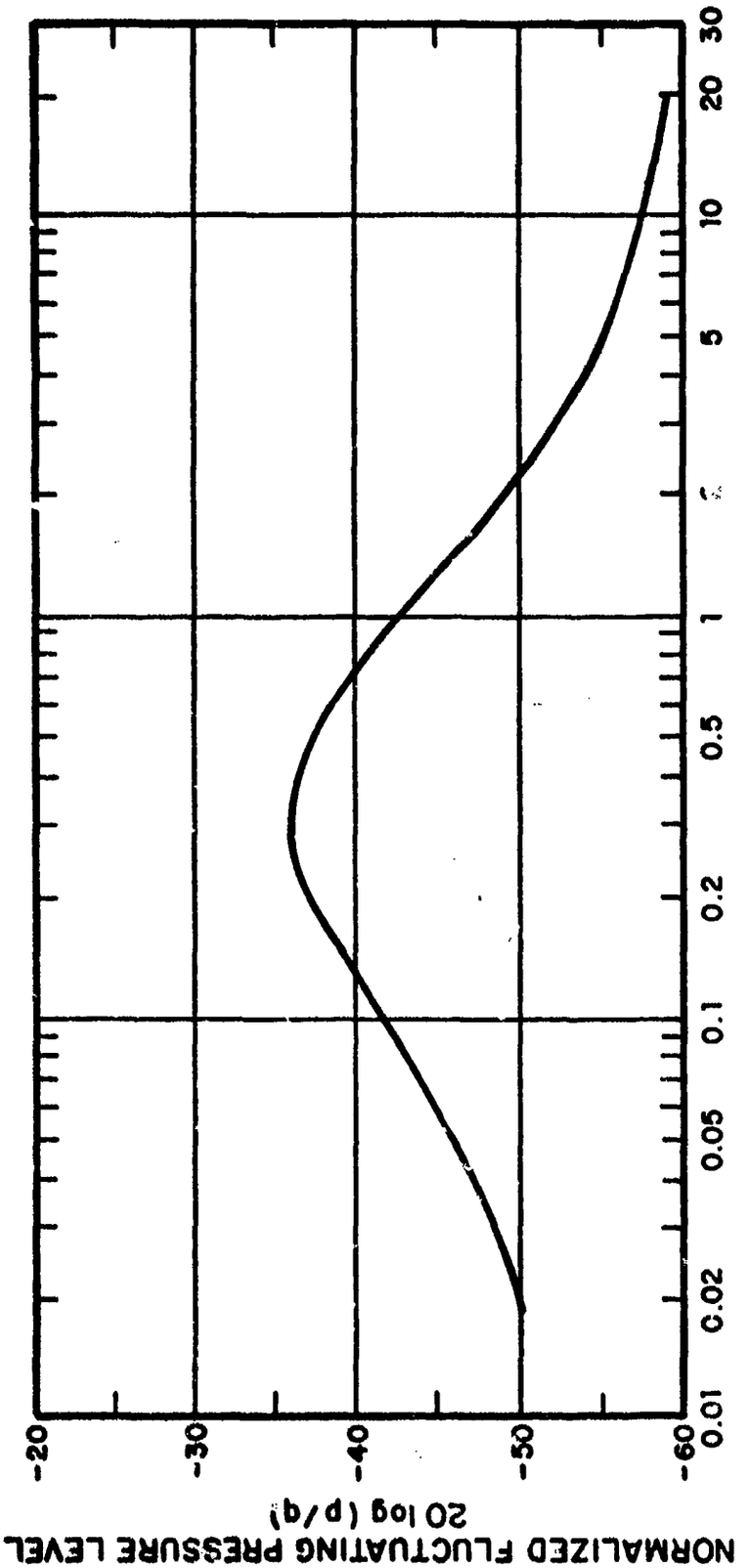

FIG. 25. NORMALIZED THIRD OCTAVE BAND FLUCTUATING PRESSURE SPECTRA ON BLOWN FLAP

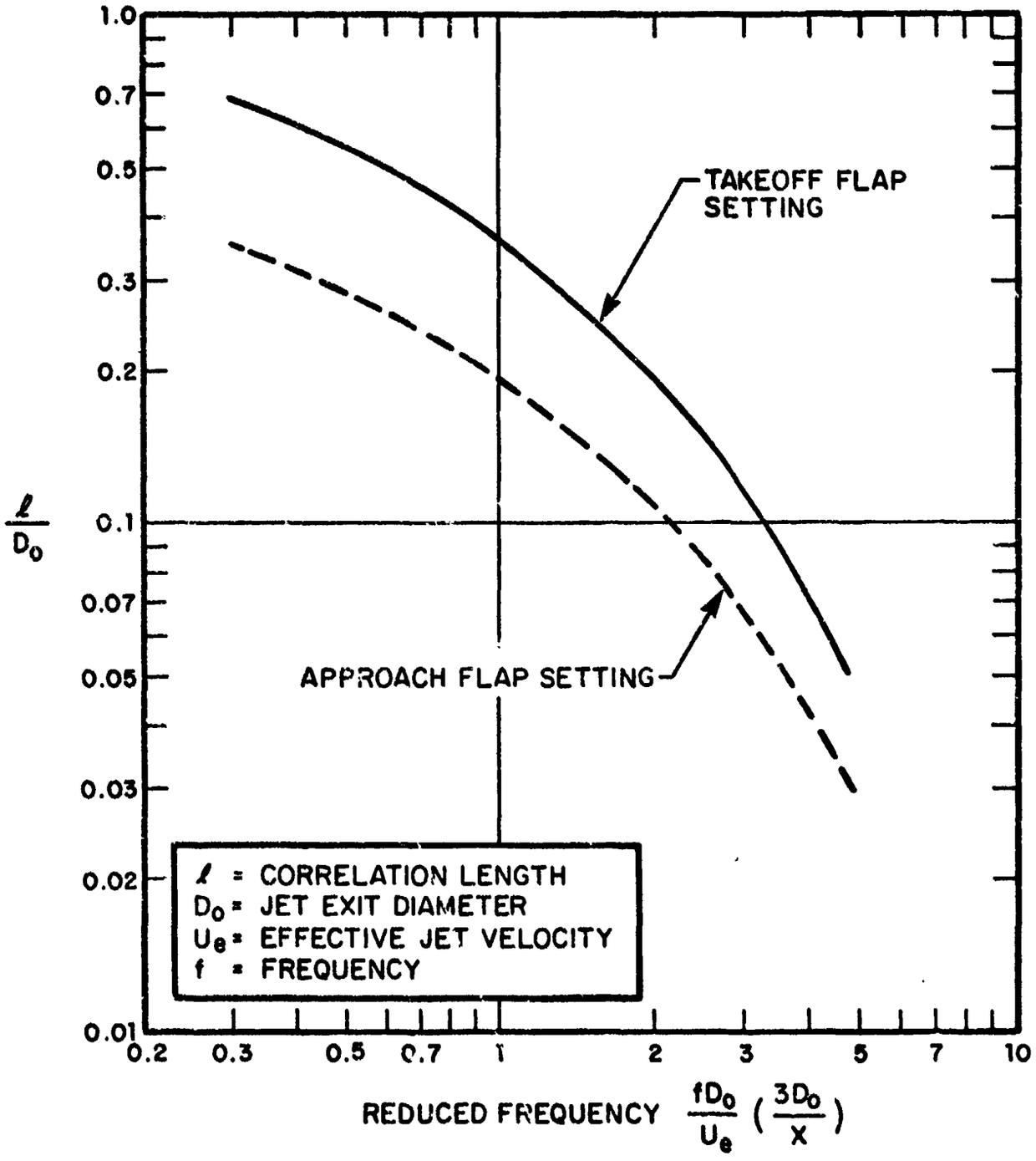

FIG. 26. SPANWISE CORRELATION LENGTH ON BLOWN FLAP

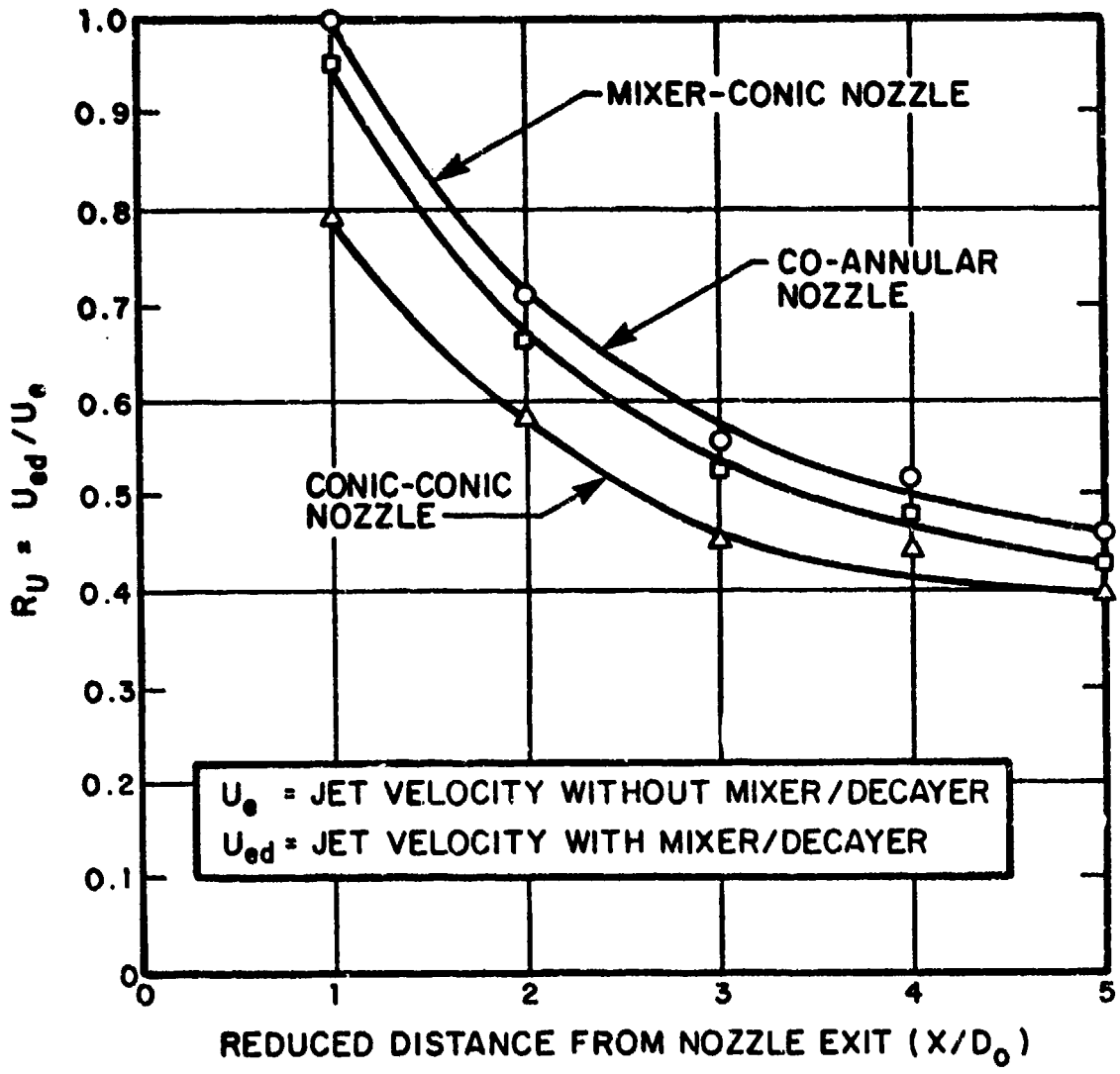

FIG. 27. EFFECT OF MIXER/DECAYER ON JET VELOCITY

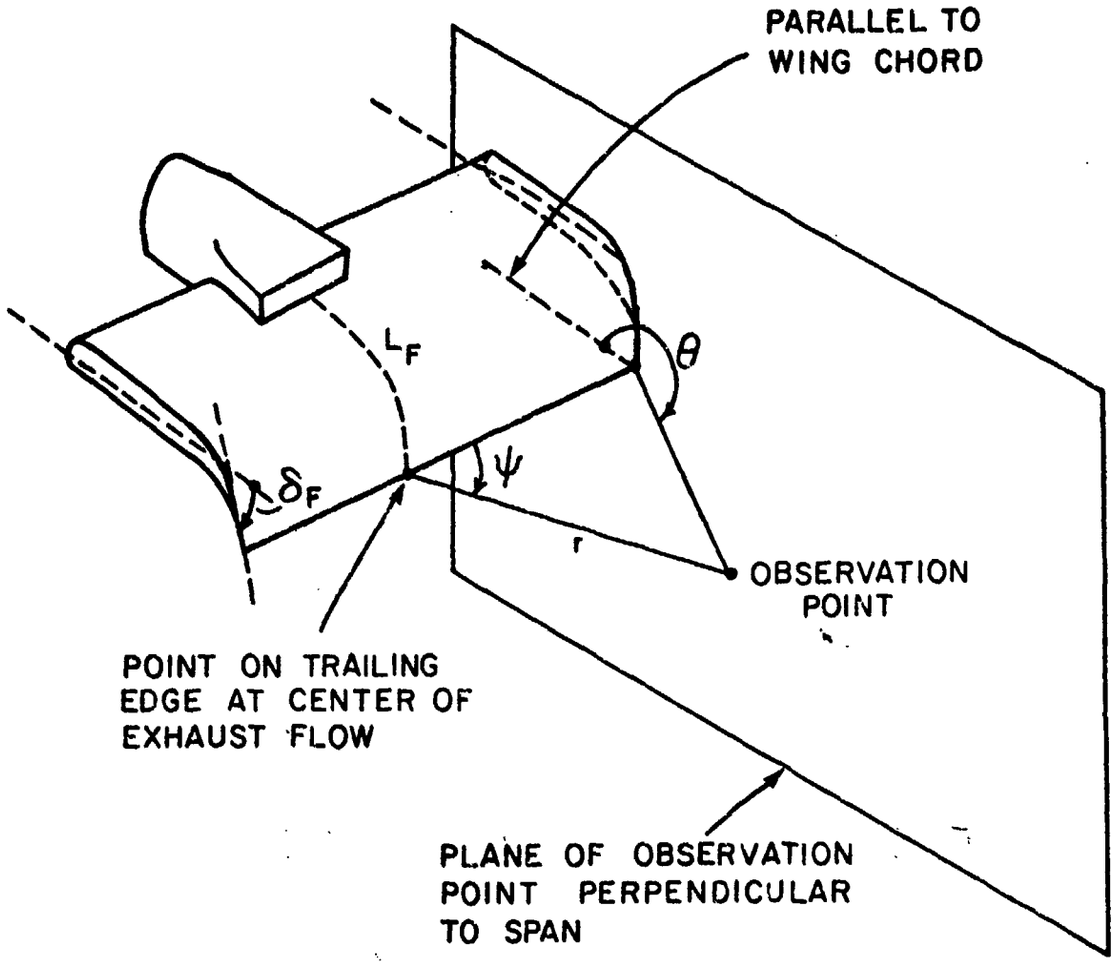

FIG. 28. COORDINATES FOR EVALUATION OF NOISE FROM UPPER SURFACE BLOWN CONFIGURATIONS

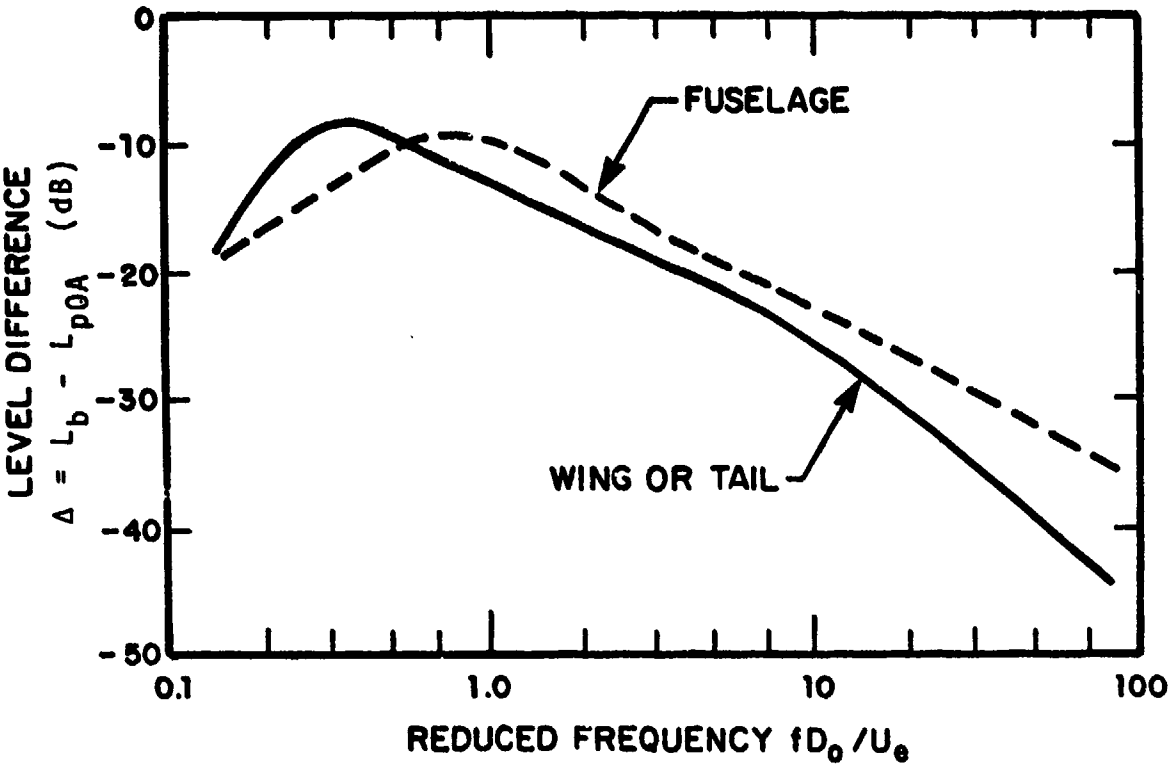

FIG. 29. RELATION BETWEEN OVERALL SOUND PRESSURE LEVEL AND LEVELS IN ONE-THIRD OCTAVE BANDS, FOR NOISE FROM UPPER SURFACE BLOWN FLAPS. (Impingement angle = 20^o nozzle aspect ratio = 4.0 all flap angles)

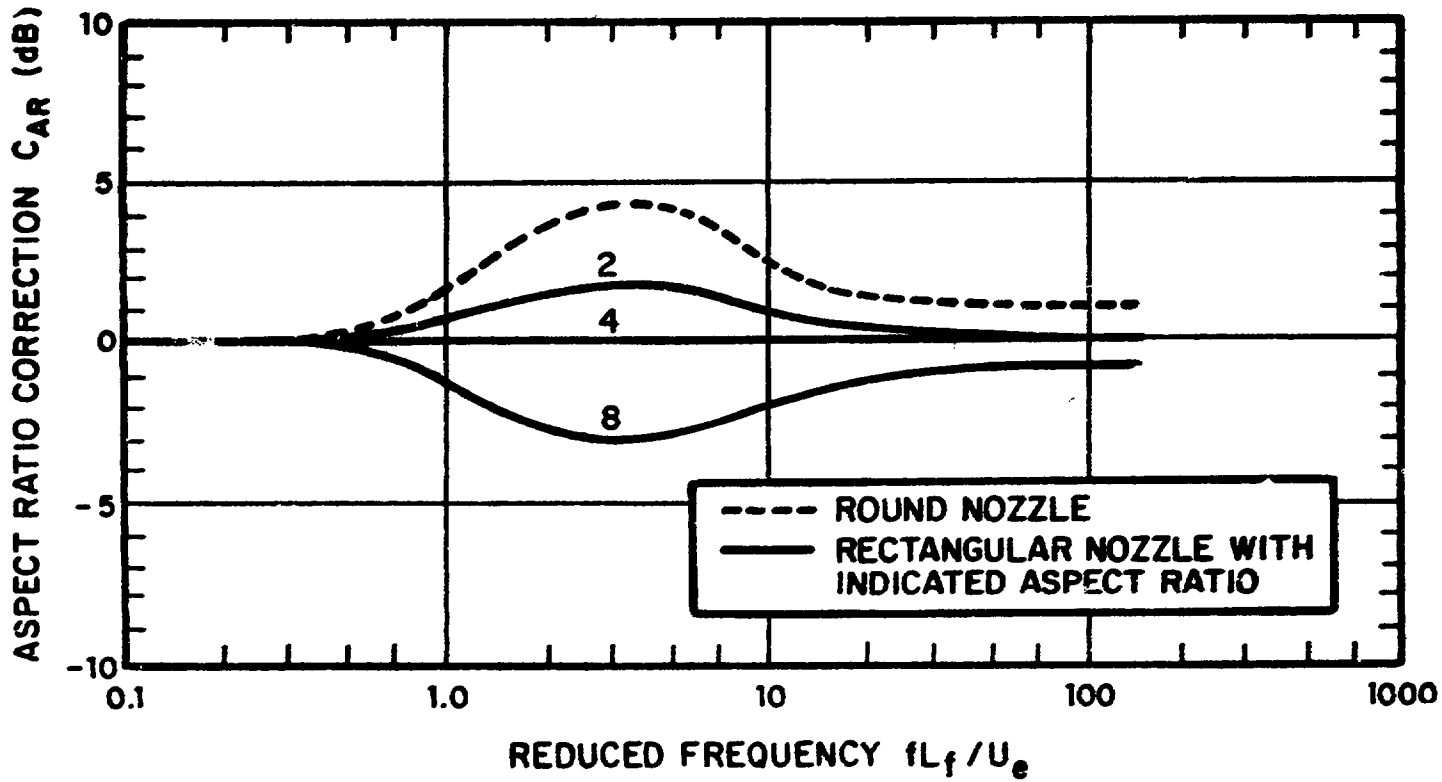

FIG. 30. NOZZLE ASPECT RATIO CORRECTION OF ONE-THIRD OCTAVE BAND SOUND PRESSURE LEVELS OF USB NOISE

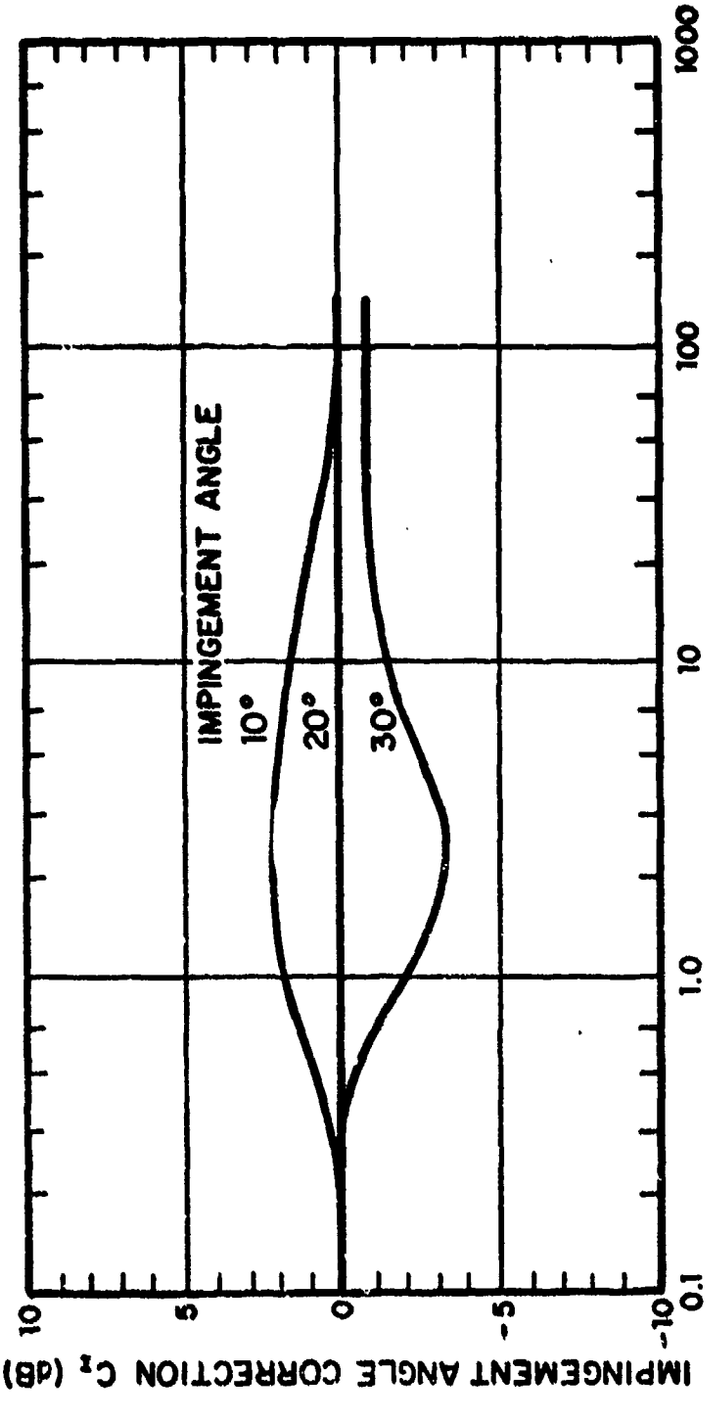

FIG. 31. IMPINGEMENT ANGLE CORRECTION OF ONE-THIRD OCTAVE BAND SOUND PRESSURE LEVELS OF USB NOISE

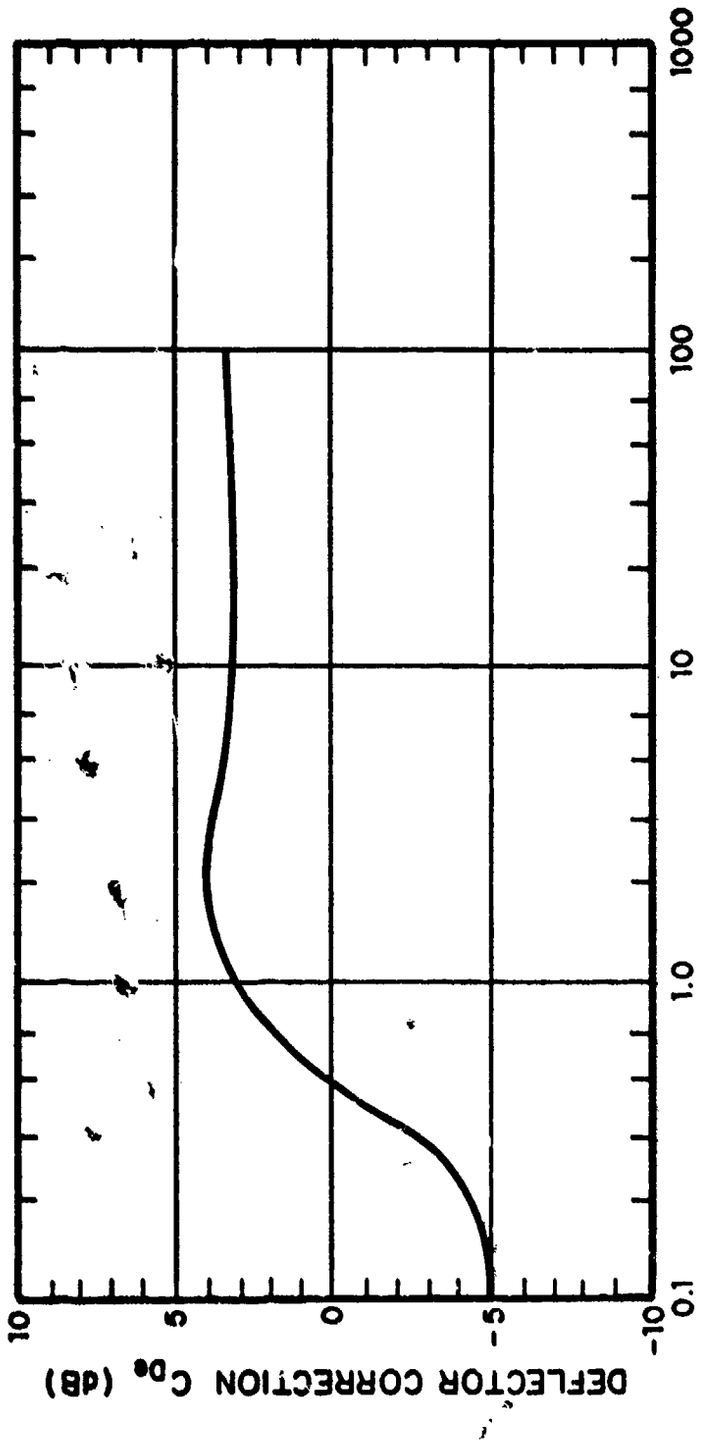

FIG. 32. CORRECTION OF ONE-THIRD OCTAVE BAND SOUND PRESSURE LEVELS OF USB NOISE FOR PRESENCE OF DEFLECTOR

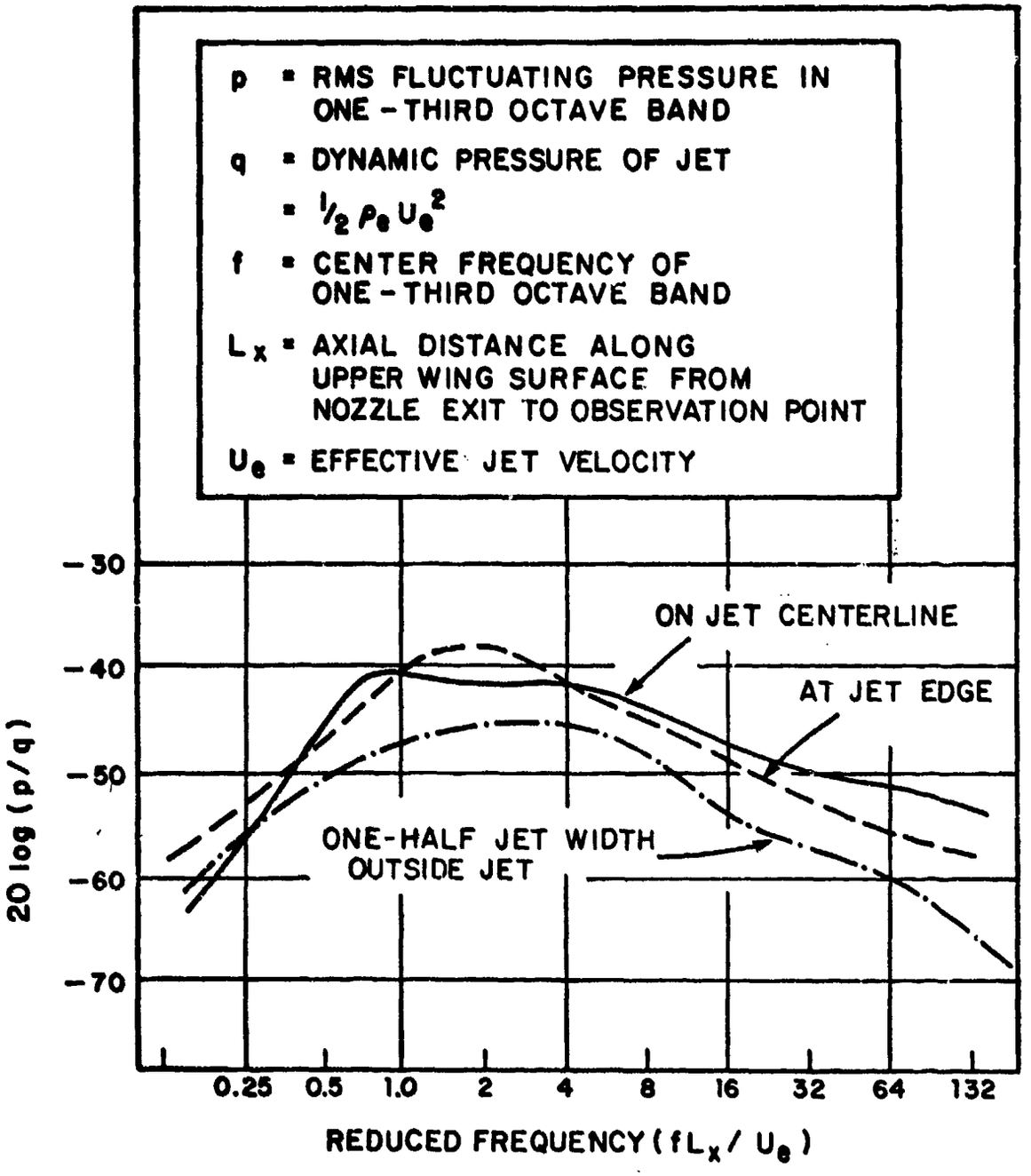

FIG. 33. SURFACE PRESSURES ON UPPER SURFACE OF USB FLAPS

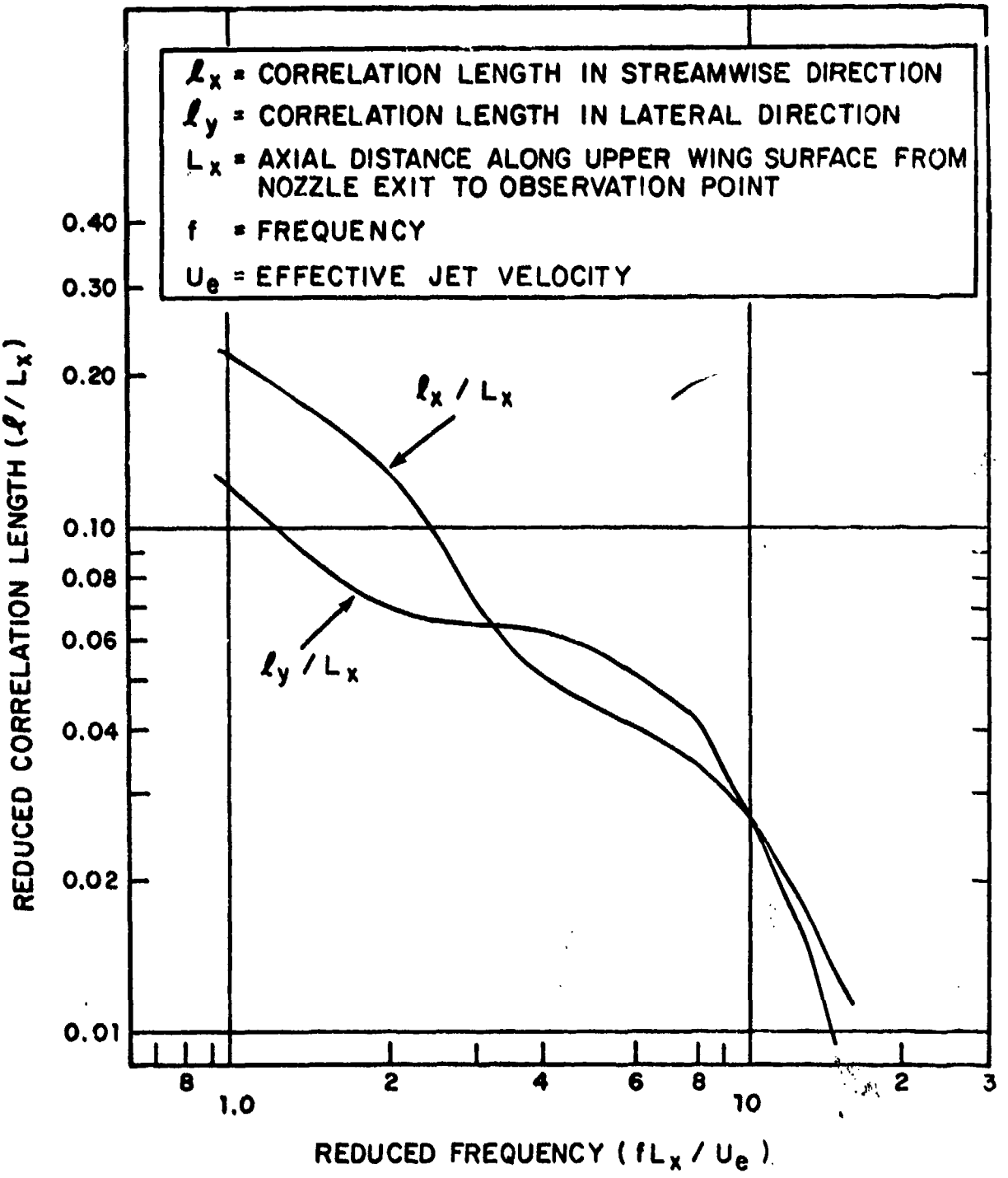

FIG. 34. CORRELATION LENGTHS OF PRESSURES ON UPPER SURFACE OF USB FLAPS

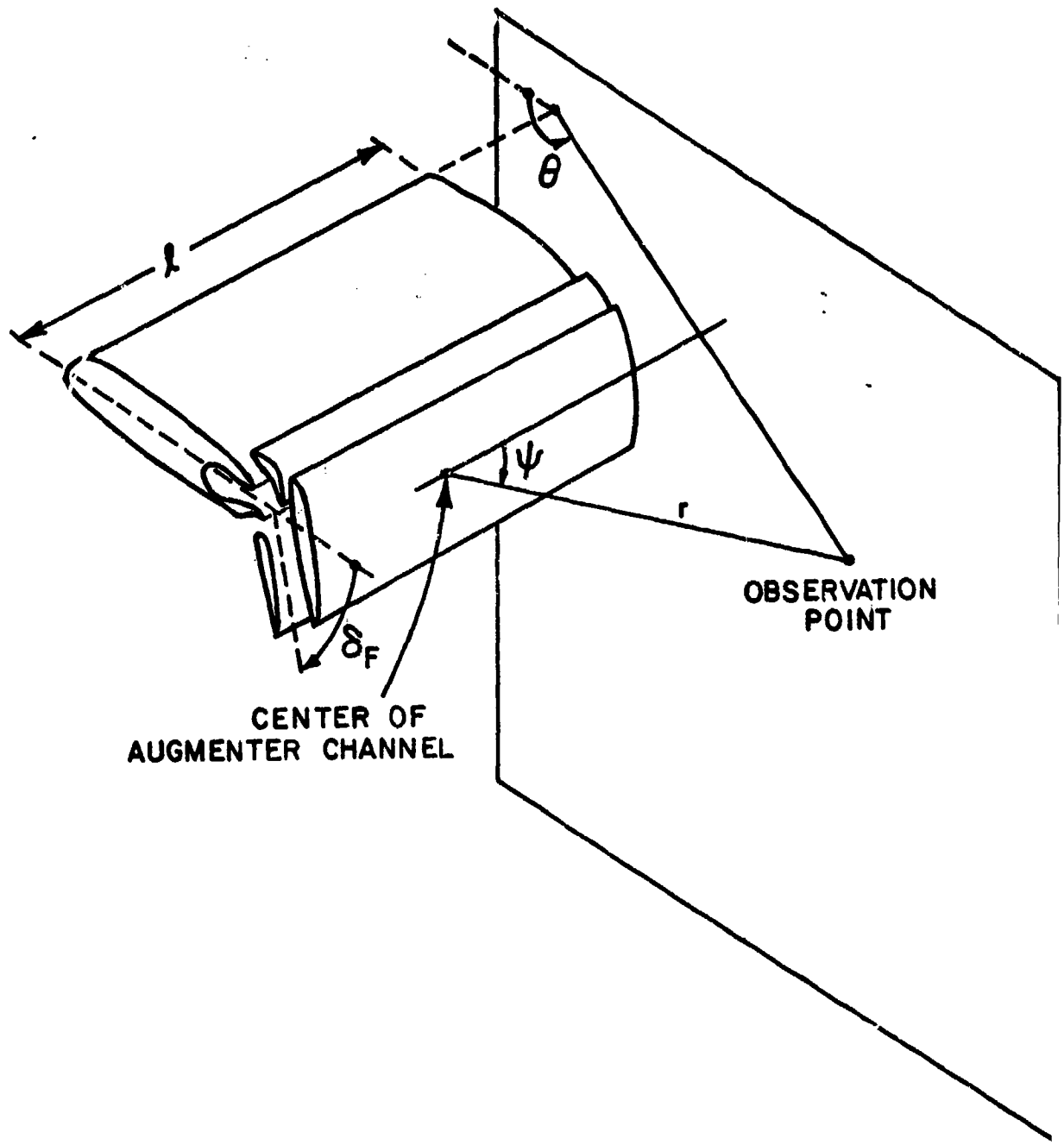

FIG. 35. COORDINATES FOR NOISE ESTIMATION OF AUGMENTER WING ELEMENT

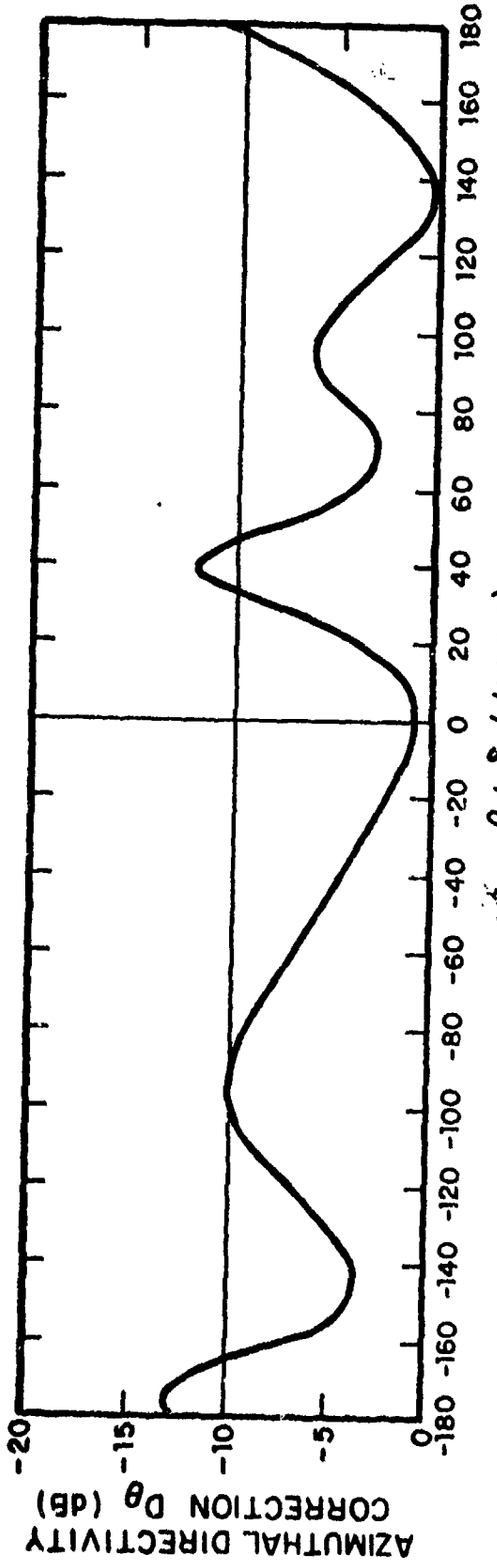

FIG. 36. AZIMUTHAL DIRECTIVITY CORRECTION FOR AUGMENTER WING NOISE

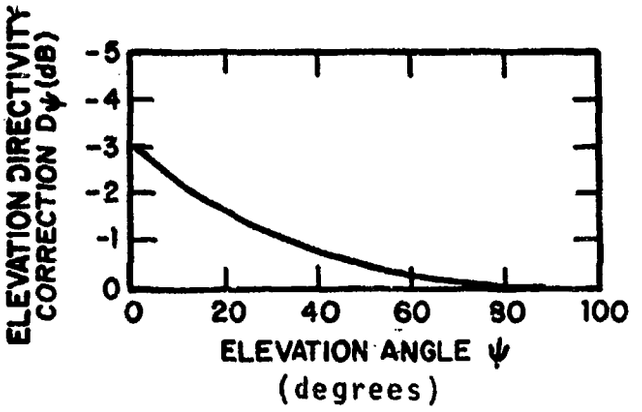

FIG. 37. ELEVATION DIRECTIVITY CORRECTION FOR AUGMENTER WING NOISE

L_p = Sound Pressure Level in One-Third Octave Band
L_{pOA} = Overall Sound Pressure Level
f = Center Frequency of One-Third Octave Band
A = Area of Wing Nozzle Cross-Section
P = Perimeter of Wing Nozzle Section Area
V_j = Velocity of Jet in Wing

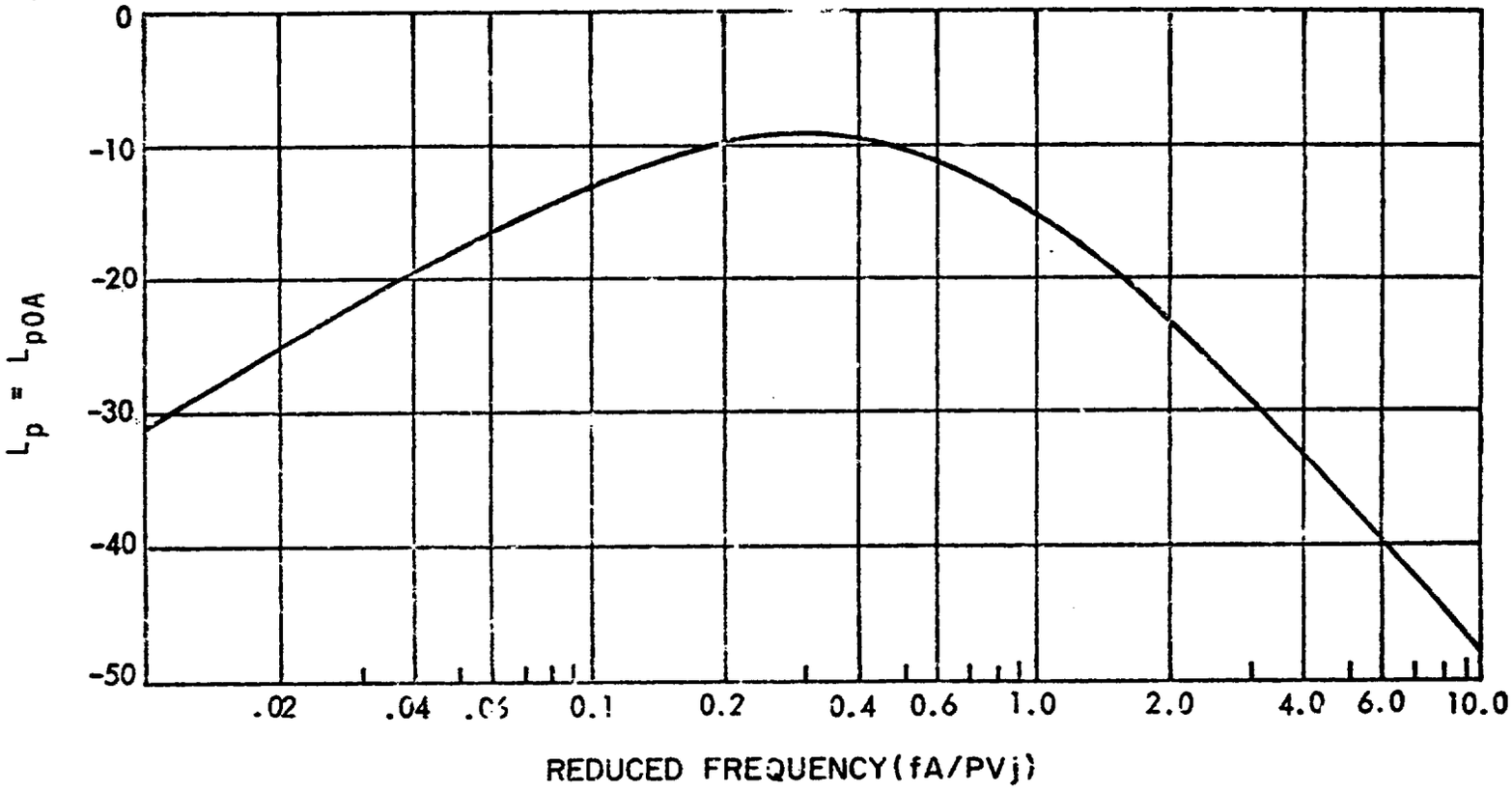

FIG. 38. REDUCED ONE-THIRD OCTAVE BAND SPECTRUM OF AUGMENTER WING NOISE

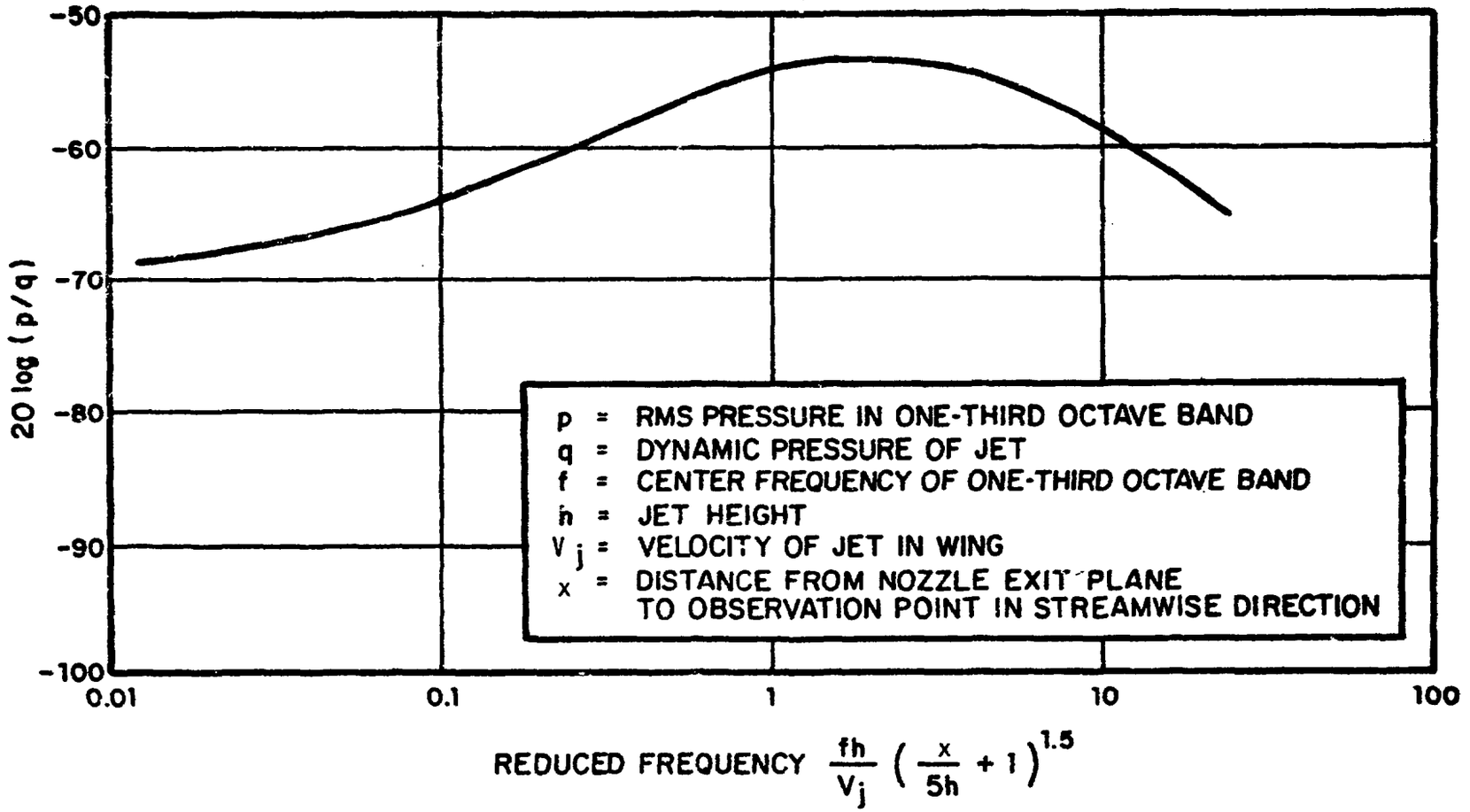

FIG. 39. NON-DIMENSIONAL ONE-THIRD OCTAVE BAND SPECTRUM OF PRESSURE ON AUGMENTER WING FLAP SURFACE (INSIDE AUGMENTER CHANNEL)

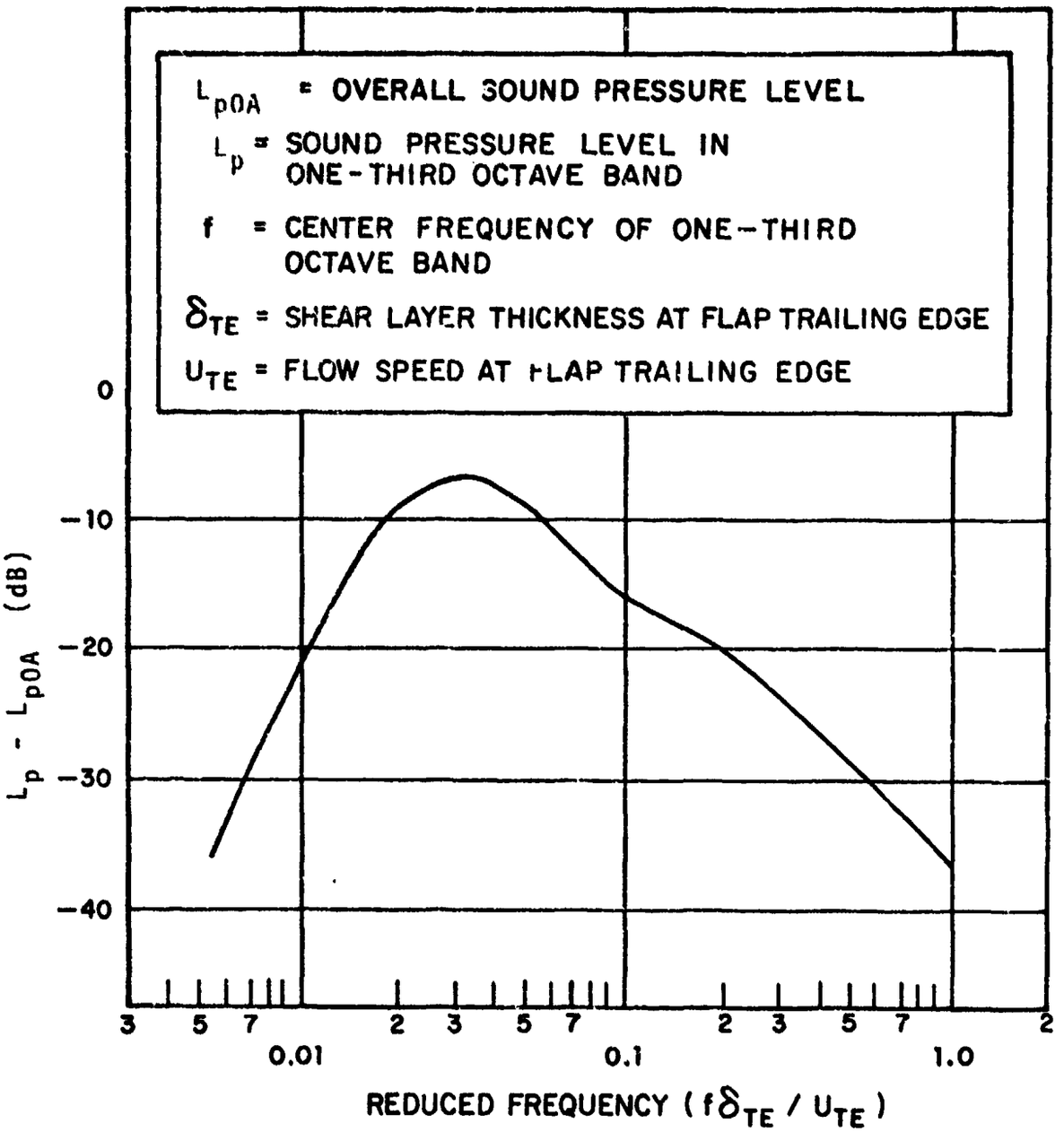

FIG. 40. NONDIMENSIONAL SPECTRUM OF JET FLAP NOISE

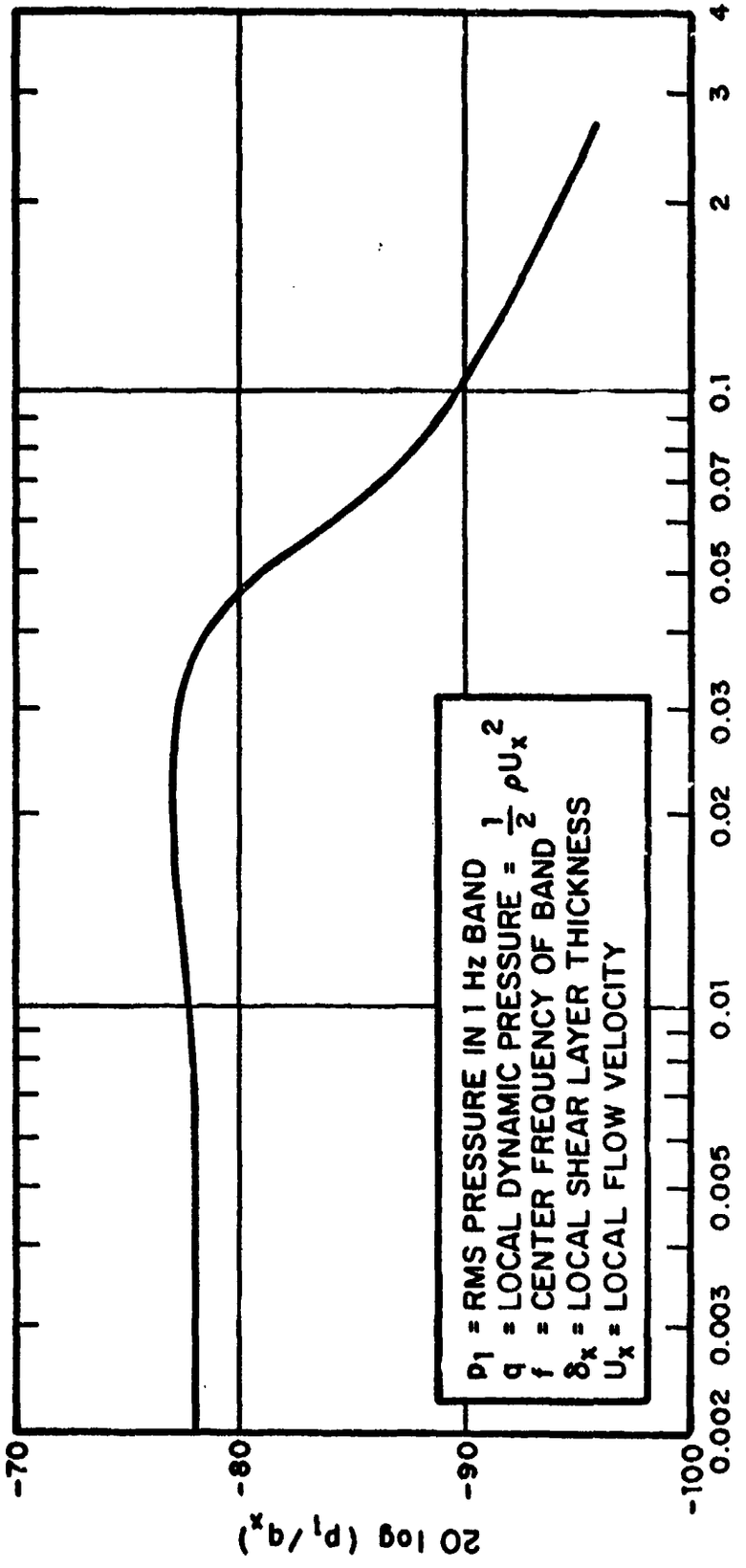

FIG. 41. NONDIMENSIONAL NARROW-BAND SPECTRUM OF PRESSURES ON UPPER SURFACE OF JET FLAP

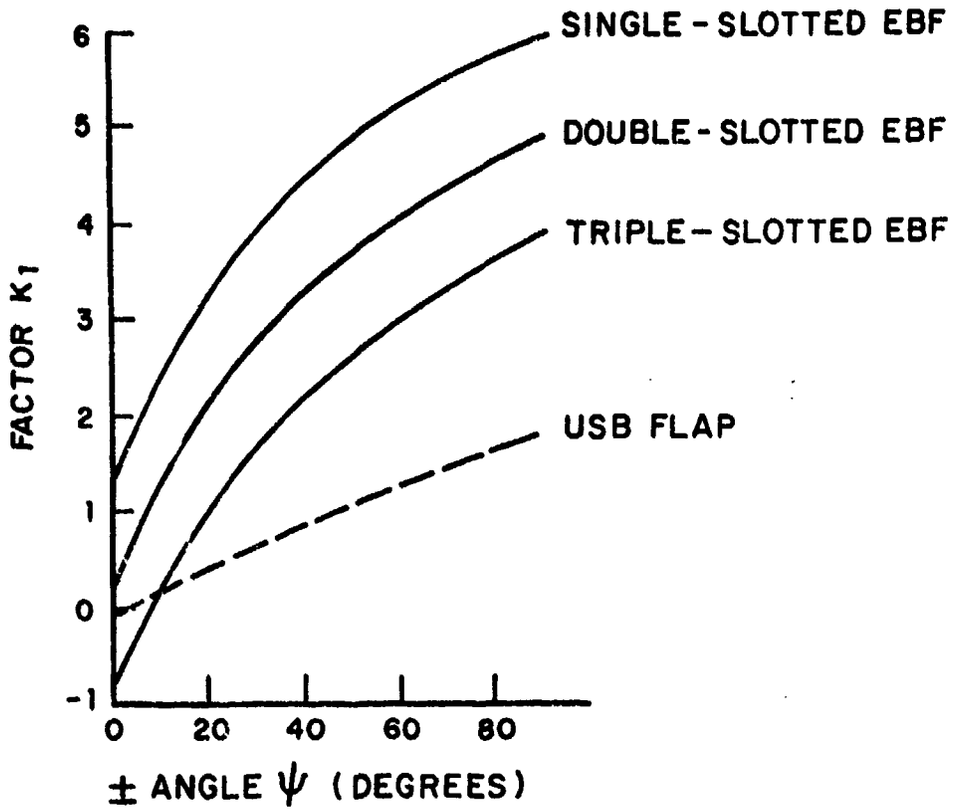

FIG. 42. FACTOR K_1 FOR FORWARD SPEED CORRECTION, EQ. [124], OF NOISE OF EXTERNALLY BLOWN CONFIGURATIONS

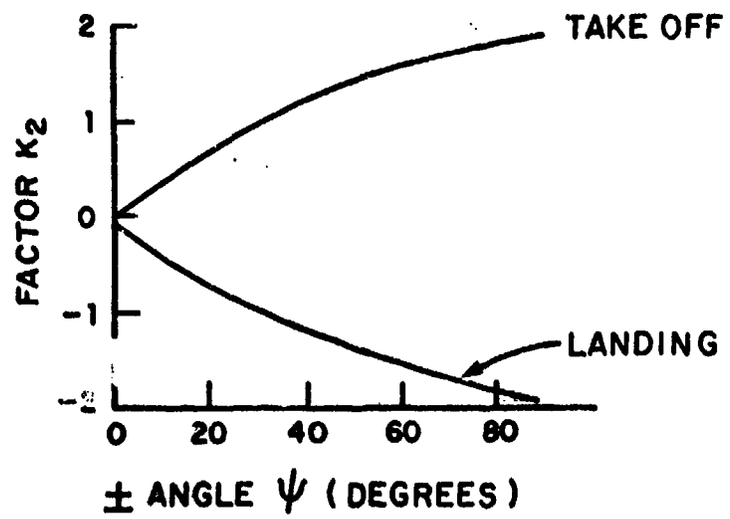

FIG. 43. FACTOR K_2 FOR FORWARD SPEED CORRECTION, EQ. [125] OF AUGMENTER WING NOISE

SECTION VI
NOISE OF PROPELLER/ENGINE SYSTEMS

6.1 General

Fluctuating surface pressures on propeller-driven aircraft result both from the propellers and from the prime mover.

Pressures due to propellers are treated in Sec. 6.2; these pressures are likely to predominate in the vicinity of the propeller disk. The noise from the engines may play a significant role at locations near the engines; this noise is addressed in Sec. 6.3.

6.2 Propeller Noise

6.2.1 Introduction

Noise Components and Mechanisms

Propeller noise generally is considered in terms of two parts:

(1) Rotational noise, which consists of discrete-frequency components at the blade-passage frequency and its harmonics (i.e., at integral multiples of the blade-passage frequency); and

(2) Vortex noise, which has broadband characteristics.

Rotational noise usually predominates, particularly at low frequencies. This noise is associated with (1) the rotation of the steady forces that act on the propeller blades to produce thrust and torque, and (2) unsteady loads acting on the blades due to spatial variation of the inflow to the propeller disk.

Vortex noise is caused primarily by (1) turbulent boundary layer flow off the trailing edges of the propeller blades, and (2) turbulent inflow to the propeller. The latter is negligible in standard tractor propeller installations. Because broadband noise is significant principally in the mid and high-frequency regions, its acoustic nearfield is important only at locations that are much nearer to the propeller disk than is the case for rotational noise.

Limitations of Available Prediction Techniques

Prediction methods for the sound pressures associated with propeller thrust and torque are reasonably well validated, but the associated spatial distributions have not been verified experimentally.

The technical literature includes no discussion or data pertaining to the nearfield of propeller vortex noise. Therefore the method presented here is based on a farfield prediction technique, whose validity for the nearfield remains to be established.

Corrections Required

Corrections for reflections from the aircraft surface are included in the prediction methods presented in this section. For aircraft near the ground, ground reflections must be considered; see Section 3.2.

No corrections to account for the effects of aircraft forward speed are required here beyond those indicated.

6.2.2 Rotational noise (freefield)

(a) Locate the coordinates x, z of the observation point (See Figure 44).

x = axial distance of observation point ahead of propeller plane

z = radial distance of observation point from edge of propeller disk.

(b) If z is less than the propeller diameter D, use the procedure of Section 6.2.2 ; otherwise, use Section 6.2.2.

*Observation Point Between One and Two Propeller Diameters from Axis; 0<z<D (Based on Ref. [6.2.1])**

(a) Calculate the propeller tip Mach Number M_t from

$$M_t = \pi D\ (RPM)/60c \tag{128}$$

and the blade passage frequency f_1 from

$$f_1 = n\ (RPM)/60 \tag{129}$$

where

D = propeller diameter (ft)

RPM = rotational speed (revolutions/min)

c = ambient speed of sound (ft/sec)

n = number of blades

---

* See Sec. 6.2.5 for references for Sec. 6.2.

(b) Find the overall freefield sound pressure level OA
in the propeller plane from

$$OASPL_o = 20 \log W - 40 \log D + 36.6\ M_t + 75.8 - (33.4 - 24.4\ M_t) \log (z/D) + 20 \log (3/n) - 10 \log [(460 + T)/528] \quad (1$$

where

W = power supplied to propeller (hp)

T = temperature of ambient air (°F)

(c) Find the overall freefield sound pressure level L_{pOA} at the observation point from

$$L_{pOA} = OASPL_o + \Delta L, \quad (131)$$

using Figure 45 to find the adjustment term ΔL for the proper reduced axial distance x/D of the observation point.

(d) Calculate the helical tip Mach number M_h from

$$M_h = \sqrt{M_t^2 + M_a^2} \quad (132)$$

where

M_a = Mach number of aircraft.

Then use Figure 46 to find the freefield sound pressure levels at the blade passage frequency and its multiples.

(b) Find the overall freefield sound pressure level $OASPL_o$ in the propeller plane from

$$OASPL_o = 20 \log W - 40 \log D + 36.6 M_t + 75.8 - (33.4 - 24.4 M_t) \log (z/D) + 20 \log (3/n) - 10 \log [(460 + T)/528] \quad (130)$$

where

W = power supplied to propeller (hp)

T = temperature of ambient air (°F)

(c) Find the overall freefield sound pressure level L_{pOA} at the observation point from

$$L_{pOA} = OASPL_o + \Delta L, \quad (131)$$

using Figure 45 to find the adjustment term ΔL for the proper reduced axial distance x/D of the observation point.

(d) Calculate the helical tip Mach number M_h from

$$M_h = \sqrt{M_t^2 + M_a^2} \quad (132)$$

where

M_a = Mach number of aircraft.

Then use Figure 46 to find the freefield sound pressure levels at the blade passage frequency and its multiples.

(e) For observation points on or near the aircraft surface and located axially at $-0.25D<x<0.25D$, correct the freefield levels (to account for reflection) by adding the correction values indicated in Figure 52. For other observation point locations, see Section 3.2.1.

Observation Point Beyond One Propeller Diameter from Edge of Disk; z>D (Based on Ref. [6.2.2])

(a) Find the partial level L_1 from Figure 47.

(b) Calculate the tip Mach number M_t from Equation (128). Use Figure 48 to determine the correction ΔL for tip Mach number and reduced radial distance z/D from the edge of the propeller disk.

(c) Find the correction ΔL_θ directivity from the "average" curve of Figure 49.

(d) Calculate the overall sound pressure level L_{pOA} at the observation point from

$$L_{pOA} = L_1 + \Delta L + \Delta L_\theta + 20 \log (4/n) + 40 \log (15.5/D) - 20 \log r \qquad (133)$$

where

n = number of blades
D = propeller diameter (ft)
r = distance of observer from center of propeller (ft)

(e) Calculate the helical tip Mach number from Equation (132); then use Figure 50 to find the sound pressure levels at the blade passage frequency and its harmonics.

(f) For observation points on or near the aircraft surface and located axially at $-0.25D<x<0.25D$, correct the above calculated freefield levels by adding the correction values given by Figure 52. For other observation point locations, see Section 3.2.1.

6.2.3 Broadband noise (based on ref [6.2.3])

(a) Find the peripheral speed U (ft/sec) of the propeller at 0.7 of its radius from

$$U = 0.7\pi \text{ (RPM) } D/60 \tag{134}$$

and calculate the overall acoustic power level OAWL from

$$OAWL = -40 + 10 \log A_b + 60 \log U \tag{135}$$

where

A_b = Total blade area projected onto blade disk (ft^2)

(b) Evaluate the projected blade thickness d_p from

$$d_p = d \cos\alpha + b \sin\alpha \tag{136}$$

where

d = blade thickness

b = blade chord length

α = blade angle of attack,

all evaluated at the 70% radius position.

(c) Calculate the spectrum peak frequency f_{pk} from

$$f_{pk} = 0.28\ U/d_p \tag{137}$$

and use Table 7 to develop an estimate of the octave band spectrum of acoustic power level PWL.

(d) For each observation point of interest, find the sound pressure level SPL that corresponds to each power level PWL from

$$L_p = PWL - 3 - 20 \log r + 10 \log [1 - J_o(2\beta) \cos 2\theta] \tag{138}$$

where

r = distance of observation point from center of propeller (ft)
β = pitch angle of propeller at 0.7 radius
θ = angle between propeller axis and line from propeller center to observation point

and Figure 51 may be used to evaluate the function $J_o(2\beta)$.

(e) For observation points on or near the aircraft surface and located axially at $-0.25D<x<0.25D$, correct the above calculated freefield levels by adding the correction values given by Figure 52. For other observation point locations, see Section 3.2.1.

6.2.4 Spatial distributions

Rotational Noise

Rotational noise from thrust, torque and thickness effects has a phase pattern that is fixed relative to the propeller blades and rotates with them. The phase (propagation) speeds in the radial and axial directions are sonic, but a Doppler correction must be applied for the axial direction, to account for forward motion of the aircraft.

For the ith order component of noise from an n-bladed propeller, the wavelengths (ft) in the radial, circumferential, and axial directions with respect to the propeller are given by

$$\lambda_r = \lambda_o/s$$

$$\lambda_c = \pi(s + R)/ni$$

$$\lambda_x = \lambda_o[(1 - s^2)^{-\frac{1}{2}} - U/c] \qquad (139)$$

where

$$s = \frac{\sin\theta \left[\frac{1-M_a^2}{M_a}\right]}{-\cos\theta + \sqrt{\cos^2\theta - 1 + \frac{1}{M_a^2}}} \qquad (140)$$

and $\lambda_o = c/f$ denotes the wavelength of sound in air.

Rotational noise due to inflow nonuniformities has a circumferential phase pattern that depends on the spatial distribution of the inflow and that is fixed with respect to the aircraft. The radial and axial wavelengths are the same as those given above for rotational noise due to thrust, torque and thickness effects.

Vortex Noise

No information is available on which to base a method for estimating the spatial correlations associated with vortex noise.

6.2.5 References for Sec. 6.2

6.2.1 Franken, P.A., *et al.* "Methods of Flight Vehicle Noise Prediction" WADC TR 58-343, November 1958

6.2.2 Metzger, , Magliozzi, , Towk, and Gray, "A Study of Propeller Noise Research" United Aircraft 1961

6.2.3 Ungar, E. E, *et al.* "A Guide for Predicting the Aural Detectability of Aircraft" AFFDL - TR-71-22; March 1972

6.2.4 Hubbard, H. H. and Regier, A. A. "Free-Space Oscillating Pressures Near Tips of Rotating Propellers" NACA TR 996; 1960

6.2.6 List of Symbols for Sec. 6.2

Symbol	Definition	Units*	
A_b	total propeller blade area projected onto blade disk	ft^2	(m^2)
D	propeller diameter	ft	(m)
$J_0(2\ )$	function of Fig. 51	---	
$L_p(f_i)$	sound pressure level at rotational noise frequency f_i	dB	
L_pOA	overall sound pressure level	dB	
M_a	Mach number of aircraft	---	
M_h	helical tip Mach number	---	
M_t	propeller tip Mach number	---	
R	propeller radius	ft	(m)
RPM	rotational speed	rpm	
T	temperature of ambient air	°F	
U	peripheral speed of propeller at 0.7 radius	ft/sec	(m/s)
W	power supplied to propeller	Hp	
b	blade chord length	ft	(m)
c	speed of sound in ambient air	ft/sec	(m/s)
d	blade thickness	ft	(m)
d_p	projected blade thickness (see Eq. B.6)	ft	(m)
f_i	blade passage frequency	Hz	
f_{pk}	frequency at spectrum peak	Hz	
n	number of blades	---	
r	distance of observer from propeller center	ft	(m)

*SI units are given in parentheses, where appropriate. The units shown here are typical ones. Where use of specific units is required for certain calculations, this is indicated in the text.

Symbol	Definition	Units	
x,z	coordinates (see Fig. 44)	ft	(m)
α	blade angle of attack	deg	
β	pitch angle of propeller at 70% of radius	deg	
θ	angle of r with propeller axis (see Figs. 44, 49)	deg	
λ_c	wavelength in circumferential direction	ft	(m)
λ_r	wavelength in radial direction	ft	(m)
λ_x	wavelength in axial direction	ft	(m)
λ_0	wavelength of sound in air	ft	(m)

TABLE 7

OCTAVE-BAND SPECTRUM OF PROPELLER VORTEX NOISE

f_{OB}/f_{pk}	½	1	2	4	8	16
$L_{WOA} - L_W$	8	4	8	9	13	14

f_{OB} = center frequency of octave band

f_{pk} = peak frequency of vortex noise spectrum

L_{WOA} = overall acoustic power level

L_W = acoustic power level in octave band

6.3 Engines

6.3.1 Turboshaft engines

The noise of a turboshaft engine contains contributions from the compressor and the exhaust jet. In this regard it is like a turbojet engine, and the same estimation procedures apply for these components. However, a turboshaft engine may also generate a significant amount of "mechanical noise" or "casing noise," which combines with that due to the other two major sources to constitute the total noise.

The empirical prediction methods described below are of questionable reliability, since they are based on field data [6.3.1, 6.3.2]* obtained on stationary power-plant gas turbine engines. Although these methods also do not take directivity into account and although their applicability to the nearfield is not known, they are the best available.

Jet Exhaust

Proceed as in Section 4.2.

If insufficient information is available to apply those techniques, proceed as in Section 6.3.1. for casing noise, but use the reduced spectra of Figure 54 instead of those of Figure 53.

Compressor

Proceed as in Section 4.3.

If insufficient information is available to apply these techniques, proceed as in Section 6.3.1 for casing noise, but

---

* See Sec. 6.3.3 for references.

use the reduced spectra of Figure 55 instead of those of Figure 53.

CASING

(a) Calculate the shaft frequency f_s and the blade passage frequency f_B from

$$f_s = RPM/60$$

$$f_B = N \cdot f_s \qquad (141)$$

where RPM denotes the shaft RPM and N the number of compressor blades.

(b) Use Figure 53 to develop two octave-band power level spectra; one based on f_s, one based on f_B.

(c) Develop a single power level spectrum, as follows:

i) For frequencies below f_s, use the levels from the spectrum based on f_s.

ii) For frequencies between f_s and $f_B/4$, use the higher of the levels given by the two spectra developed above.

iii) For frequencies above $f_B/4$, use the levels from the spectrum based on f_B.

(d) Determine the octave-band sound pressure level values L_p from the sound power level values determined above by using

$$L_p = L_w - 20 \log R - 1 \qquad (142)$$

where R is the distance from the engine to the observation point, in feet.

6.3.2 Piston engines

The noise of a piston engine typically contains contributions from the exhaust and intake, as well as "mechanical" or "casing" noise, which remains if the intake and exhaust are fully muffled. The same empirical estimation approach is used here for each of the three noise components.

The empirical prediction technique described below is based on correlation [6.3.1] of data for about 50 engines rated between 9 and 3850 Hp and operating at between 225 and 1800 rpm [6.3.2]; none of these engines were of the aircraft type. Although this technique also includes no directivity and specific nearfield corrections, it is the only generally useful one available.

(a) Calculate the engine firing frequency f_F from

$$f_F = (RPM)N_c/60\eta \qquad (143)$$

where RPM represents the engine rpm, N_c the number of cylinders, and η the number of revolutions per firing (for one cylinder).*

(b) Evaluate the octave-band power-level spectrum associated with each noise component by using Figure 56.

(c) Use Equation (142) to convert each power level spectrum to a sound pressure level spectrum.

6.3.3 Rotary combustion (wankel) engines

As for a piston engine, the noise of a rotary combustion engine is made up of contributions from the exhaust, intake, and casing. The same empirical estimation approach is used here for

* Most spark-ignition engines take two revolutions for completion of a four-stroke cycle, so that $\eta = 2$. For two-stroke cycle engines, a firing occurs for each revolution, and $\eta = 1$.

each of the three components.

The empirical prediction technique described here is based on a very limited amount of data [6.3.3] based on three different double-rotor engines yielding between 30 and 105 hp and running at 2500 to 5000 rpm. Applicability of this technique to grossly different engines is questionable.

(a) Evaluate the octave-band power level spectrum associated with each component by using Figure 57.

(b) Use Equation (142) to convert each power level spectrum to the corresponding pressure level spectrum.

6.3.3 References for Sec. 6.3

6.3.1 Ungar, E.E., *et al.*, "A Guide for Predicting the Aural Detectability of Aircraft," AFFDL-TR-71-22

6.3.2 Miller, L., "Acquisition and Study of Noise data of Diesel and Gas Engines," BBN Report No. 1476.

6.3.3 Berkowitz, M., Hermes, W., and Lamping, H., "Rotating Combustion Engine Evaluation for Low Noise Aircraft Applications," Curtis-Wright Corp., Report CW-WR-69-078.F, January 1970.

6.3.4 List of Symbols for Sec. 6.3

Symbol	Definition	Units*
H_p	engine power output	H_p
$(H_p)_{rated}$	rated engine power	H_p
L_p	sound pressure level	dB
L_W	sound power level in octave band	dB
N	number of compressor blades	---
N_c	number of cylinders	---
R	distance from engine to observation point	ft
RPM	engine speed	rpm
f	center frequency of octave band	Hz
f_B	blade passage frequency	Hz
f_F	firing frequency	Hz
f_s	shaft rotation frequency	Hz
n	number of revolutions per firing	---

*The estimation techniques of this section require use of the specific units indicated here.

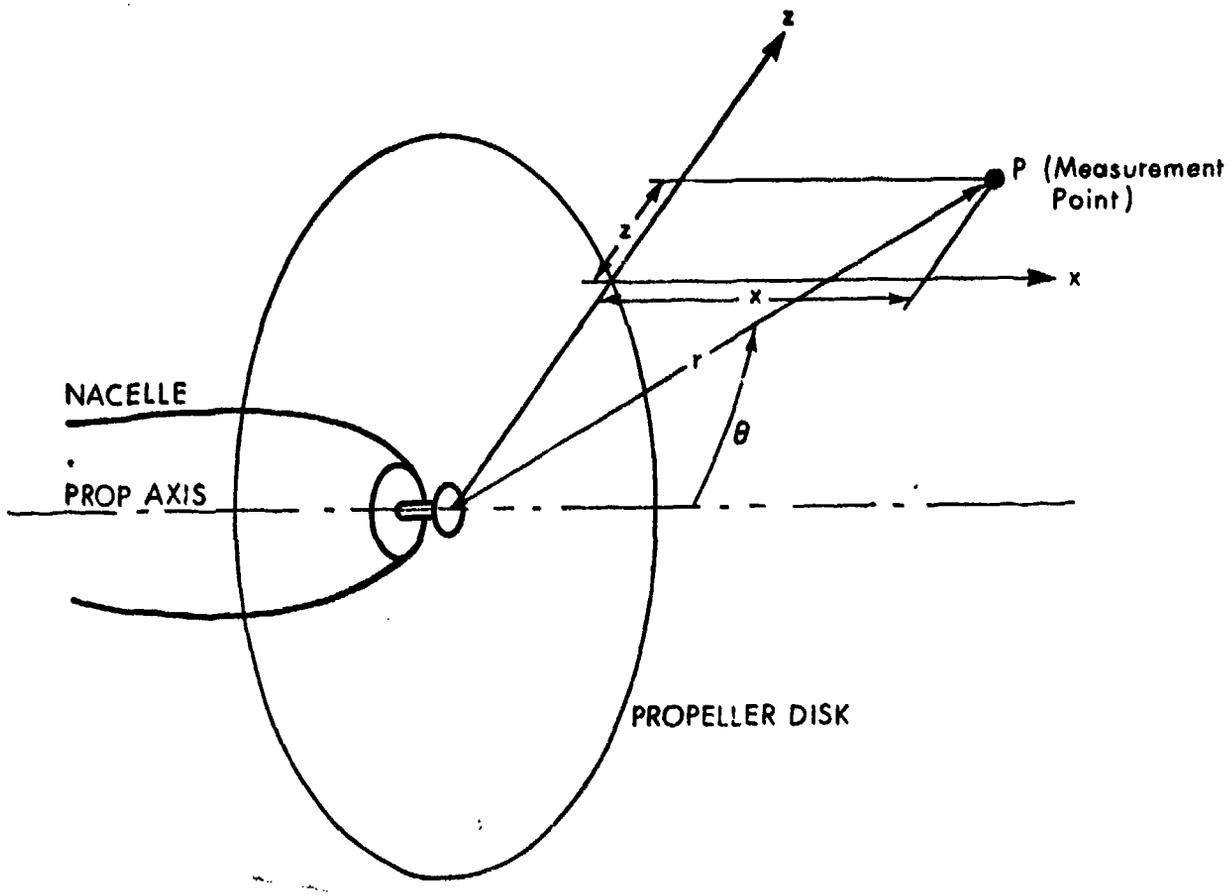

FIG. 44. COORDINATES OF OBSERVATION POINT RELATIVE TO PROPELLER

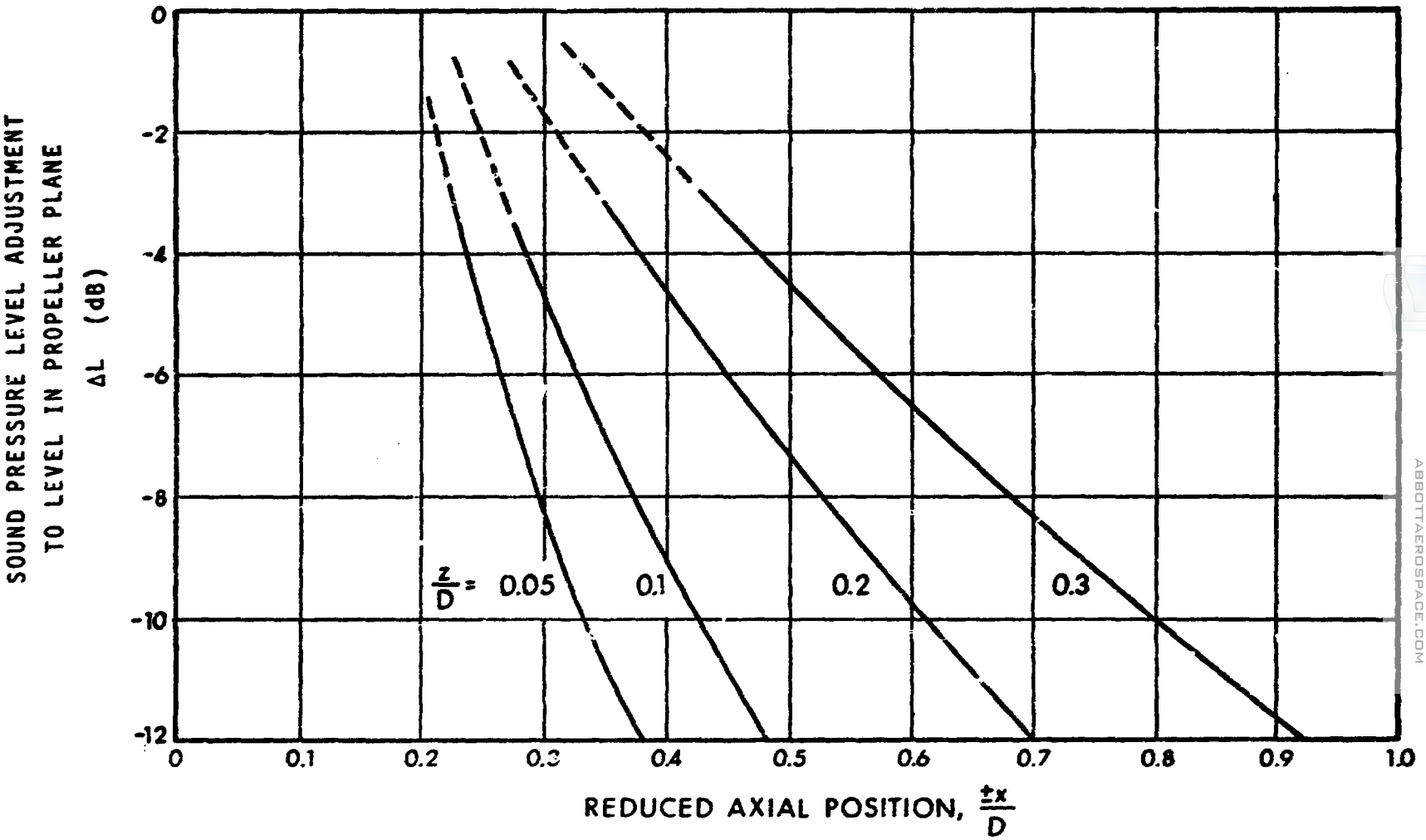

FIG. 45. CORRECTION OF OVERALL, FREE-SPACE PROPELLER NOISE LEVELS FOR AXIAL POSITION FORE AND AFT OF PROPELLER PLANE.

$L(f_i)$ = Sound pressure level of ith harmonic (dB, re 2×10^{-5} N/M^2)

L_{pOA} = Overall sound pressure level

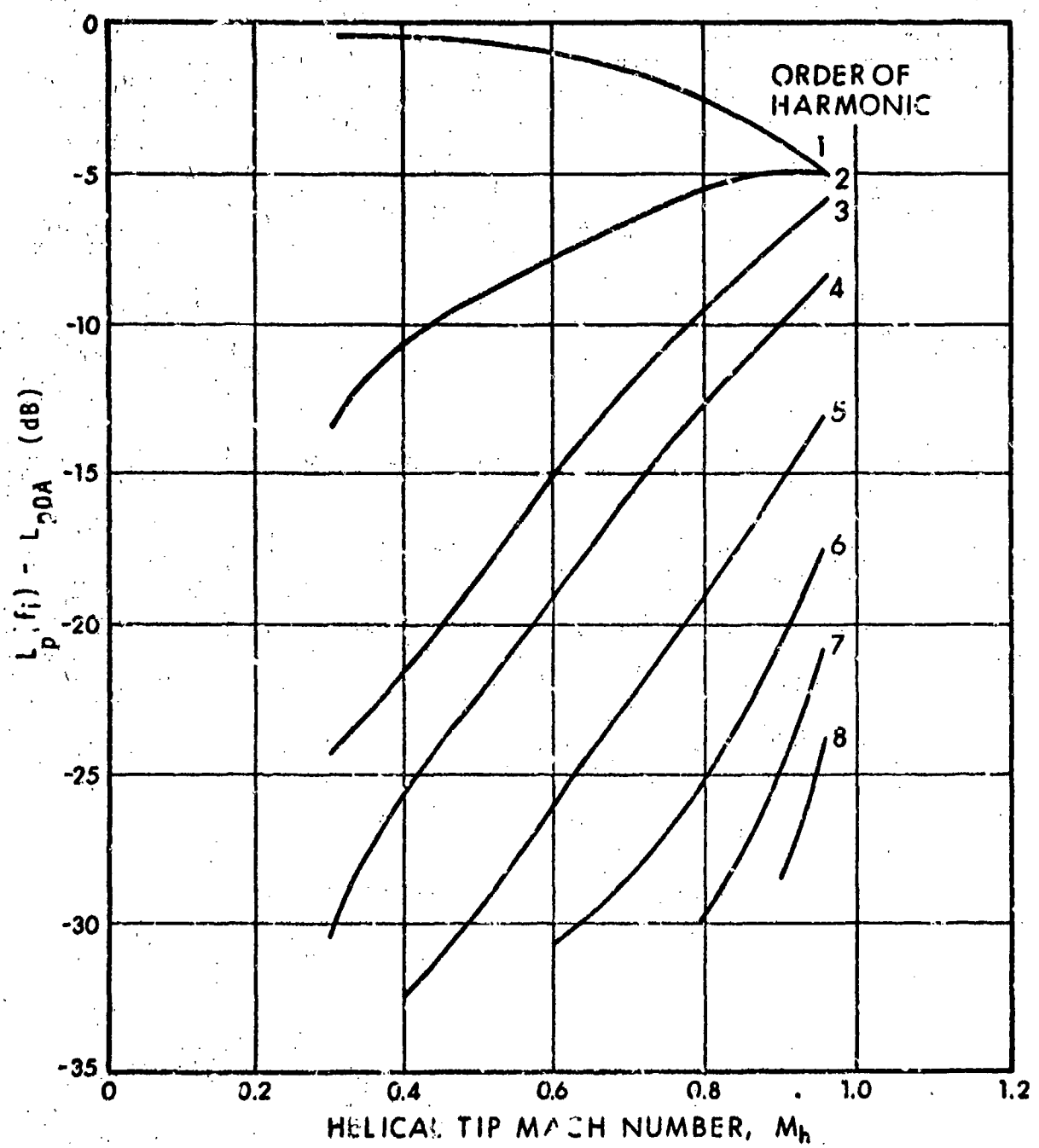

FIG. 46. SOUND PRESSURE LEVELS AT ROTATIONAL NOISE FREQUENCIES f_i

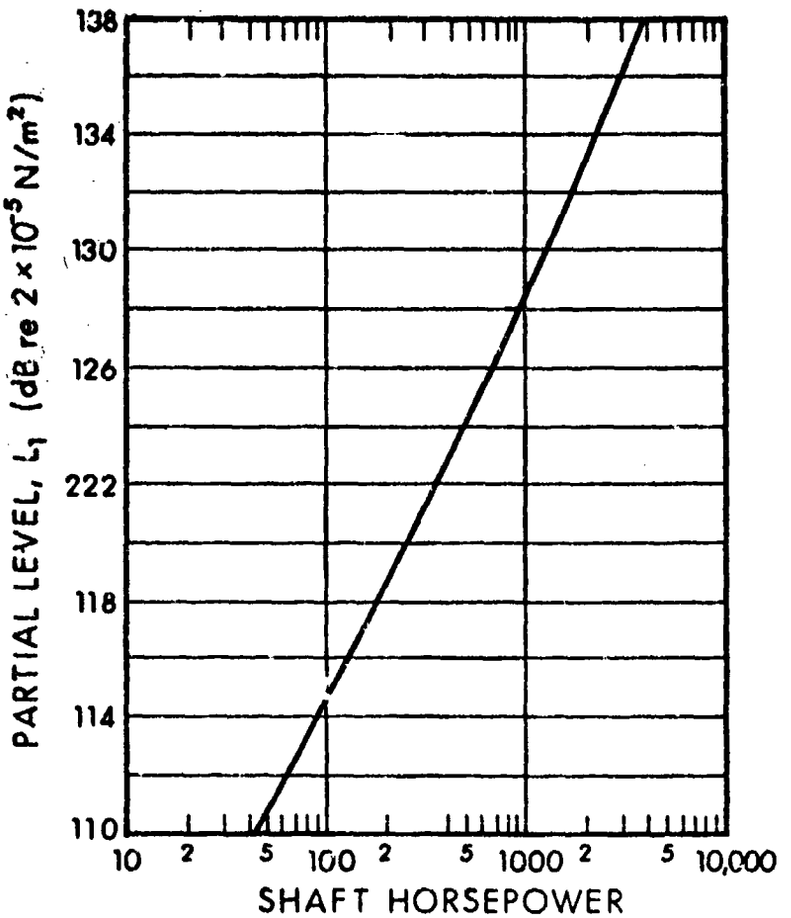

FIG. 47. PARTIAL LEVEL OF PROPELLER ROTATIONAL NOISE

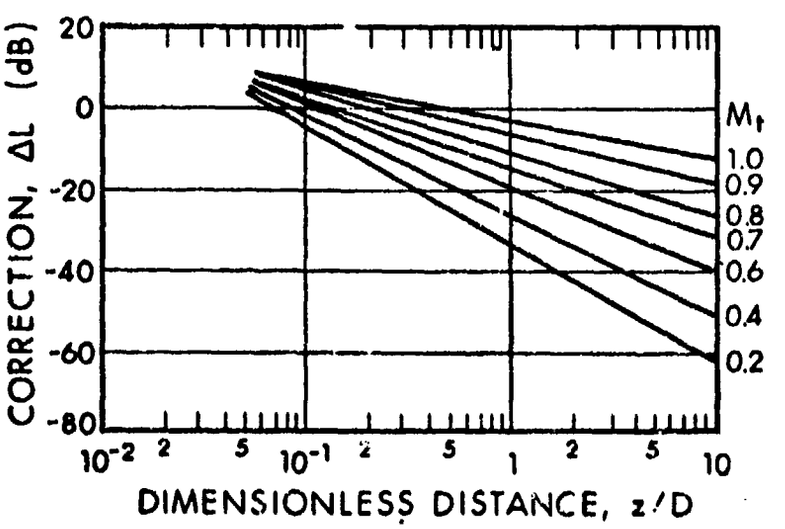

FIG. 48. CORRECTION OF PROPELLER ROTATIONAL NOISE FOR SPEED, TIP MACH NUMBER AND RADIAL DISTANCE.

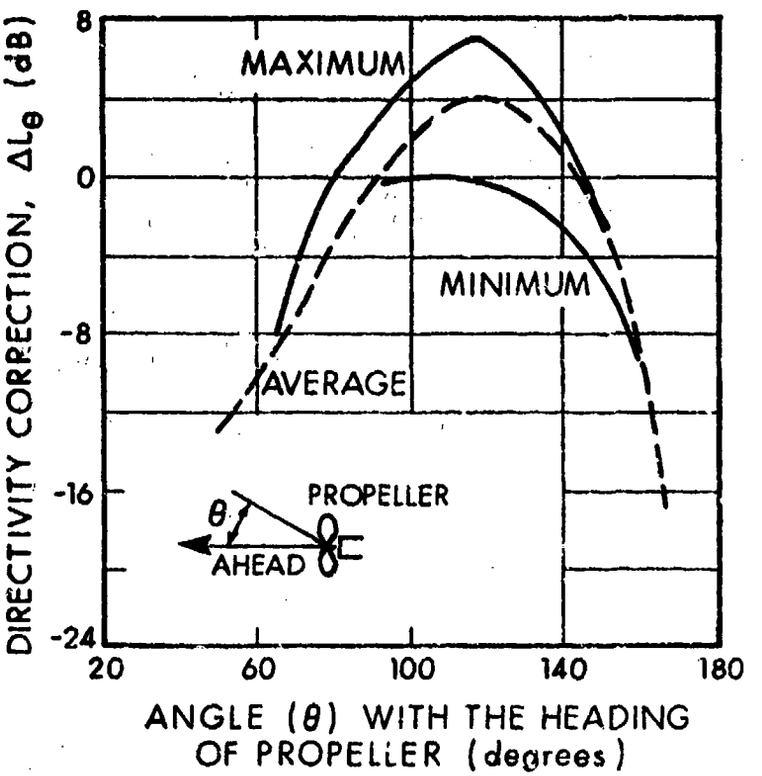

FIG. 49. CORRECTION FOR DIRECTIVITY OF PROPELLER ROTATIONAL NOISE

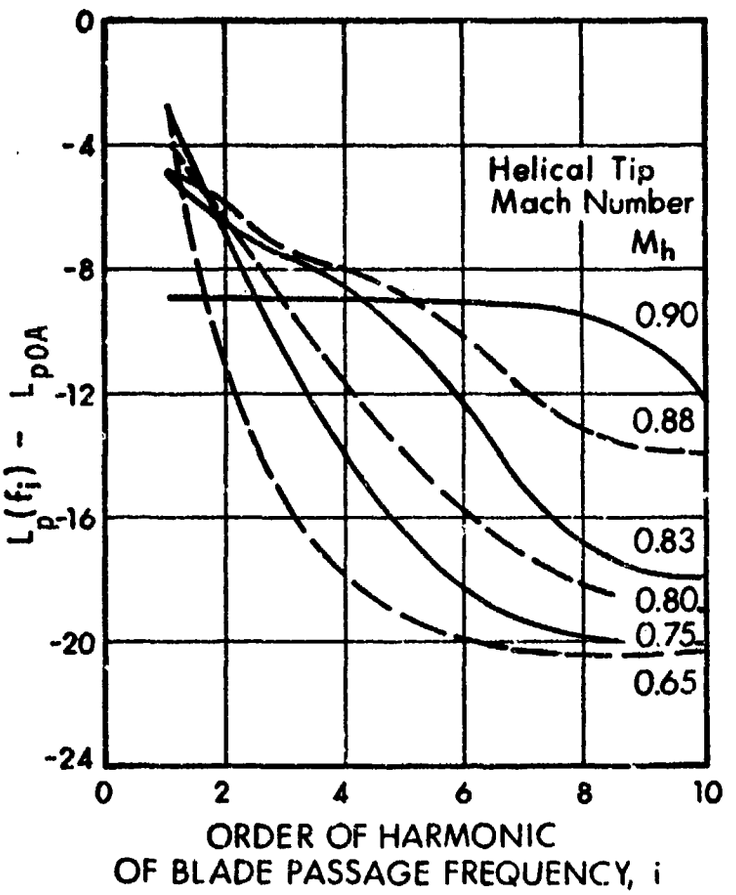

FIG. 50. SOUND PRESSURE LEVELS AT ROTATIONAL NOISE FREQUENCIES $f_i = if_1$
(i=1 corresponds to blade passage frequency)

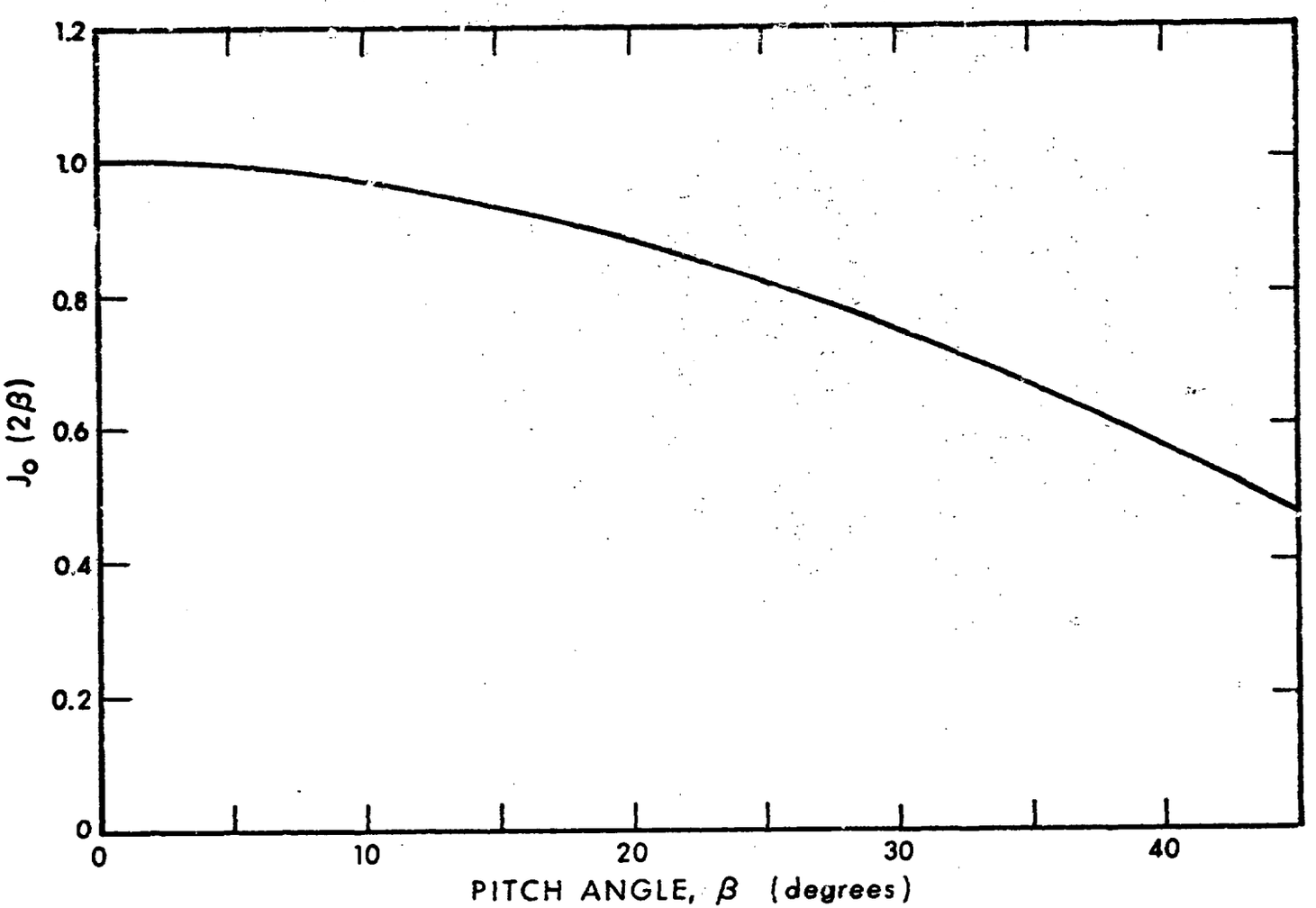

FIG. 51. THE FUNCTION J_0 OF EQ. [138].

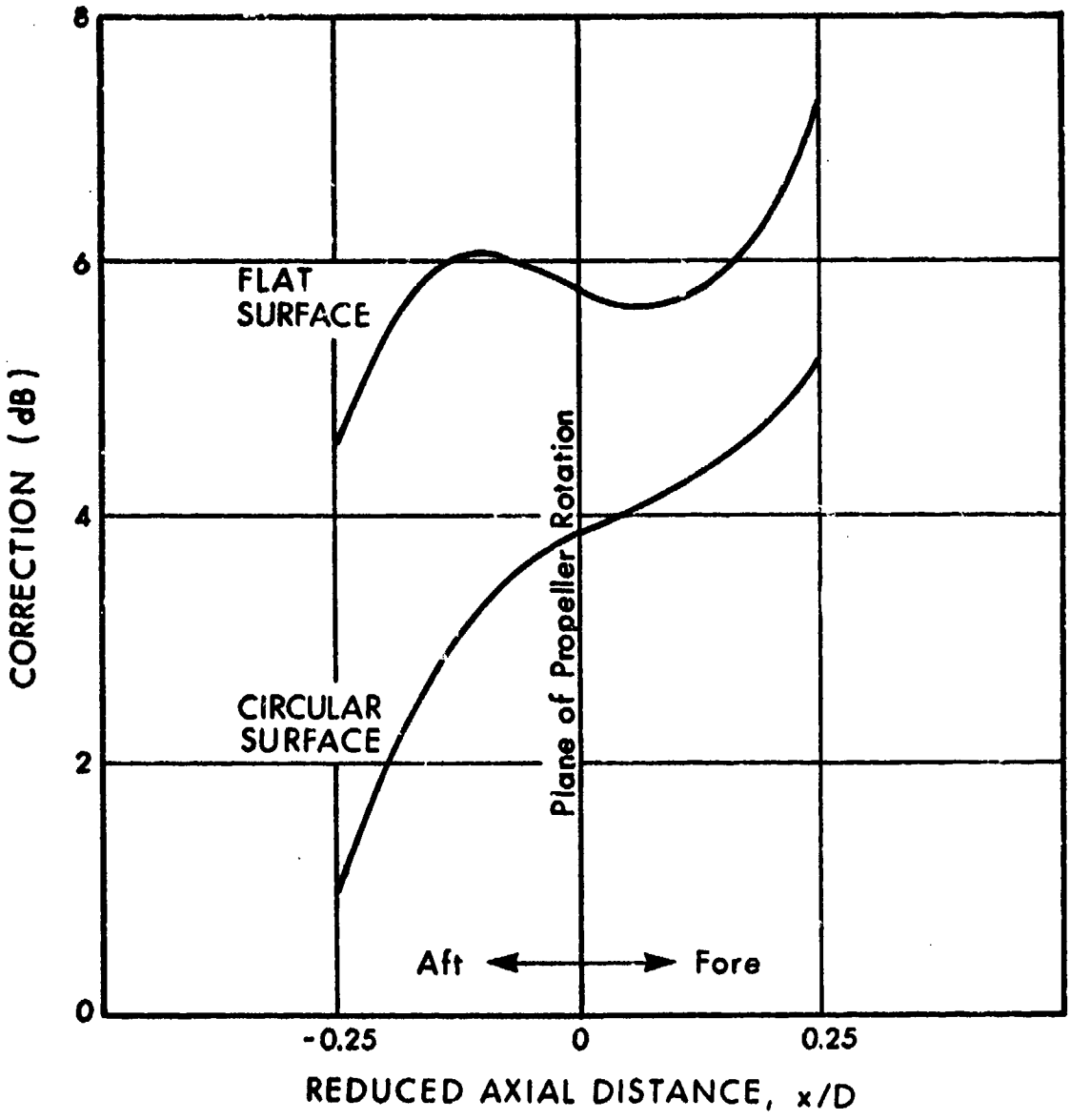

FIG. 52. CORRECTION FOR PROPELLER NOISE REFLECTION AT AIRCRAFT SURFACE [6.2.2, 6.2.4]

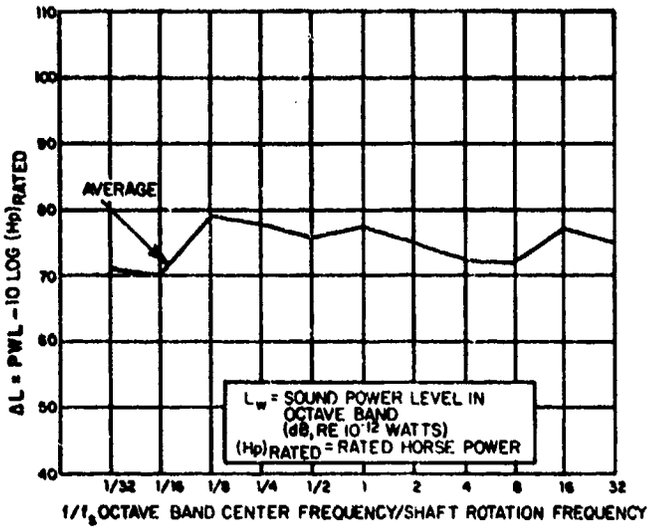

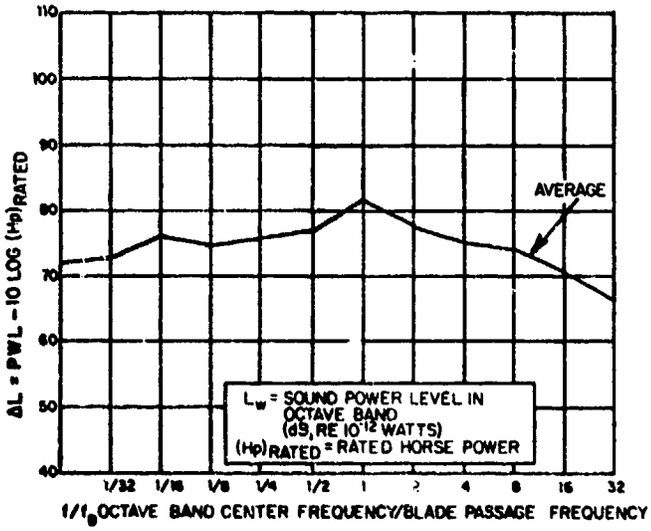

FIG. 53. REDUCED CASING NOISE SPECTRA OF TURBOSHAFT ENGINES [6.3.1].

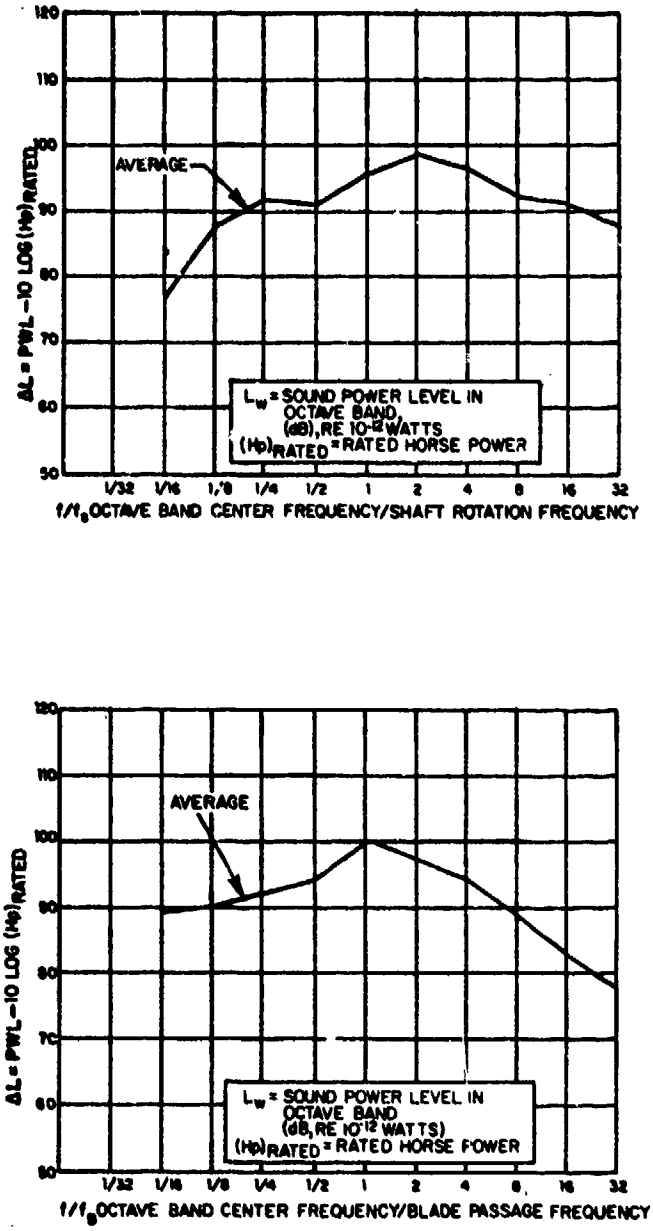

FIG. 54. REDUCED EXHAUST NOISE SPECTRA OF TURBOSHAFT ENGINES [6.3.1].

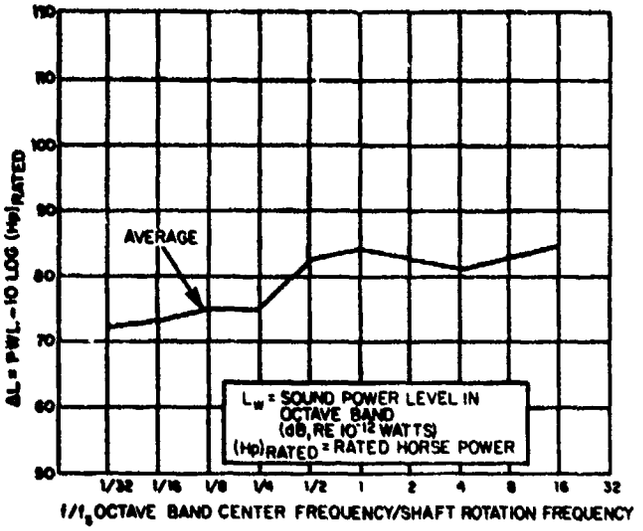

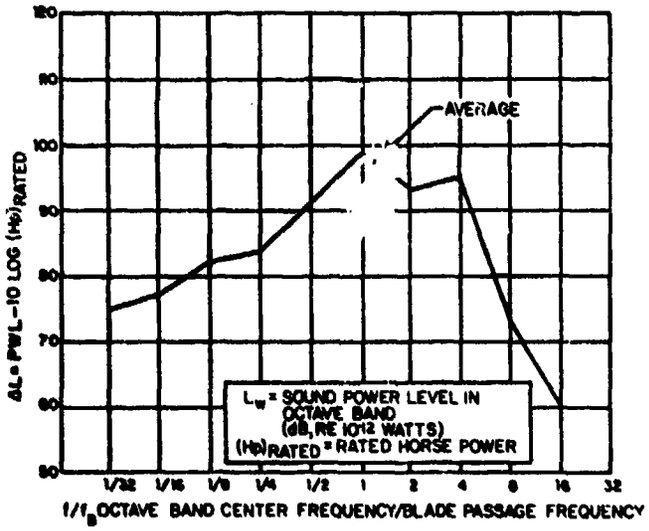

FIG. 55· REDUCED INLET NOISE SPECTRA OF TURBOSHAFT ENGINES [6.3.1].

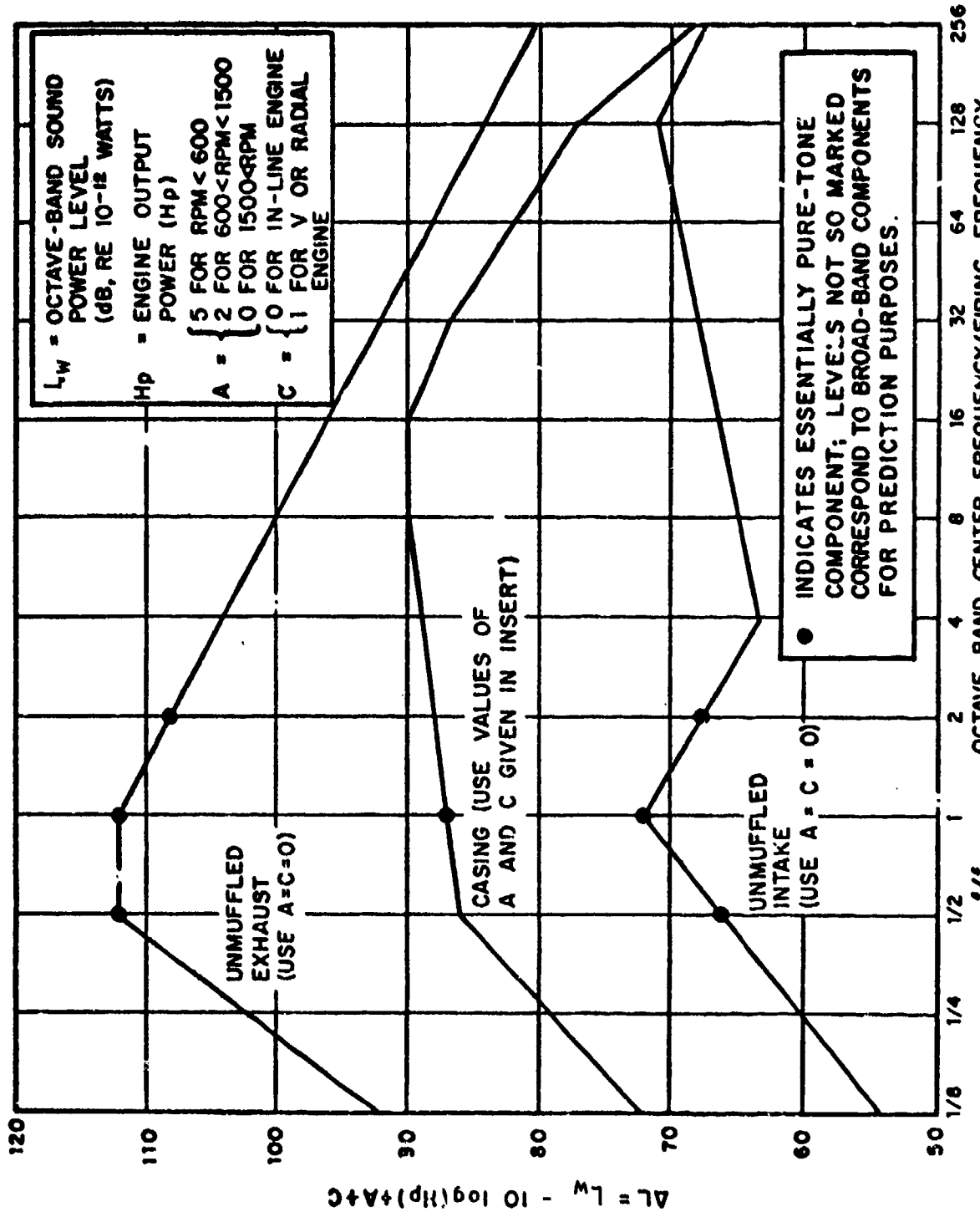

FIG. 56. REDUCED SPECTRA FOR ESTIMATION OF NOISE OF PISTON ENGINES.

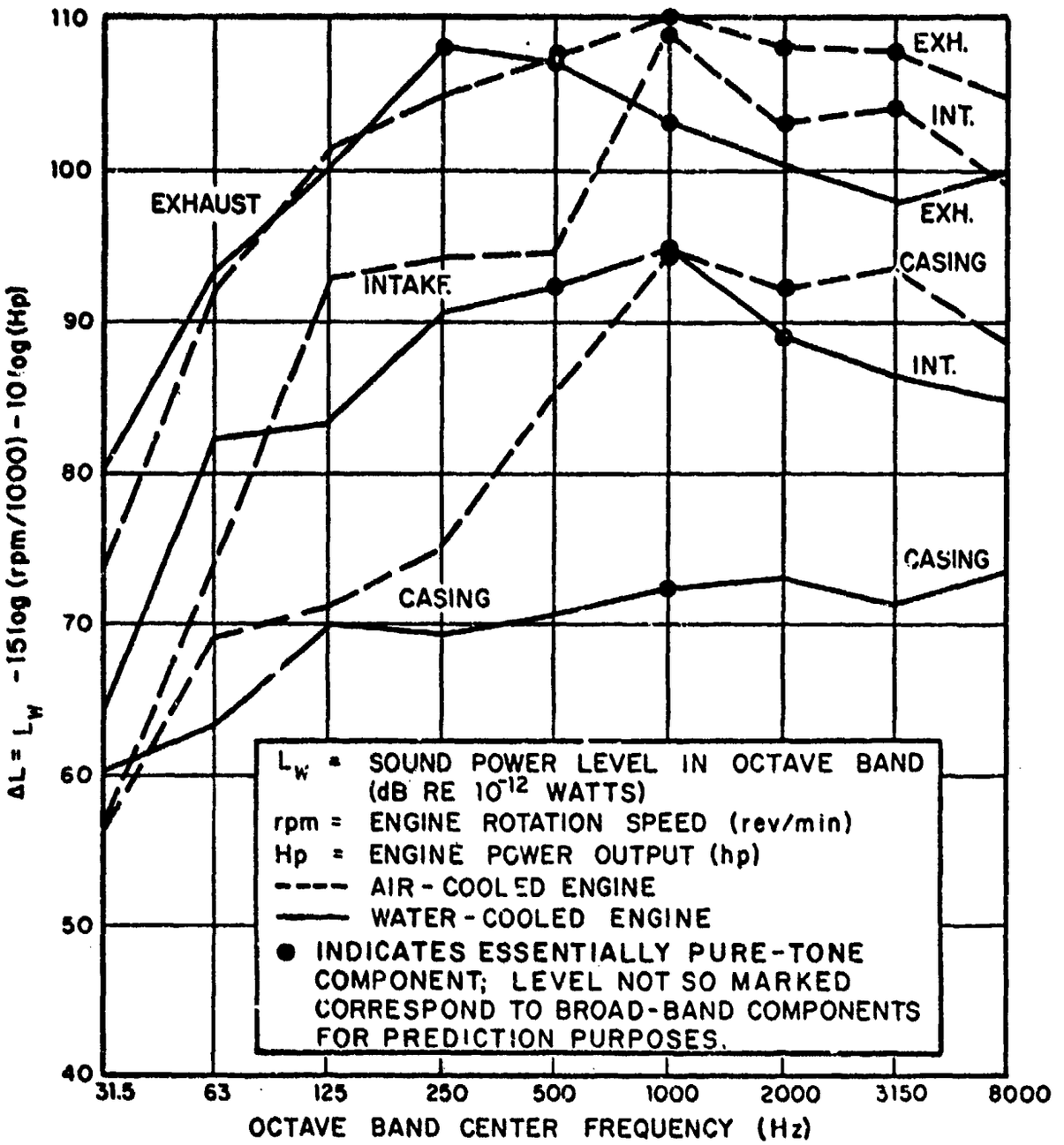

FIG. 57. REDUCED SOUND POWER SPECTRA OF ROTARY COMBUSTION ENGINES.

SECTION VII

BLAST PRESSURES DUE TO ARMAMENT

7.1 Closed Breech Weapons

Each firing of a round produces a blast due to the rapid escape of the propellant gases from the nozzle. The blast overpressure (measured from ambient atmospheric conditions) at a given observation point rises very rapidly to its peak value, then decays more slowly and typically overshoots the zero value slightly toward the negative. For practical estimation purposes, the pressure signature of a single blast may be represented as a triangular pulse with zero rise-time; that of blasts from an automatic weapon may be represented as a sawtooth-like series of such pulses. (See Figure 58.)

7.1.1 Peak Overpressure

The estimation methods presented here apply to the free-field; i.e., in absence of any reflecting surfaces. These values must be corrected as indicated in Section 3.2.1, to account for reflection at the receiving surface.

Stationary Aircraft

(a) Determine the axial and lateral distances x and R of the observation point from the end of the barrel, and find the reduced (dimensionless) distances x/C and R/C, where C denotes the caliber of the weapon (i.e., the inside diameter of the barrel).

(b) For $-30<x/C<80$ and $0<R/C<90$, use Figure 59 to determine the value of the reduced peak overpressure $\Delta P\ C^2 b/E$, extrapolating the given curves and interpolating between them, as needed.

For observation point locations outside the above-mentioned range, calculate the angle θ that a line drawn from the muzzle to the observation point makes with the direction of projectile travel, using

$$\theta = \arctan(R/x) \tag{144}$$

Then find where a line drawn from the origin of Figure 59 at that angle intersects the outermost curve; read the corresponding value $(\Delta P\ C^2b/E)_a$ and the coordinates x_a/C, R_a/C of the intersection*. Calculate the reduced overpressure at the observation point from

$$\Delta P\ C^2b/E = (\Delta P\ C^2b/E)_a \left(\frac{x_a^2 + R_a^2}{x^2 + R^2}\right)^{3/4} \tag{145}$$

(c) From the value of $\Delta P\ C^2b/E$ determine as above, calculate the peak overpressure ΔP. Here b represents the barrel length and E the energy release from the gun blast.

Moving Aircraft

The effect of aircraft motion is to increase the pressure ahead of the barrel and to reduce it in the aft region. In order to account for this effect, multiply the value of ΔP obtained for stationary aircraft by

$$\frac{(\Delta P)_{\text{moving}}}{\Delta P} = \left(1 + \frac{U^2}{2n}\right)\left(0.7\cos\theta + \sqrt{1 - 0.49\sin^2\theta}\right)^3 \tag{146}$$

* Note: The subscript a has been appended to the symbols representing values read here from Fig. 59.

where U denotes the aircraft speed in the direction of projectile travel, η represents the energy released per unit mass of propellant, and Θ is given by Equation (144).

7.1.2 Impulse, pulse duration, and spectrum

The impulse I associated with a gun blast is defined as the area under the positive portion of the overpressure-vs-time curve; see Figure 58. Typical units of I are psi-msec. Estimation of the impulse is required for estimation of the pulse duration and frequency spectrum. The procedures described here apply for moving, as well as for stationary aircraft.

Impulse

(a) Determine the reduced axial and radial distances, x/C and R/C, of the observation point from the end of the barrel.

(b) For $-30<x/C<90$ and $0<R/C<90$, use Figure 60 to determine the value of the reduced Impulse $IC^{5/4}b^{3/4}/E$ corresponding to the observation point location. Extrapolate and interpolate from Figure 60, as necessary.
For observation point locations outside of the aforementioned range, calculate the angle Θ from Equation (144), and draw a corresponding line from the origin of Figure 60. Determine where this line intersects the outermost curve on the Figure, and read the corresponding values* of x_i/C, r_i/C and $(IC^{5/4}b^{3/4}/E)_i$.

*Note: The subscript i has been appended to the symbols representing values determined here from Fig. 60.

Then calculate the reduced impulse at the observation point from

$$IC^{5/4}b^{3/4}/E = (IC^{5/4}b^{3/4}/E)_i \left[\frac{x_i^2 + R_i^2}{x^2 + R^2}\right]^{3/8} \qquad (147)$$

(c) Calculate I from the value of $IC^{5/4}b^{3/4}/E$ determined above.

Pulse Duration

Find the duration T_I of the pulse (see Figure 58) from

$$T_I = 2I/\Delta P \qquad (148)$$

Spectrum

For a single pulse (Figure 58 a), the frequency content is best described by the spectral density $S(\omega)$. If the idealized pulse is approximated by a triangular shape, its spectral density is given by

$$S(\omega) = \frac{(\Delta P)^2}{2\pi^2\omega^4 T_I^2}\left[(\omega T_I)^2 + 2(1-\cos\omega T_I - \omega T_I \sin\omega T_I)\right] \qquad (149)$$

For a pulse train (Figure 58b), the spectrum consists of components at discrete frequencies $f_n = n/T_R$; n = 1, 2, 3, ..., where T_R denotes the time between pulses. The amplitude A_n of the component at frequency f_n is given by

$$A_n = \frac{\Delta P}{2\pi^2 n^2 \alpha}\left[(2\pi\alpha n)^2 + 2\,(1-\cos 2\pi\alpha n - 2\pi\alpha n \sin 2\pi\alpha n)\right]^{1/2} \qquad (150)$$

where

$$\alpha = T_I/T_R \quad . \qquad (151)$$

7.1.3 Spatial correlation

(a) Approximate the surface at the location of interest by a plane. Determine the distance r_o of this plane from the center of the muzzle. (Note: this distance is measured along a line perpendicular to the plane.)

(b) Calculate the correlation length ℓ for the component at frequency f from

$$\ell = \left[\frac{C}{2\pi f} \left(2r_o - \frac{C}{2\pi f}\right)\right]^{\frac{1}{2}} \quad \text{for } f > \frac{C}{4\pi r_o} . \tag{152}$$

For $f \leq C/2\pi r_o$, the correlation length is essentially zero.

(c) Find the correlation coefficient corresponding to a separation distance ξ (in any direction along the surface of interest) from

$$\rho(\xi) = \begin{cases} \exp(-\xi/\ell) & \text{for } f > C/4\pi r_o \\ 0 & \text{for } f \leq C/4\pi r_o \end{cases} \tag{153}$$

7.2 Open-Breech (Recoilless) Weapons

Recoilless weapons emit a forward blast from the muzzle, as well as a rearward blast from the open breech. The nozzle blast predominates near the muzzle and forward of the weapon; the breech blast predominates near and behind the breech. Both blasts may make similar contributions directly at the side of the weapon; in general, the contributions from both blasts must be evaluated and superposed.

Little is known about the effect of aircraft flight speed on the blast fields produced by recoilless weapons. Because of this absence of information and because such weapons typically are used

only at relatively low flight speeds, the estimation techniques indicated here may be used for all flight speeds of usual interest.

The pressures and pressure spectra found by the methods given below pertain to the freefield. Effects of reflections at aircraft surfaces must be taken into account as indicated in Sec. 3.2.1.

7.2.1 Muzzle blast

(a) Calculate the peak overpressure ΔP (psi) at the observation point from

$$\Delta P = 11.8 \times 10^{-3} P_c (C/R)^{1.1} \qquad (154)$$

where P_c represents the chamber pressure (psi), C the caliber (inside barrel diameter, in.), and R the distance from the center of the muzzle to the observation point.

(b) Calculate the corresponding impulse I (psi-sec) from

$$I = (0.335)\ (P_c E^2)^{1/3}\ (C/R)^{0.208} \qquad (155)$$

where E represents energy in the propellant minus the kinetic energy of the projective.

(c) Estimate the pulse duration T_I from Equation (148).

(d) Determine the corresponding spectral density from Equation (149).

(e) Determine the corresponding pressure correlations from Sec. 7.1.3.

7.2.2 Breech blast

(a) Determine the angle Θ (degrees) between the centerline of the weapon and a line drawn from the center of the breech to the observation point, where $\Theta = 0$ corresponds to the direction directly toward the rear of the weapon.

(b) Calculate the peak overpressure ΔP (psi) at the observation point from

$$\Delta P = 10^{-3} P_c (R/C)^{0.006630 - 1.48} \exp(5.82 - 0.0428\,\Theta) \tag{156}$$

where, as in Equation (154), P_c represents the chamber pressure (psi), C the caliber of the weapon (in.), and R the distance (in.) from the center of the muzzle to the observation point.

(c) Calculate the corresponding impulse I (psi-sec) from

$$I = 0.1\,(P_c E^2)^{1/3}\,(R/C)^{0.003790 - 0.904} \exp(6.30 - 0.3620\,) \tag{157}$$

(d) Determine the pulse duration T_I by use of Equation (148) and calculate the spectral density from Equation (149).

(e) Evaluate the corresponding pressure correlations by application of Sec. 7.1.3.

7.3 List of Symbols for Sec. VII

Symbol	Definition	Units*	
A_n	amplitude of pressure component	lb/ft^2	(N/m^2)
C	caliber (inside diameter of barrel)	ft	(m)
E	energy release from gun blast	ft-lb	(Nm)
I	impulse	$lb\text{-}sec/ft^2$	(NS/m^2)
P_c	chamber pressure	lb/in^2	(N/m^2)
R	lateral distance of observation point from end of barrel	ft	(m)
$S(\omega)$	spectral density	$sec^2lb^2ft^{-4}$	$(S^2N^2m^{-4})$
T_I	pulse duration	sec	(s)
T_R	time between pulses	sec	(s)
U	aircraft speed in direction of projective travel	ft/sec	(M/S)
b	barrel length	ft	(m)
f	frequency	Hz	
ℓ	correlation length	ft	(m)
r_0	distance of surface plane from muzzle	ft	(m)
x	axial distance of observation point from end of barrel	ft	(m)
ΔP	overpressure	lb/in^2	(N/m^2)
α	T_2/T_R	---	
η	energy released per unit mass of projectile	ft lb/slug	(mN/kg)
θ	angle between barrel axis and line from muzzle to observation point	deg	
ξ	separation distance	ft	(m)
ρ	correlation coefficient	---	
ω	radian frequency	rad/sec	

*SI units are shown in parentheses where appropriate. The units indicated here are typical ones; where equations require the use of specific units, this is indicated in the text.

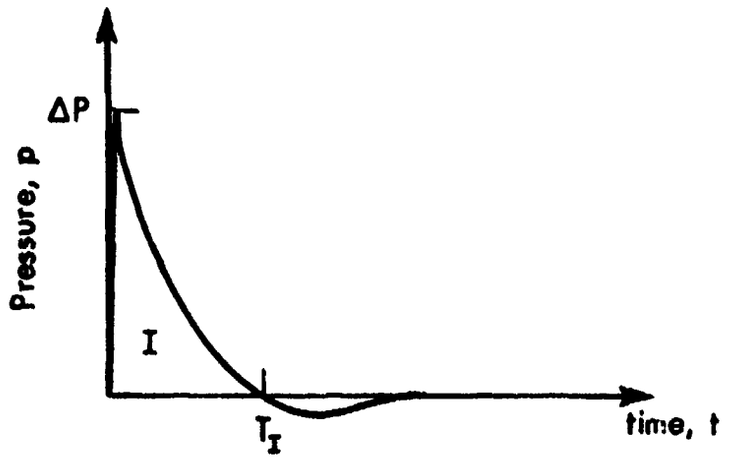

a. TYPICAL SINGLE PULSE

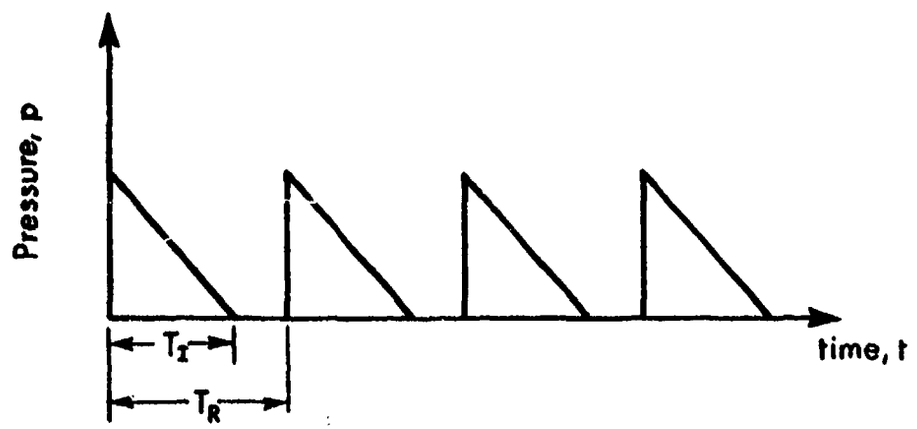

b. IDEALIZED PULSE TRAIN FOR AUTOMATIC WEAPON

FIG. 58. IDEALIZED GUN-BLAST OVERPRESSURE PULSES

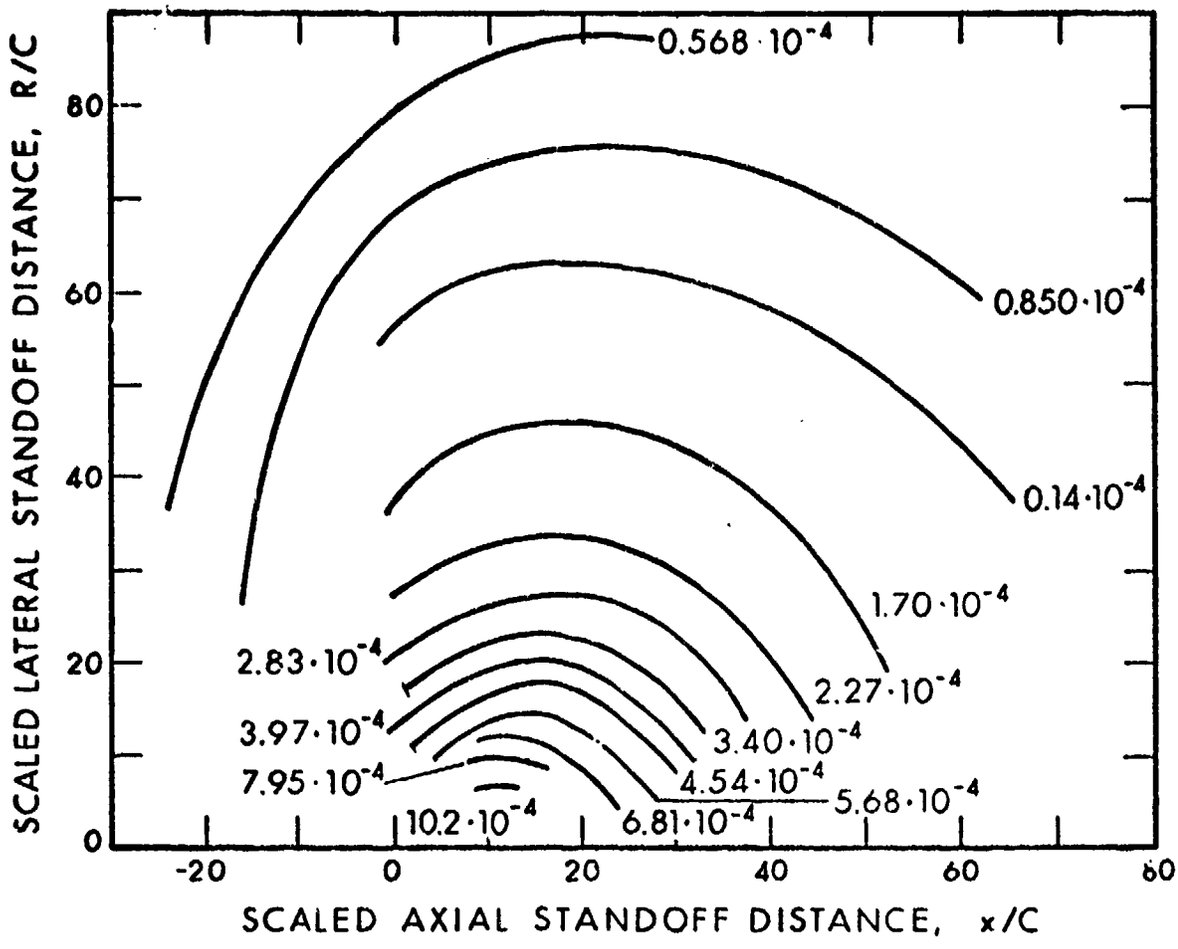

FIG. 59. CURVES OF CONSTANT SCALED OVERPRESSURE $\Delta P \cdot C^2$ b/E FOR CLOSED-BREECH WEAPONS [6.2].

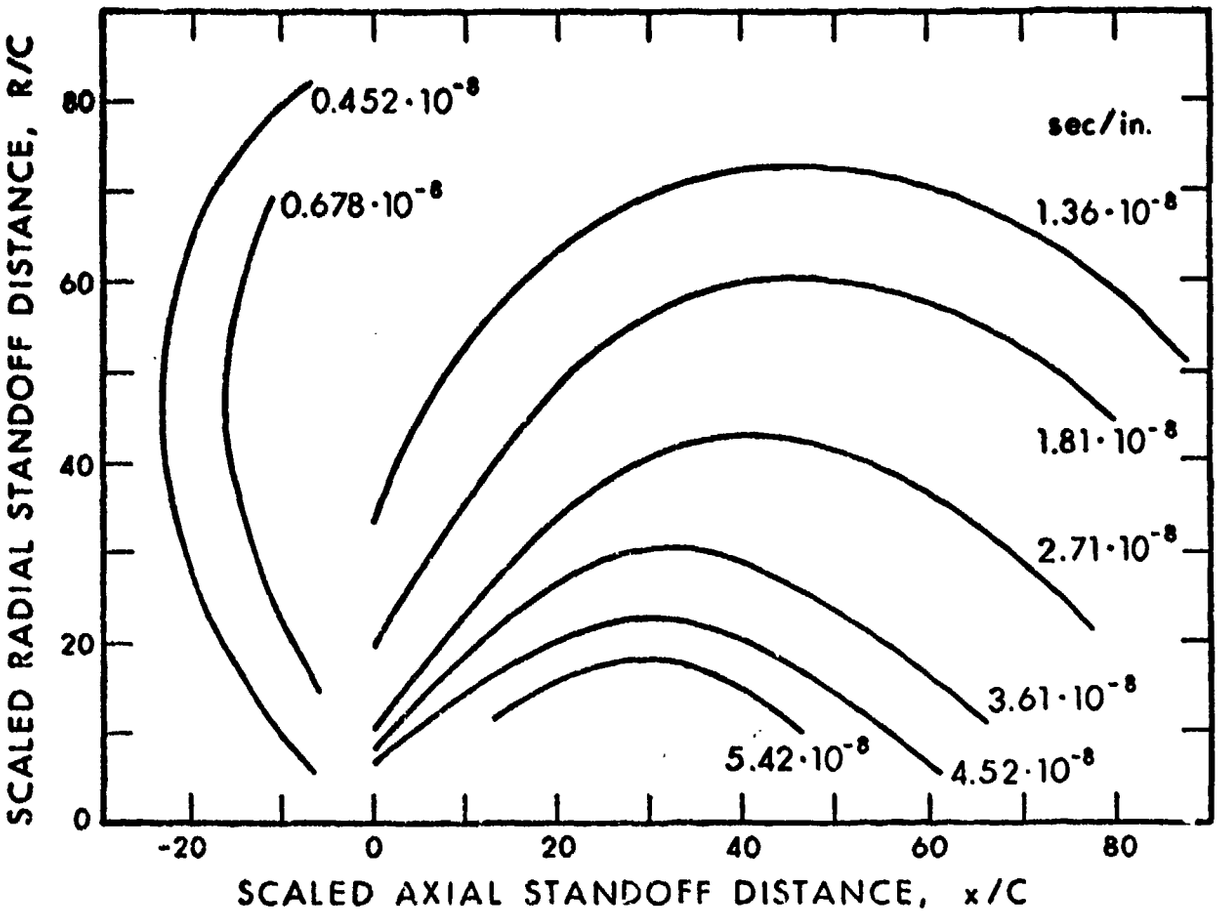

FIG. 6.0. CURVES OF CONSTANT SCALED IMPULSE $IC^{5/4} b^{3/4}/E$ FOR CLOSED-BREECH WEAPONS [6.2].

SECTION VIII
BOUNDARY LAYER PRESSURE FLUCTUATIONS

8.1 Turbulent Boundary Layers

Boundary layers develop as a consequence of the effect of viscosity; they are smooth (laminar) at low Reynolds numbers and become turbulent at Reynolds numbers that exceed a critical value. This critical value depends on the local pressure gradient; for zero pressure gradient the critical Reynolds number based on the distance of the observation point from the point of streamline reattachment is of the order of 5×10^6, but for non-zero gradients it may be smaller or greater than this value by a factor of about 100.

The structure of a turbulent boundary layer (and thus the pressure it exerts on a surface to which it is attached) depends not only on the Reynolds and Mach numbers, but also on the surface roughness, the pressure gradient, and the velocity field outside of the boundary layer. For prediction of the fluctuating pressures associated with a turbulent boundary layer, one needs to know its local properties, particularly its displacement thickness. There exists no simple analytical method for predicting this thickness for practical configurations. If this displacement thickness and other aerodynamic parameters are not known from wind-tunnel or flight tests, use of very approximate empirical prediction relations is indicated.

8.1.1 Rms pressure

Estimate the root-mean-square pressure $\bar{p}$ at a point under a turbulent boundary from

$$\bar{p}/q = \begin{cases} 0.006/(1 + 0.14\ M^2) & \text{for } M < 5 \\ 0.00133 & \text{for } M \geq 5 \end{cases} \qquad (158)$$

where q and M denote the dynamic pressure and Mach number, respectively, both as measured in the free-stream.

8.1.2 Power Spectral Density

For subsonic free-stream flows ($M < 1$) find the power spectral density S(f) from*

$$S(f) = \frac{2}{\pi} \frac{\bar{p}^2\ \delta^*}{U} \left[1 + \left(\frac{2\pi f \delta^*}{U}\right)^2\right]^{-1} . \qquad (159)$$

For supersonic free-stream flows ($M > 1$), find the power spectral density S(f) from

$$S(f) = \frac{2\ \bar{p}^2\ \delta^*}{U} \left[1 + \left(\frac{4\pi f \delta^*}{U}\right)^{0.9}\right]^{-2} \qquad (160)$$

Here δ^* denotes the boundary layer displacement thickness, U the free-stream flow speed, f the frequency (in Hertz), and $\bar{p}^2 = (\bar{p})^2$ the mean-square pressure as found from equation

8.1.3 Pressure levels in frequency bands

For subsonic free-stream flows calculate the mean-square pressure $p^2_{\Delta f}$ in a band between frequencies f_1 and f_2 from

---

* Where δ^* is not known from data, take $\delta^* = \delta/8$ for $M < 1$, where δ denotes the boundary layer thickness.

$$p^2_{\Delta f} = \bar{p}^2 \frac{1}{\pi^2} \left[\arctan\left(\frac{2\pi f_2 \delta^*}{U}\right) - \arctan\left(\frac{2\pi f_1 \delta^*}{U}\right) \right] \tag{160}$$

For supersonic free-stream flows, calculate $p^2_{\Delta f}$ by integrating S(f) of Equation (160) between f_1 and f_2. (Numerical integration is indicated here, because no closed form solution is available.)

Alternately, calculate $p^2_{\Delta f}$ approximately by multiplying the values found from Equation (160) by $F(f_c)$, where

$$F(f_c) = \frac{\pi + 20\pi f_c \delta^*/U}{1 + 20\pi f_c \delta^*/U} \tag{162}$$

$$f_c = (f_1 + f_2)/2$$

Find the corresponding sound pressure levels by use of Equation (8).

8.1.4 Spatial correlations

The pressure correlation coefficient at radian frequency ω may be estimated from

$$\rho(\xi,\eta) = A_\xi A_\eta \cos(\omega\xi/U_c) \tag{163}$$

where

$$A_\xi = \exp(-0.1\,\omega\xi/U_c)\,[0.5 + 0.5\exp(-0.07\xi/\delta^*)]$$

$$A_\eta = \begin{cases} \exp(-1.4\,\omega\eta/U_c)\,[0.3 + 0.7\exp(-0.055\eta/\delta^*)] & \text{for } \alpha \le 0.7\theta. \\ \exp(-0.223\omega\eta/U_c)\,[0.73 + 0.27\exp(-0.135\eta/\delta^*)] & \text{for } \alpha \ge 0.7\theta. \end{cases} \tag{164}$$

and

$$U/U_c = 0.675 + 0.3\exp(-0.11\omega\delta/U) - 0.25\exp(-0.38\xi/\delta) \tag{165}$$

Here ξ and η denote the separation distances in the streamwise and lateral directions, respectively, U_c represents the convection velocity, α denotes the angle of attack, and θ the half angle of a cone approximating the surface locally.

8.2 Transitional Boundary Layers

In a transitional boundary layer, the boundary layer structure changes from laminar to fully turbulent. Transition is a sensitive phenomenon that depends strongly on Reynolds number, surface roughness, surface discontinuities, and pressure gradients. Because of the complexity and parameter sensitivity of transitional boundary layers, their characteristics can be estimated only roughly.

8.2.1 Rms pressure

Estimate the rms pressure $\bar{p}$ under a transitional boundary layer from

$$\bar{p}/q = 0.006 \Big/ (1 + 0.013M^2) \quad , \tag{166}$$

where q and M denote the dynamic pressure and Mach number in the free stream.

8.2.2 Power spectral density

Estimate the power spectral density S(f) from

$$S(f) = \frac{2}{\pi} \frac{\bar{p}^2 \ \delta_t}{U} \left[1 + \left(\frac{2\pi f \ \delta_t}{U}\right)^2\right]^{-1} \tag{167}$$

where the rms pressure $\bar{p}$ is found from Eq.(166) , U represents the local free-stream velocity, f the frequency (in Hertz), and δ_t the transitional flow length. If δ_t is not known from aerodynamic data, estimate it from

$$\delta_t/\delta^* = 2.9 \ (1 + 0.013M^2)^2 \ , \tag{168}$$

where δ^* denotes the boundary layer displacement thickness.

8.2.3 Pressure levels in frequency bands

Use Eqs. (161) and (162), but with δ^* replaced by δ_t, to find the mean square pressure in each band of interest. Find the corresponding sound pressure level by use of Eq. (8).

8.2.4 Spatial correlations and convection velocities

Find the turbulent boundary layer convection velocity U_c by use of Eq. (164); estimate the convection velocity U_{ct} for the transitional boundary layer from

$$U_{ct} = 0.7\, U_c \quad . \tag{169}$$

Estimate the spatial correlations by use of Eqs. (163), with

$$A_\xi = \exp\left(-0.06\omega\xi/U_{ct}\right)\left[0.6 + 0.4 \exp\left(-0.024\xi/\delta^*\right)\right]$$

$$A_\eta = \exp\left(-\beta\cdot\omega\eta/U_{ct}\right)\left[0.6 + 0.4 \exp\left(-0.024\eta/\delta^*\right)\right] \tag{170}$$

$$\beta = \begin{cases} 0.68 & \text{for } \alpha \le 0.7\theta \\ 0.446 & \text{for } \alpha > 0.7\theta \end{cases}$$

8.3 Separated Flows

Separated flow occurs where a boundary layer detaches itself from a surface, resulting in a region of flow reversal often characterized by unsteadiness and the formation of large turbulent eddies or vortices.

In general, separation is associated with a sharp edge or corner, or with an adverse pressure gradient. The separated flow behind bluff bodies is a special case, called base flow, and is treated in Sec. 8.4. In supersonic flow, flow separation and shocks often occur simultaneously and interact to produce a shock oscillation phenomenon that can generate intense fluctuating pressures.

8.3.1 Rms pressures

Estimate the rms pressure $\bar{p}$ in a separated flow region from

$$\frac{\bar{p}}{q} = \begin{cases} 0.045/(1 + M_e^2) & \text{for expansion regions} \\ 0.022 & \text{for compression regions} \\ 0.14/(1 + .5M^2) & \text{for locations where flow separates or attaches, where shocks may be present.} \end{cases} \tag{171}$$

Here, M_e denotes the Mach number downstream of the expansion, q the upstream dynamic pressure, and M the upstream Mach number.

8.3.2 Power spectral density

Estimate the power spectral density S(f) from

$$S(f) = \frac{5.9\ \bar{p}\delta_e}{U_e}\left[1 + \left(\frac{0.17\ f\ U_e}{\delta_e}\right)^{0.83}\right]^{-2.15} \tag{172}$$

where $\bar{p}$ denotes the rms pressure found from the appropriate expression of Eq. (170), δ_e represents the upstream boundary layer thickness, U_e the free-stream velocity upstream of the separation region, and f the frequency (in Hertz).

8.3.3 Pressure levels in frequency bands

Find the mean square pressure $p^2_{\Delta f}$ in any band extending from frequency f_1 to f_2 by integrating Eq. (172) numerically between f_1 and f_2.

Alternatively, approximate $p^2_{\Delta f}$ by multiplying S(f) from Eq. (171) by $F(f_c)$ given by Eq. (162).

Find the corresponding sound pressure level by applying Eq. (8).

8.3.4 Convection velocities and spatial correlations

Because for separated flows the narrowband convection velocities vary strongly with wavenumber and frequency, broadband convection velocities have relatively little meaning.

Estimate the narrowband convection velocity U_c at frequency f from

$$U_c/U_e = 0.6 + \log (f\, x_s/U_e) \quad , \tag{173}$$

where U_e denotes the freestream velocity upstream of the separation, and x_s represents the streamwise distance of the observation point from the flow separation point.

Estimate the pressure correlation coefficient at frequency f from

$$\rho(\xi,\eta) = A_\xi A_\eta \cos (2\pi f \xi/U_c) \quad , \tag{174}$$

where

$$A_\xi = \begin{cases} \exp [-0.75\xi] & \text{for} \quad B < 1 \\ \exp [-0.75\xi\, B] & 1 < B < 10 \\ \exp [-1.5\xi] & B > 10 \end{cases} \tag{175}$$

$$A_\eta = \begin{cases} \exp\,[-0.75\eta] & \text{for } B < 1 \\ \exp\,[-0.75\eta\, B^{0.3}] & B > 1 \end{cases} \qquad (176)$$

$$B = f\delta/(6 \times 10^{-3} U_e) \quad . \qquad (177)$$

Here, ξ and η denote the separation distances in the streamwise and cross-stream directions, respectively, δ represents the upstream boundary layer thickness, and U_e the freestream velocity upstream of the separation region.

8.4 Base Flows

Base flow is separated flow that occurs behind the blunt termination of a body. Typical base flow is characterized by flow recirculation and turbulent vortex shedding.

8.4.1 Rms pressure

Estimate the rms pressure $\bar{p}$ in a base flow from

$$\frac{\bar{p}}{p_b} = \frac{0.01\, M_b^2}{1 + 0.04\, M_b^2} \quad , \qquad (178)$$

where p_b denotes the base static pressure and M_b the Mach number of the flow just outside the base wake.

8.4.2 Power spectral density

Determine the power spectral density $S(f)$ associated with a base flow from

$$S(f) = \frac{2\,\bar{p}^2 d}{U_b}\left[1 + \left(\frac{\pi f d}{U_b}\right)^2\right]^{-1} \quad , \tag{179}$$

where $\bar{p}$ is found from Eq. (178), f denotes frequency, U_b represents the flow velocity just outside the base flow region, and d is the diameter of the base.

8.4.3 Pressure levels in frequency bands

Calculate the mean-square pressure $p^2_{\Delta f}$ in any band extending from frequency f_1 to frequency f_2 from

$$p^2_{\Delta f} = \frac{2}{\pi}\,\bar{p}^2\left[\arctan\left(\frac{\pi d f_1}{U_e}\right) - \arctan\left(\frac{\pi d f_2}{U_e}\right)\right] \quad . \tag{180}$$

Use Eq. (8) to find the corresponding sound pressure level.

8.5 List of Symbols for Sec. VIII

Symbol	Definition	Units*	
B	reduced frequency (Eq. 177)	---	
$F(f_c)$	averaging function, Eq. 162)	---	
M	Mach number	---	
M_b	Mach number outside base wake	---	
M_e	Mach number downstream of expansion	---	
$S(f)$	power spectral density	lb sec/ft	(N s/m)
U	free-stream flow speed	ft/sec	(m/s)
U_c	convection velocity	ft/sec	(m/s)
U_{ct}	convection velocity for transitional boundary layer	ft/sec	(m/s)
U_e	free-stream velocity upstream of separation	ft/sec	(m/s)
f	frequency	Hz	
f_c	average frequency	Hz	
f_1, f_2	limiting frequencies of band	Hz	
$\bar{p}$	root-mean-square pressure	lb/ft^2	(N/m^2)
p_b	base static pressure	lb/ft^2	(N/m^2)
p_Δ^2	mean-square pressure in frequency band Δf	(lb^2/ft^4)	(N^2m^4)
q	dynamic pressure	lb/ft^2	N/m^2)
x_s	streamwise distance of observation point from flow separation point	ft	(m)
α	angle of attack	deg	
δ	boundary layer thickness	ft	(m)
δ^*	boundary layer displacement thickness	ft	(m)

*SI units are given in parentheses. Units given are typical; a consistant set must be used in any particular calculation.

Symbol	Definition	Units*	
δ_e	boundary layer thickness upstream of expansion	ft	(m)
δ_t	transitional flow length	ft	(m)
θ	cone half angle	deg	
ξ,η	separation distances in streamwise and cross-flow directions	ft	(m)
ω	radian frequency	Hz	

SECTION IX
CAVITY NOISE

9.1 Introduction

High-speed flow over cavities in aircraft surfaces frequently produces intense pressure fluctuations in the cavity and attendant radiated sound. Oscillatory pressures in the cavity are produced essentially by the flow shear layer interacting with the cavity pressure modes and with the cavity trailing edge. Typically, cavity oscillations begin to occur at low Mach numbers, become most intense in the transonic regime, and tend to decrease at high Mach numbers.

Cavity pressure oscillations typically involve strong pure tone components at the few lowest resonance frequencies of the cavity, and also a broadband noise component. The radiation of noise from these pressure oscillations to regions outside the cavity is poorly understood. At supersonic speeds, the radiation appears to be highly directional and concentrated largely in the direction normal to the cavity mouth; at low subsonic speeds the radiation is nearly uniform in all directions. The pressures experienced by aircraft surfaces surrounding the cavity may be expected to be of the same order as the pressures in the cavity, for a distance equivalent to about one cavity depth from the cavity edges.

Data and estimation methods are available only for shallow cavities, i.e., for cavities with length/depth ratios greater than about 2.0. For deep cavities, one can estimate the resonance frequencies reasonably well, but one can only make a very rough guess at the amplitudes.

Cavities arranged in arrays or placed one behind the other generally do not interact significantly, and each may be analyzed independently of the others.

The presence of stores in a cavity generally has only minor effects on the cavity pressure oscillations, provided the stores do not occupy a major fraction of the cavity volume and do not interfere with the shear layer over a substantial fraction of the cavity mouth. If such shear layer interference does occur, then there often result dramatic reductions in the fluctuating pressures.

9.2 Pressures Inside Cavity

(a) Refer to Figure 61 and determine the dimensions D, L, W corresponding to a rectangular cavity that approximates the actual configuration of interest.

(b) Calculate L/D.

9.2.1 Shallow cavities ($L/D \geq 2$)

(a) Calculate the oscillation frequencies f_1, f_2, f_3 corresponding to the lowest three modes from

$$f_n = \frac{(n - 0.25)\ U/L}{1.75 + M\ (1 + 0.2\ M^2)^{-\frac{1}{2}}} \quad ; \quad n = 1, 2, 3 \qquad (181)$$

where

U = free stream air speed
M = aircraft Mach number

(b) Calculate the peak sound pressures $\hat{P}_n$ associated with the one-third octave bands containing three lowest modes from

$$\begin{aligned} 20 \log (\hat{P}_2/q) &= -27 - 3.3\ L/D + 25\ \text{sech}\ (2M - 2) \\ 20 \log (\hat{P}_1/q) &= 20 \log (\hat{P}_2/q) + 1.5\ L/D - 13 \\ 20 \log (\hat{P}_3/q) &= 20 \log (\hat{P}_2/q) - 13M + 9 \end{aligned} \qquad (182)$$

where q denotes the dynamic pressure.

(c) Find the length-wise distribution of the sound pressures associated with the first three modes from

$$20 \log [P_n(x)/q] = 20 \log (\hat{P}_n/q) - 10 \left[1-\left|\cos\left(\alpha_n x/L\right)\right| + (.33L/D - .6)(1 - x/L)\right] \quad (183)$$

where

$$\alpha_n = \begin{cases} 3.5 \text{ for } n = 1 \\ 6.3 \text{ for } n = 2 \\ 10.0 \text{ for } n = 3 \end{cases} \quad (184)$$

and

x = distance from cavity leading edge.

The pressures given by Equation (183) are assumed to be constant along the cavity depth and width.

(d) Determine the one-third octave band sound pressure levels due to broadband noise in the cavity by applying Figure 62.

9.2.2 Deep cavities (L/D < 2)

(a) Calculate estimates of the oscillation frequencies f_1, f_2, f_3 corresponding to the lowest three modes from

$$f_n = \left(\frac{2n - 1}{4}\right)\left(\frac{c}{D}\right), \qquad n = 1, 2, 3 \quad (185)$$

where c = speed of sound in air.

(b) Estimate the sound pressure p_b acting on the cavity bottom by using

$$20 \log (p_b/q) \approx 9.0 - 3L/D + 20 \log (2M-M^2-0.7) \quad (186)$$

where q = dynamic pressure.

Note that this estimate is a very approximate one.

(c) Estimate the corresponding pressure distribution in the depth direction from

$$p(y) = p_b \cos \left[\frac{(2n-1)\pi}{2} \frac{y}{D} \right] \quad (187)$$

where

y = distance measured from the floor of the cavity.

Assume that the pressure distribution is uniform in the length and width direction.

(d) Assume the broadband noise component is negligble.

9.3 Pressures on Surfaces Around Cavity Mouth

9.3.1 Below Mach 0.3 (M < 0.3)

(a) Calculate the Strouhal number $S_n = f_n L/U$ associated with the pure-tone component at frequency f_n from Equation (181)

(b) Find the pure-tone sound pressure p_{sn} at the observation point of interest (at the frequency f_n) from

$$p_{sn} = 0.035 \, q \, S_n W/r_s \quad (188)$$

where

q = dynamic pressure
W = cavity width
r_s = distance from center of cavity trailing edge to observation point.

(c) For a deep cavity (L/D < 2), neglect the broadband noise contribution. For a shallow cavity (L/D $\geq$ 2), use Figure 62 to find the broadband sound pressure levels L_p in the cavity and then calculate the sound pressure level L_s at the surface point of interest from

$$L_s = L_p - 20 \log (r_s/r_c) \qquad (189)$$

where

r_c = distance from center of cavity trailing edge to cavity edge point nearest observation point.

9.3.2 Above Mach 0.3 (M > 0.3)

Locations Within 2D From a Cavity Edge

At locations less than 2D from a cavity edge, where D denotes the cavity depth, the pressure is equal to that on the nearest cavity interior (bulkhead) surface, which pressure is estimated by means of the approach described in Section 9.2.

Locations Beyond 2D From a Cavity Edge

(a) Calculate the sound pressure level L_p at the location on the cavity interior that is nearest to the surface point of interest, using the procedure of Section 9.2.

(b) Find the sound pressure level L_d at the surface point of interest from

$$L_d = L_p - 20 \log (r_s/r_d) \qquad (190)$$

where

r_d = distance from center of cavity trailing edge to cavity edge location for which L_p is calculated

r_s = distance from center of cavity trailing edge to observation point on surface

9.4 List of Symbols for Sec. IX

Symbol	Definition	Units*	
D	cavity depth	ft	(m)
L	cavity length	ft	(m)
L_c	sound pressure level in 1/3 octave band, relative to dynamic pressure	dB	
L_p	sound pressure level in cavity, referred to 2×10^{-5} N/m^2	dB	
L_s	sound pressure level in 1/3 octave band at surface point (re 2×10^5 N/m^2)	dB	
M	aircraft Mach number	---	
$\hat{p}_n$	peak sound pressure for nth mode	lb/in^2	(N/m^2)
S, S_n	Strouhal number	---	
U	free-stream airspeed	ft/sec	(m/s)
W	cavity width	ft	(m)
c	speed of sound in air	ft/sec	(m/s)
f_1, f_2, f_3	oscillation frequencies for lowest three cavity modes	---	
n	number of mode	---	
p_b	sound pressure on cavity bottom	lb/ft^2	(N/m^2)
p_{sn}	pure-tone sound pressure at frequency f_n	lb/ft^2	(N/m^2)
q	dynamic pressure	lb/in^2	(N/m^2)
r_c	distance from center of cavity trailing edge to cavity edge point nearest observation point	ft	(m)

*SI units are shown in parentheses. Units given here are typical ones; a consistant set must be used for any particular calculation.

Symbol	Definition	Units*	
r_s	distance from center of cavity trailing edge to observation point outside cavity	ft	(m)
x	distance from cavity leading edge	ft	(m)
y	distance from cavity floor	ft	(m)
α_n	distribution adjustment factor	---	

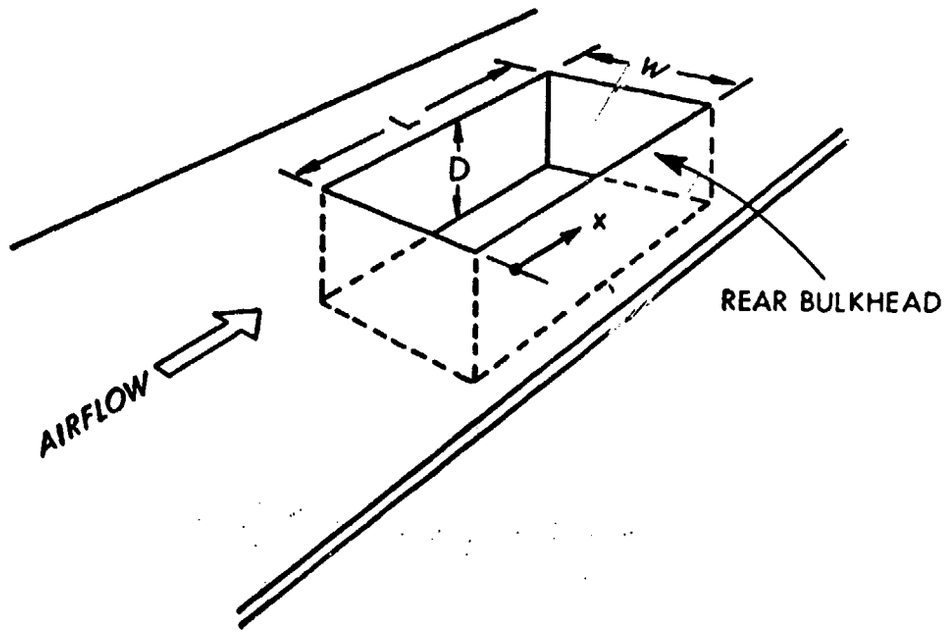

FIG. 61. RECTANGULAR CAVITY

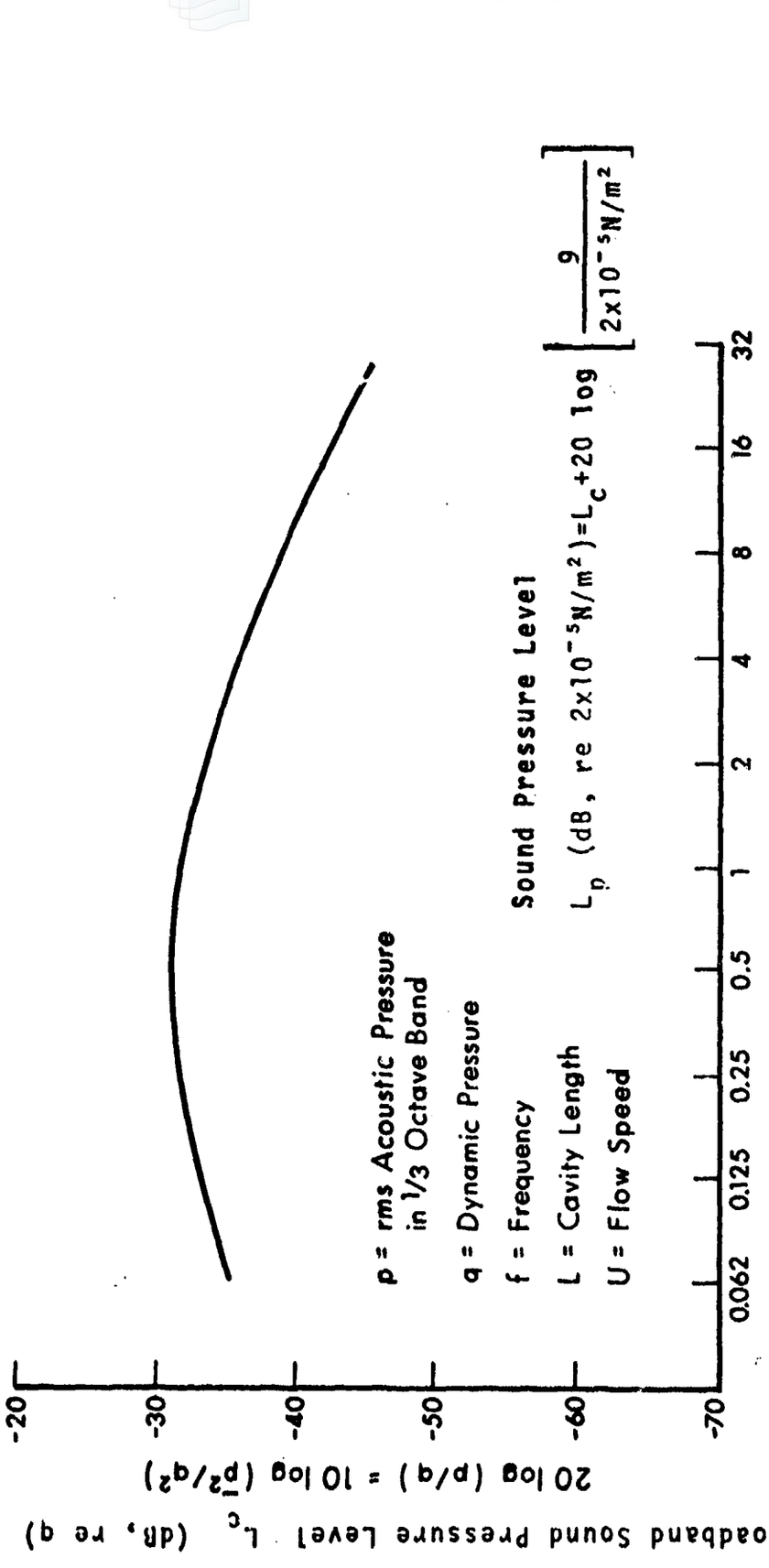

FIG. 62. NONDIMENSIONAL 1/3-OCTAVE BAND SPECTRUM OF CAVITY BROADBAND NOISE.

☆ U. S. GOVERNMENT PRINTING OFFICE: 1977 — 757-001/383